NTNU – Trondheim
Norwegian University of
Science and Technology

Seimic analysis of Carboniferous rift basin and Triassic growth-fault basins of Svalbard; analysis of seismic facies patterns with bearing on basin geometry and growth-strata successions

Anita Sørstrønen Bjerkvik

Earth Sciences and Petroleum Engineering
Submission date: June 2012
Supervisor: Martin Landrø, IPT
Co-supervisor: Alvar Braathen, UNIS
Snorre Olaussen, UNIS

Norwegian University of Science and Technology
Department of Petroleum Engineering and Applied Geophysics

Abstract

This study analyzes 2D seismic sections of extensional growth-fault basins, covering two tectonic realms; (i) Carboniferous rifting in Central Spitsbergen, and (ii) shallow Triassic extensional basins of the SE Svalbard region. The study of the Carboniferous Billefjorden Trough in Sassenfjorden-Tempelfjorden and from Reindalen, focus on the rift infill with associated wedge and lenticular shaped depocenter geometries. The two fundamental geometries are identified by either variable fault truncation of the wedge-shaped basin fill (fault onlap relationship) or fault-tip monoclines with associated basinward offset of the related lenticular basins. The interpretation of lines from Eastern Svalbard focus on a series of Triassic, shallow basins (< 200 m; up to 150 ms deep) of which most are bound by listric faults that sole out in underlying shale successions. These observations are correlated with similar faulting with basins in cliffs of Edgeøya. The offshore Triassic faulting of Eastern Svalbard represent a first assessment, as such analysis has not been carried out before.

This study goes deeper into details on the evaporite-dominated Carboniferous Billefjorden Trough than those presented by Bælum and Braathen (2012). Some new information and characterization of the basin infill link seismic facies analysis of Carboniferous rifting to reflector belts that can be correlated with the pre-rift Billefjorden Group, the syn-rift successions of the Hultberget, Ebbadalen and Minkinfjellet formations, and the immediate post-rift (or late syn-rift) Wordiekammen Formation. The Billefjorden Trough is the result of a complex basin evolution history, and published results of outcrop studies in the northern Billefjorden area shows a basin that changes basin depocenter geometry, from a lenticular shape to a wedge shape and then back to a lenticular shape. Similar patterns are recognized by the seismic facies analysis. In a conceptual framework, the Billefjorden Trough differs from the rift basins described in Prosser (1993), in that the basin is significantly influence of fault-propagation folding, probably controlled by thick basin-center successions of low-shear strength evaporites. Encountered geometries are more similar to those of rift basins of the Gulf of Suez.

Eastern Svalbard offers world class examples of extensional fault-growth basins in mountain slopes of Edgeøya and partly Hopen. Similar faulting is encountered in the lines interpreted from the Eastern Svalbard dataset, where the intricacy of faulting and their associated shallow basins of Triassic age offer complex geometries but also challenging interpretation work because of limited seismic resolution. Revealed internal geometries include rollovers and drag-folds, offering some general geometrical similarities with the much larger Carboniferous rifts. However, the depositional systems are very different. For the Triassic, regional clinoform progradation in a northerly direction interacted with the faulting, indicating that the coastal or deltafront migration at times were arrested by the faulting. This arrest is suggested by vertically stacked sequences, before the fault systems are bypassed by renewed clinoform progradation.

Sammendrag

Denne studien analyserer 2D seismiske seksjoner av ekstensjonsvekst-forkastningsbassenger, som dekker (i) karbon rifting i sentral-Spitsbergen området, og (ii) grunne Trias ekstensjons-bassenger i sør-øst Svalbard-regionen. Studiet av Billefjorden «Trough» 'et av Karbon alder i Sassenfjorden-Tempelfjorden og fra Reindalen, fokusere på riftsedimentene med assosiert kile- og linseformede deposenter geometrier. Disse to grunnleggende geometriene er identifisert med enten variable forkastningstrunkering av de kileformede bassengesedimentene (forkastnings pålapp) eller «fault-tip» monoklinaler med assosiert offset mot bassenget av de relaterte linseformede bassengene. Tolkningen av linjene fra Øst-Svalbard fokuserer på en serie av Trias, grunne bassenger (<200 m, opp til 150 ms dype), hvorav de fleste er bundet av listriske forkastninger som såler ut i underliggende skifer suksesjoner. Disse observasjonene er korrelert med lignende forkastninger tilstede i klippene på Edgeøya. Øst Svalbards offshore Trias forkastninger representerer en første evaluering, siden en slik analyse ikke har vært utført før.

Denne studien går dypere inn i detaljene på det evaporitt-dominerte Karbon Billefjorden «Trough» 'et enn tolkningen presentert av Bælum og Braathen (2012) for det samme området (Sassenfjorden-Tempelfjorden og Reindalen). Ny informasjon og karakterisering av sedimentene som har fylt bassenget kan bli koblet opp mot seismisk facies analyse av karbonrift reflektorbelter som kan bli korrelert med pre-rift sedimenter fra Billefjorden gruppen, syn-rift suksesjonene Hultberget, Ebbadalen og Minkinfjellet formasjonene, og den umiddelbare post- rift (eller sent syn-rift) Wordiekammen formasjonen. Billefjorden «Trough» 'et er resultatet av en kompleks bassengevolusjon, og publiserte resultater fra feltstudier i det nordlige Billefjorden området viser et basseng som endrer deposenter-geometri, fra linseformet til kileformet, og deretter tilbake til linseformet igjen. Lignende mønstre er anerkjent av den seismiske facies analysen. I et konseptuelt rammeverk, avviker Billefjorden «Trough» 'et fra de riftbassengene beskrevet i Prosser (1993), i at bassenget er betydelig påvirket av forkastnings-forplantnings folding, trolig styrt av tykke basseng-senter suksesjoner bestående av evaporitter med lav skjærstyrke. Slike geometrier finner man også i riftbassenger i Suez gulf-området.

Øst-Svalbard tilbyr eksempler i verdensklasse på ekstensjons- forkastningsvekst bassenger i fjellsidene på Edgeøya og delvis Hopen. Lignende forkastninger er funnet i linjene tolket fra Øst-Svalbard datasettet, der intrikate forkastninger og deres assosierte grunne Trias basseng tilbyr komplekse geometrier, og dette gjør også tolkningsarbeidet utfordrende på grunn av begrenset seismisk oppløsning. Avdekkede interne geometrier inkludere rollovers og «drag»-folder, og tilbyr noen generelle geometriske likhetstrekk med den mye større Karbonriften. Men avsetningsmiljøene er svært forskjellige. For Trias er det regionale prograderende klinoformer i nordlig retning, påvirket av forkastninger, som indikerer at kyst -eller deltafront migrasjon til tider ble påvirket av forkastninger. Denne

påvirkningen er foreslått av vertikalt stablede sekvenser, før forkastningssystemene ble forbigått av nye prograderende klinoformer.

Acknowledgements

The following report is the result of a one semester master diploma thesis for post graduate students at the Norwegian University of Science and Technology (NTNU). It aims at detailed interpretation of extensional basins for selected seismic 2D lines from Central Spitsbergen and Eastern Svalbard.

Great thanks to those who have been involved in this study; Professor Alvar Braathen, Professor Snorre Olaussen, Post Doc. Ingrid Anell, Professor Martin Landrø and the University Centre in Svalbard (UNIS). Professor Alvar Braathen is thanked for providing relevant articles, guidance and for prominent discussion regarding the geology of the study area and seismic interpretation of extensional basins. He is also thanked for commenting and reviewing this diploma, significantly improving its content. Professor Snorre Olaussen is thanked for providing additional relevant articles and for assistance and guidance with seismic interpretation of the study area. Post Doc. Ingrid Anell is thanked for assistance with Petrel and guidance regarding the seismic interpretation of the study area. Professor Martin Landrø is thanked for being my official supervisor at NTNU, and for helping to get in contact with Professor Alvar Braathen and Professor Snorre Olaussen (UNIS).

The seismic datasets have been made available by the Norwegian Petroleum Directorate (NPD). As the seismics have some confidentiality, their location have been somewhat masked, in that shot points have been removed from figures. The Norwegian Petroleum Directorate (NPD) is thanked for granting access to the dataset from Eastern Svalbard, and for permission to publish the results of the interpretation in this diploma.

Trondheim (NTNU) and Longyearbyen (UNIS), June 19th 2012.

Table of contents

List of figures

1. Introduction

The understanding of extensional basins is important for many reasons, and especially in the exploration for hydrocarbons, since rift basins often represent potential reservoirs in play models for hydrocarbon provinces. The bounding fault mechanisms and sediments filling in the space made available through active extension have the ability to contain and preserve huge amounts of hydrocarbon reserves.

The following thesis work will study 2D lines from various parts of rift basins from Eastern Svalbard and in the Billefjorden Trough region (Tempelfjorden, Sassenfjorden and onshore Reindalen).

Summarized aim for the study: The use of 2D seismic sections to analyze various geometries of faults and associated extensional basins; key focus on 1) Carboniferous rift infill with associated wedge and lenticular fill shapes, caused by fault truncation and fault-tip monoclines, 2) Triassic shallow basins (100-150 m deep) bound by listric faults soled in underlying shale successions, with a close link to similar faulting onshore Edgeøya on E Svalbard. The latter study has a true exploration nature; as such analysis never has been performed before for this area.

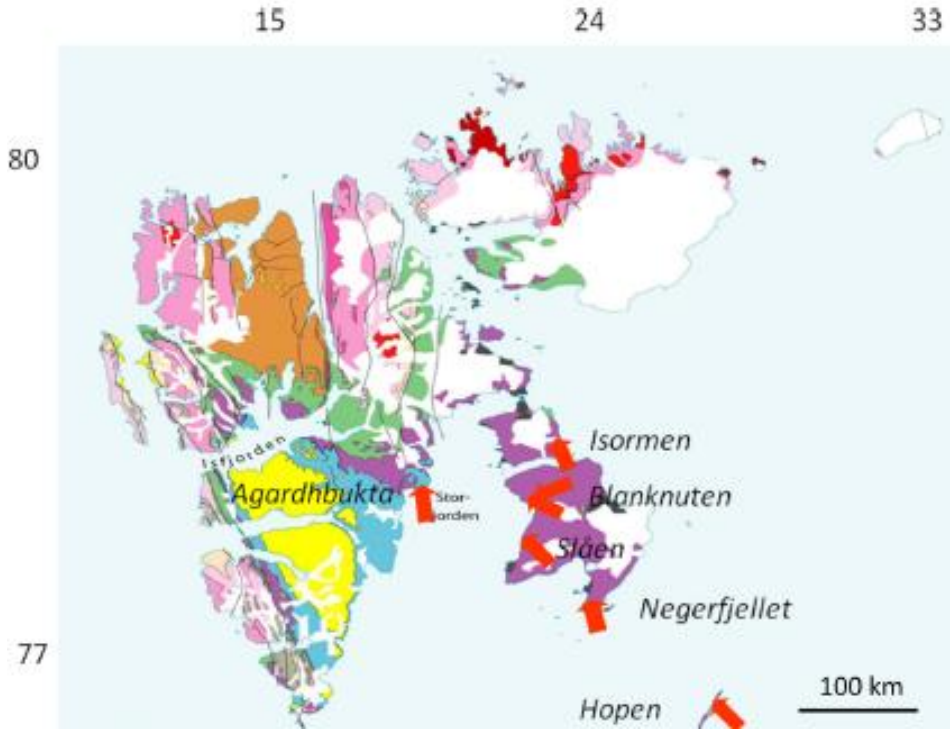

Figure 1.1 Stratigraphic overview map of Svalbard with palaeocurrent directions from eastern Svalbard. Taken from the publication by (Høy & Lundschien, 2011).

1.1 The Barents Sea

The shelf area of the Barents Sea is extensive, and in Figure 1.2 from Riis, Lundschien, Høy, Mørk, and Mørk (2008) the extent and approximate limitations are shown. The Barents Sea is an intra-cratonic basin with passive margins delineating the western and northern boundary (Grogan et al., 1999). The metamorphic basement in this region has recorded events of Precambrian age such as the Svecokarelian and Svekonorwegian orogeneses. Further, the Neoprotorozoic experienced the Baikalian event, as well expressed in eastern Finmark and nearby Russia and the SE Barents Shelf. The later Caledonian Orogeny climaxing with collision between Fennoscandia and Greenland, can be traced from the Norwegian mainland and up to Svalbard, accordingly crossing the shelf. In the Early-Middle Devonian , this major mountain chain started to collapse, or extend, allowing deposition of continental fault-bound basins (e.g., Steel & Worsley, 1984). One such basin is found in north-central Spitsbergen, another in southern Spitsbergen, and there is an extensive Late Paleozoic rift underlying the platforms south and east of Svalbard (Grogan et al., 1999).

Subsequent extension in the middle Carboniferous to Early Permian over larger areas further modified the overall deeper configuration of the shelf region. One well-studied example is the Billefjorden Fault Zone, associated with the hanging wall growth basin of the Billefjorden Trough (e.g., Maher and Braathen, 2011; Braathen et al. 2011; Bælum and Braathen, 2012). In the late Permian to Triassic time period, major orogenesis in the east represented by the Uralides, caused formation of a very deep (7-9 km) foredeep basin in the eastern shelf region. As the mountain belt was gradually denudated, a major pulse of clastic sediments was shed out from eastern source areas, first filling in the foredeep in earlier Triassic times. Subsequent infilling a shallow marine to continental, very broad shelf followed, as the shelf turned into a paralic platform (Riis et al., 2008). This infill is recorded by a series of clinoforms, sourced from the SE, and gradually building towards the NW and W (Riis et al., 2008; Høy and Lundschien 2011).

The Triassic was a relatively quiet period in the western part of the Barents Sea and Svalbard, without signs of major tectonic activity (Riis et al., 2008). The stratigraphic foundation for the Triassic basin development in the northern Norwegian Barents Sea is a succession of Carboniferous to Permian sediments (Høy & Lundschien, 2011).

In the Triassic a major system of large clinoform beds can be seen on seismic data from the Sentralbanken High to close to Kvitsøya. The same system can also be followed further west, between Edgeøya and Nordaustlandet (Høy & Lundschien, 2011). The way clinoform sets are stacked gives a good indication of how the basin settings were at the time of deposition. When the stacking of the clinoform sets is vertical, this implies creation of accommodation space and subsidence rates to be approximately equal to the rate of the infilling sediments. This setting is locally observed for the Lower and Middle Triassic successions of the Southern Barents Sea (Høy & Lundschien, 2011). When the stacking of clinoform sets has more lateral prograding geometry, it implies that the accommodation space was created before the sediments started to fill in the available space. In this case, a single clinoform set moves up a little step compared to the underlying clinoform, but also

makes a large step forward compared to the previous clinoform set. This is the case for the Northern Barents Sea Triassic clinoform system, where the sediments filled in an existing marine basin infill, hence after the accommodation space was created (Høy & Lundschien, 2011). The transport direction is believed to be mainly from the SE towards the NW, and the suggested provenance areas are Siberia, the Kola Peninsula and the Caledonides (Høy & Lundschien, 2011). These clinoforms are of interest in this study, as they should be present in the studied seismic lines from the SE Svalbard shelf area. The study area is inside the red polygon (indicating area of seismic area studied) in Figure 15.1, based in the article of Høy and Lundschien (2011).

Subsequent development of the Barents Shelf include Jurassic and Cretaceous rifting. However, these rift zones are seen as deep fault bound basins along southern and southwestern parts of the shelf, generally becoming younger to the west. As such tectonism has not been documented on Svalbard; these events are of limited interest for this study. On the other hand, a nearly continuous Jurassic to Early Cretaceous record of mainly shallow marine and partly continental deposits are widespread on Svalbard. An erosional event in the Late Cretaceous has removed part of this succession. Further, the Paleocene to Eocene formation of the West-Spitsbergen fold-thrust belt caused crustal thickening and uplift in the west, and deposition in a foredeep basin to the east, the Tertiary Central Basin of Spitsbergen. The associated forebulge should accordingly be located farther east, probably along the east coast of Spitsbergen, which shows a very gentle anticline (Braathen, Osmundsen, & Olaussen, 2011b). The final event of the Svalbard region is oblique rifting occurring between Spitsbergen and Greenland since the Oligocene, causing additional uplift of the western Svalbard as a passive margin progressively developed (e.g., Leever, Gabrielsen, Faleide, & Braathen, 2011, and references therein).

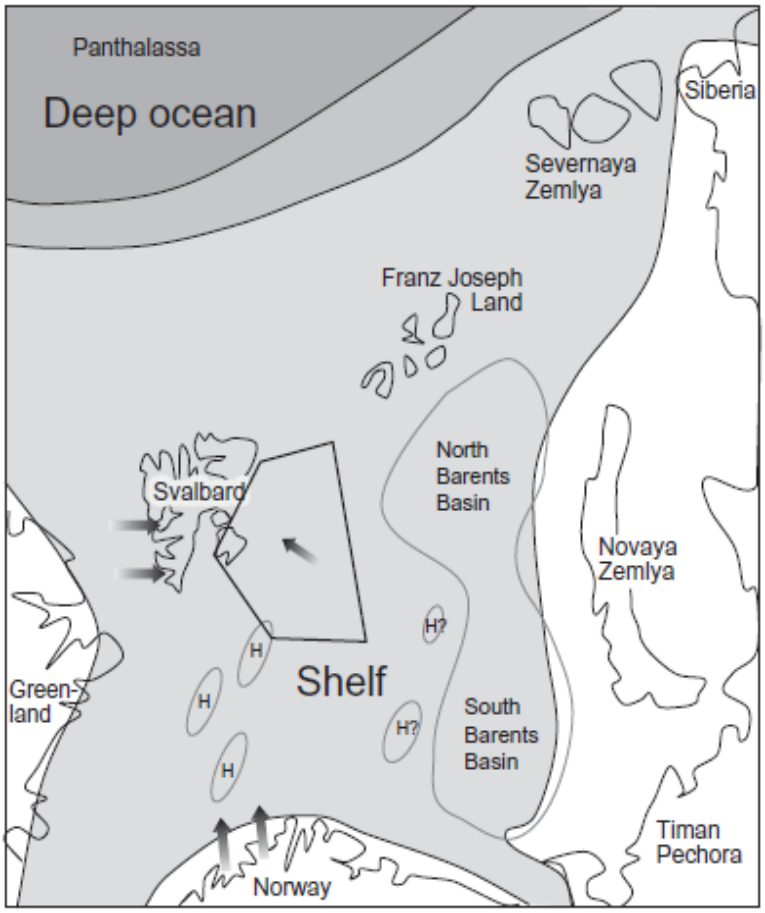

Figure 1.2 Reconstruction of the regional setting of the Barents Sea in early Triassic times, showing the continents at this time, the area of deposition in Triassic and suggested direction of sediment supply with arrows. This figure is from the publication by Riis et al. (2008), modified from Cocks and Torsvik (2007).

1.2 Conceptual models based in onshore studies Observations of rift basins

As this study address extensional faults and associated hanging wall basins, some background information of more conceptual nature is given on such tectonic systems.

The majority of folding as encountered in deformed crustal sections is commonly found in areas affected by contractional tectonics driven by compressional or transpressional forces as well as around salt and mud diapirs. However, many folds/flexures are also observed for extensional environments (e.g., Schlische, 1995). Some common examples of folding structures in extensional regimes are rollover folds and drag folds, both associated with normal faulting.

Outcrop datasets and analyses from the Sinai rift shoulder of the Suez Rift, which offers world-class examples of extensional faults and rift basins, shows that growth faults and fault-tip folds to a large extent control the development of the syn-rift stratigraphic facies (Sharp, Gawthorpe, Underhill, & Gupta, 2000). Investigation of the extensional basins of the Gulf of Suez rift also show that fault-parallel folds formed in response to fault-propagation folding, which has been ascribed as a key structural factor for sedimentation during the initiation of rifting processes (Jackson, Gawthorpe, & Sharp, 2006). The exposed and studied master faults of the Suez-Rift show footwall anticlines and hanging wall synclines which are parallel to the master fault (Jackson et al., 2006). These major structures are believed to be formed simultaneously with the extensional faulting, and are thus not a product of post-rift processes such as fault and basin inversion (Jackson et al., 2006). In recent publications of the Billefjorden Trough (Maher and Braathen 2011; Braathen et al., 2011), the so-called inversion monoclines in this basin have been re-interpreted as extensional monoclines, in accordance with the conceptual models of Suez Rift. Accordingly, there is an intimate link between folding and deposition in the basin. As some of the presented seismic lines image the Billefjorden Trough, this knowledge is of great importance for the interpretation work.

1.3 Rift basin geometry and depocenter characteristics in seismic sections

In the publication by Prosser (1993) it is stated that the spatial distribution and temporal evolution of depositional systems in basins bounded by active faulting are seen as to be significantly influenced by tectonics. Further, the fault movement and the stage of basin development are considered to be controlling the potential for erosion, sediment flux and deposition (Prosser, 1993). Several general and idealized stages of rift evolution are recognized, named S2-S5. In Figure 1.3 there are examples of S2-S5 reflectors in a rift basin setting, illustrating their typical appearance. The S2 is defined as the rift initiation when the subsidence rate and the sedimentation rate are approximately equal. S2 can be recognized by wedge shaped reflector packages that thin and end high on the hanging wall slope, often showing hummocky internal seismic facies. S3 represents the rift climax, at the time when the rate of fault displacement is highest with reflector packages characterized by increased aggradation. In such cases, the rate of subsidence could exceed the sedimentation rate and there is an increased area available for deposition. The reflectors close to the footwall dip-slope can have a chaotic appearance for seismic sections, especially for data with low resolution. The S4 is recognized as the post rift stages of rift basin evolution (Prosser, 1993). The general data quality of the 2D seismic lines I will interpret in this report will most likely not have sufficient resolution to observe detailed S2-S5 facies. Still, the indications of pre-, syn- and post-rift sediments for the lines showing the large scale Billefjorden Trough is recognizable to some extent.

Eustatic sea-level fluctuations that occur during basin formation will have profound effects on the depositional systems and their seismic expression. However, they will not necessarily dominate or mask the tectonic effects, especially in the areas most affected by local relief, in practice found closest to the active faults (Prosser, 1993; Jackson et al., 2006; Braathen et al., 2011).

In Figure 1.4 an idealized log of the vertical lithostratigraphy through the basin center is shown. This log, interpret the expression of changing tectonic control on the depositional system. For this study, this conceptual link between seismic expression and lithology represent a useful guide when seismic facies are linked to stratigraphy and lithology.

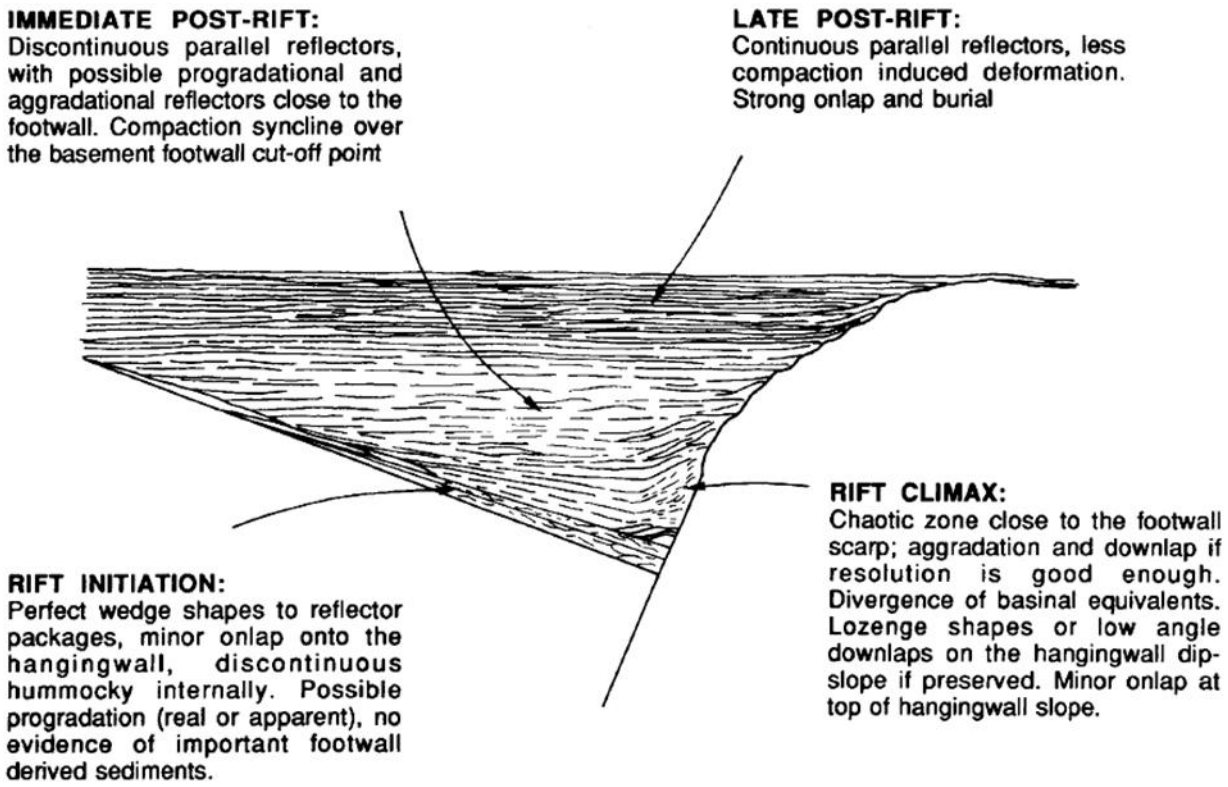

Figure 1.3 Taken from the publication by Prosser (1993), showing a near ideal case of rifting and rift basin.

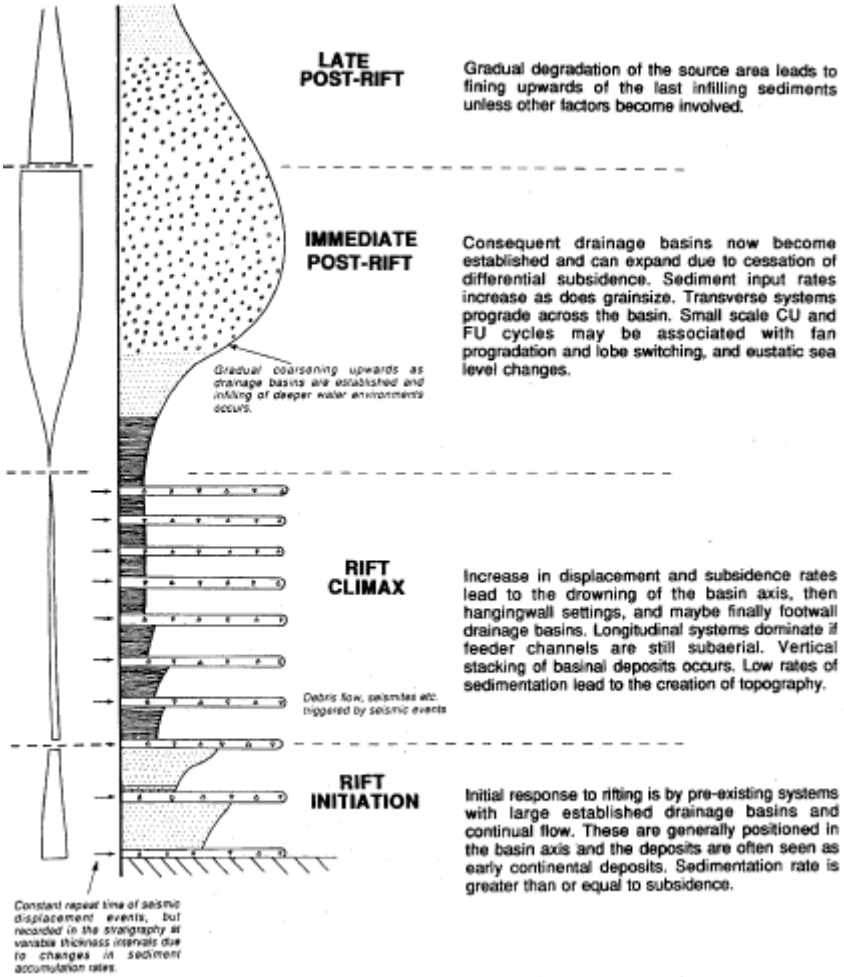

Figure 1.4 Taken from the publication by Prosser (1993), showing an idealized log of lithostratigraphy trough the basin center.

1.4 The Billefjorden Trough and the Billefjorden Fault Zone

The Billefjorden Trough is one of many Carboniferous rift basins of the Barents Shelf. These Carboniferous basins are important as exploration targets for the oil industry, especially further south, on the Loppa High, where such basins have an interesting depth. A significant part of the Billefjorden Trough is found on-shore, which makes it accessible and ideal for field studies. Accordingly, this Carboniferous rift basin is the best studied of these Carboniferous basins of the Barents Shelf (e.g., Braathen et al., 2011; Bælum & Braathen, 2012; and references therein). The Billefjorden Trough itself has an overall westward dip of the basin floor, outlining a half-graben structure that is deepest next to the master fault (Billefjorden Fault Zone) in the west. This is well expressed in Figure 3.2 showing the position of the Billefjorden Trough in the hangingwall (east) of the Billefjorden Fault Zone. There are source rocks in the Billefjorden Trough such as organic-rich syn-tectonic evaporittic rocks in addition to pre-tectonic lacustrine and bog-type coal deposits (e.g., Braathen et al., 2011). The reservoir potential is linked to the siliciclastic alluvial fan and delta systems, and to carbonate sections deposited as syn-rift sediments in the basin, showing both fracturing and locally karstification. Some carbonate build-ups have also been recognized along the high-standing blocks of the basin realm.

The Billefjorden Fault Zone stretches for a minimum of 110 km along strike, with a hanging wall basin that is approximately 20-30 km wide at the most (Bælum & Braathen, 2012). The major fault zone has an approximate north-south trend, and is possible to trace from the NW shelf, across Spitsbergen, and southwards to Storfjorden (McCann & Dallmann, 1996). The larger fault segments of the fault zone are the Odelfjellet, Balliolbreen and Drønbreen faults (Bælum & Braathen, 2012). In this study, the focus is on the Billefjorden Fault Zone where it extends south of Billefjorden, in the Sassenfjorden and Tempelfjorden region. Farther south, one seismic line from the Reindalen valley is included. All these lines show the Billefjorden Through.

The Billefjorden Fault Zone developed during three major tectonic events. In the latest Devonian, a contractional event (Svalbardian event) caused large-scale folding and reverse faulting, as especially seen in the Devonian basin just east of the Billefjorden Fault Zone (Bergh, Maher, & Braathen, 2011; Nøttvedt, Livbjerg, Midbøe, & Rasmussen, 1993). During this event, the eastern basement block was thrust up on top of the Devonian basin, with an indicated vertical separation of around 10 km (Bergh et al., 2011; Bælum and Braathen, 2012). Subsequently, the latest Devonian landscape was denudated, before the pre-rift sediments of the Billefjorden Group were deposited. They are made up of coarse, mature sandstones and pebbly sandstones of braided river affinity, intercalated with coals with an origin from swamps and lakes. During the middle Carboniferous, the Billefjorden Fault Zone was reactivated as a normal fault,with rejuvenation parallel to - and east of the Devonian master faults. This faulting offset the Billefjorden Group with as much as 2500 meters near Pyramiden (Bælum and Braathen 2012). The developing rift basin, the Billefjorden Trough, was subsequently filled with an up to 2500 m succession of syn-rift sediments; spanning

from sandstones that are more common near the margins, to mainly evaporites and carbonates in the basin center. It has been argued that faults of the basin were reactivated in the early Tertiary in association with formation of the fold-thrust belt; however, much of the ascribed basin inversion has been rejected in recent contributions (Maher and Braathen, 2011; Braathen et al. 2011) that document that mainly rifting-related structures are seen in the basin.

The syn-rift sedimentary succession starts with the Hultberget Formation with continental fluvial deposits of fine to medium sandstone alternating with muddy siltstone (Braathen, Bælum, Maher Jr, & Buckley, 2011; Johannessen & Steel, 1992; Nøttvedt et al., 1993; Riis et al., 2008). The overlying Ebbadalen Formation starts with the Ebbaelva Member that consists of shales with interbedded sandstone and carbonates, gradually becoming more influenced by evaporites towards the top. The following succession has been described as alluvial fan deposits of the Odellfjellet Member near the Billefjorden Fault Zone, interfingering with basin center evaporites and carbonates of the Tricolorfjellet Member. The so-called syn-rift succession is topped by the heterolithic Minkinfjellet Formation, starting with a fairly thick carbonate mud unit, then hosting meter-thick layers of sandstone, shale, evaporites and carbonate. The overlying marine, cancerous Wordiekammen Formation has commonly been regarded as post-rift; however, both Maher and Braathen and Braathen et al. (2011) document thickness variations in this unit around fault-tip monoclines, consistent with ongoing tectonism for the lower part of this unit.

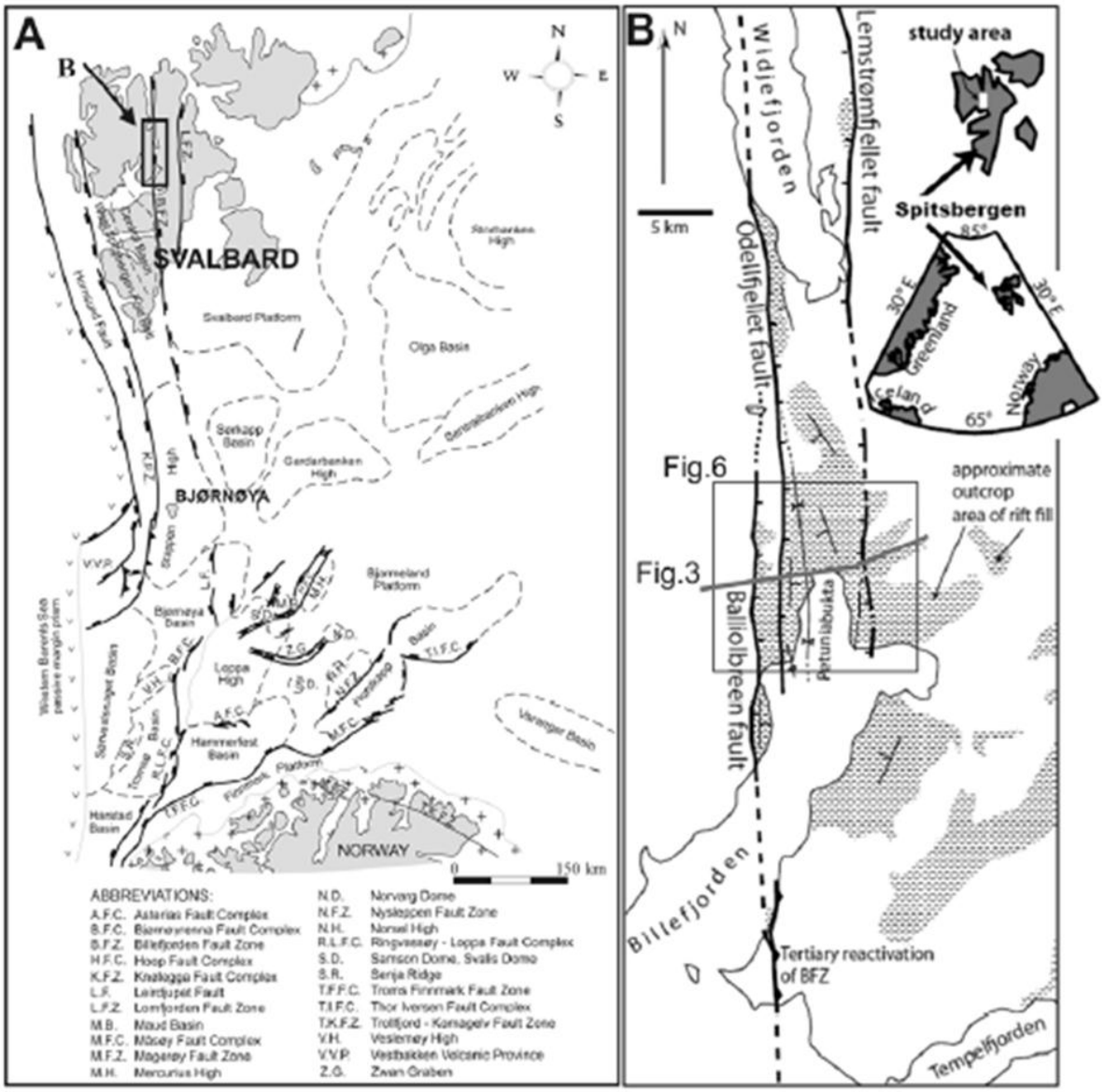

Figure 1.5 Overview of major faults and fault zones from the Billefjorden area, from the publication by Braathen et al. (2011), modified from Maher Jr and Braathen (2010).

1.5 Triassic extension in the Barents Shelf

This study brings the first seismics to the table that focus on potential Triassic extensional faulting of the area between Sørkapp, Hopen and Edgeøya. Figure 1.6 and Figure 1.7 from Braathen et al. (2011; pers. comm.) show the structural style of Triassic faulting on Edgeøya and Hopen. The initial interpretation by Edwards (1976) is that this faulting and basin formation relates to delta front collapse. On the contrary, Braathen et al. (2011) documents a regional extent of this type of faulting, identifying such faults over a distance exceeding 200 km, thereby underlining the likelihood of a regional tectonic event. Further, there seems to be a link between deep-rooted faults, and shallower listric faults that sole out in pro-delta shales. With a regional extent, such faults should be visible in seismic sections of the region. With this in mind, screening of available seismics resulted in identification of some potential fault systems of similarity to those seen on land. The shallow depth and complexity of these basins; however, represent a major challenge in seismic interpretation due to the limited resolution.

Figure 1.6 Photograph's of extensional listric faults with Triassic growth basins in the hanging wall from Kvalpynten, SSW Edgeøya. The view is to the east. Photographs by A. Braathen.

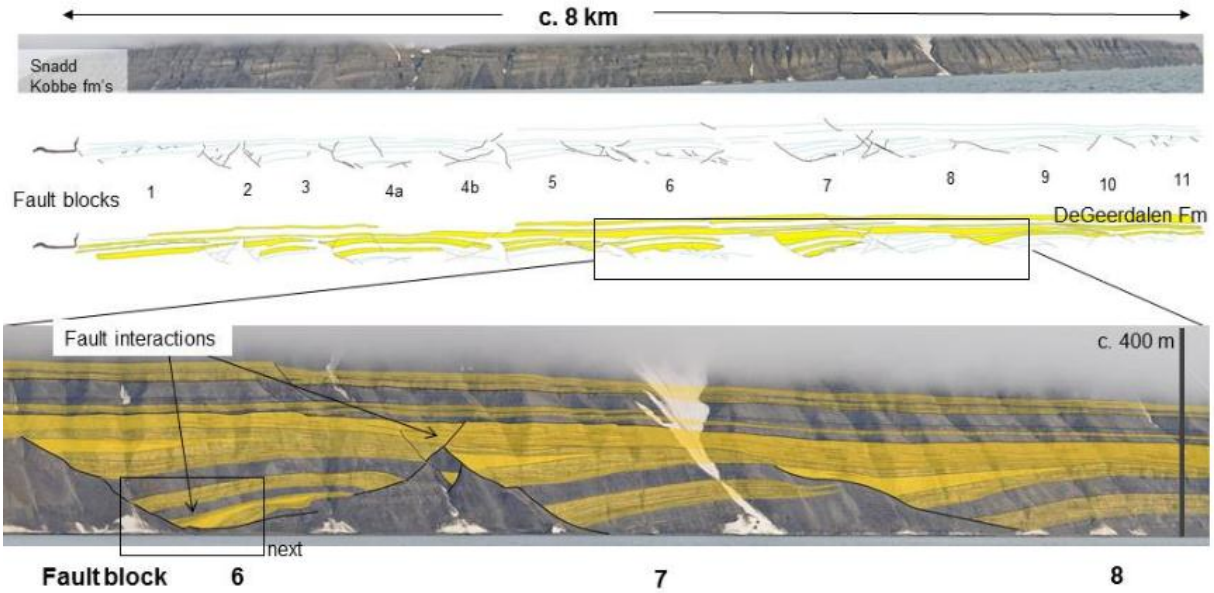

Figure 1.7 Photograph's with interpretations of extensional listric faults with Triassic growth basins in the hanging wall from Kvalpynten, SSW Edgeøya. The view is to the east. Photographs by A. Braathen.

2. Datasets and method

The seismic 2D lines interpreted in the following chapter are from different seismic campaigns on Svalbard. I have chosen to include the detailed interpretation for selected areas on 7 lines in total; 3 lines from Eastern Svalbard (lines 2045-92 A, 2145-92 and 2300-81), all from the same dataset, 3 lines from the area of Sassenfjorden and Tempelfjorden (lines NH8706-210/404/405) and 1 line from Reindalen (NH8802-32).

Line NH8802-32, located in Reindalen, is from the terrestrial campaign NH8802. This line was collected in 1988 using a 60 channel 1500 meter snow streamer which was pulled by a bandwagon (reviewed in Bælum & Braathen, 2012). The source used was dynamite (Dynacord) charges of 2-4 kg/shot (Bælum & Braathen, 2012). This method of collecting seismic is highly susceptible to noise, which can be hard to process away from the seismic afterwards. For instance, wind conditions, snow layer composition and noise created by motor vehicles will affect the signal to noise ratio in a negative way. This is almost inevitable for this kind of terrestrial seismic campaign.

The marine 2D data from the NH8706 campaign was collected in 1987 with a 160 channel 2000 meter streamer, and with an airgun SWAG array as source (Bælum & Braathen, 2012). There are some issues with regards to water depth in the fjords of Svalbard, which are highly variable (Bælum & Braathen, 2012).

The lines interpreted in detail from the Eastern Svalbard dataset are named 2045-92 A, 2145-92 and 2300-81. Note that only selected parts of these lines are interpreted. This is indicated with a red line in the overview maps showing the position of all lines from this dataset. In general, the seismic surveys covering areas of Storfjorden and Eastern Svalbard are exposed to various noise-generating artifacts, especially dolerite intrusions with high velocities. Intrusions frequently occur in these areas, offering a series of effects on other reflectors, and especially side-sweep reflections in the seismic image can be misleading. Also, cemented zones and high velocity layers (carbonates, evaporites, intrusions, etc.) can cause multiples and disturb the seismic ray patterns.

A near-top Permian (ntP) reflector is established for all interpreted lines in my Petrel project (and also for many additional lines from the Eastern Svalbard dataset not further addressed here), to have a reference horizon. This horizon is in general a very strong and consistent reflector, which is a good place to start the interpretation. The work also tried to establish a near top Wordiekammen (ntW) for all lines in the interpretation, but this horizon appears to not be as reliable as the ntP. The reason for this, amongst other things, is that it is not a very straightforward horizon to interpret for some of the lines, and can change laterally from a clear, strong and continuous reflector to becoming nearly invisible, or simply blend in with other reflectors.

The method used for the detailed interpretation mainly involves interpretation by hand. Transparent paper for was used for tracing out all reflectors, then this sheet was used without the seismic line to mark discontinuities such as faults and other boundary surfaces outlined by onlap, toplap, and downlap terminations. Finally, an identification of seismic

facies was performed. Further, areas of special interest on the selected lines were addressed by numbering them (1, 2...etc.) for the discussion of observations.

The seismics from Eastern Svalbard was delayed, and did not arrive before the middle of March (2012). The late arrival of the dataset delayed the start of the interpretation of the Triassic extensional basins from the Eastern Svalbard 2D lines. The dataset was also sent with wrong coordinates, but this was possible to correct for in Petrel. Before the seismic from Eastern Svalbard arrived, the focus was on the line from Reindalen and the lines from Sassenfjorden and Tempelfjorden.

Around the detailed interpretation work - where there truncation/termination and onlap, downlap or toplap reflectors, a boundary surface (green) or fault (red) is marked as appropriate depending on the overall situation of the reflectors and identified facies. Where the reflectors seem to be cut and end abruptly (possibly also related to a blurry zone in the seismics), faults are marked in red. Exactly where the fault start and end is at times challenging to decide, as the data often is blurry in the fault zones, and some of the interpreted faults have small offset. It can be especially challenging to distinguish between boundary surfaces and faults with low angle, which is the case for the East Svalbard study, especially as the quality of the data in all lines is moderate.

The workflow for the detailed interpretation of the lines presented in the following subsections is to first draw up reflectors on transparent paper, without any further interpretation of the reflectors. The second step is to draw up faults, termination patterns (onlap, downlap, and toplap), boundary surfaces (as a consequence of termination of reflectors with onlap, toplap and downlap patterns) and erosional surfaces if they were visible. The last step in the detailed interpretation is to interpret seismic facies (A, B, etc.), and to preferably be able to assign the seismic facies to its related formation and lithology. Only the final figures are presented in the following sections, whereas the step-wise line-drawing figures have been included as “raw” data in the Appendix.

All indications of time (y-axis) on the seismic plots are two-way-travel time (TWT). Due to uncertainties concerning possible restrictions from The Norwegian Petroleum Directorate (NPD) regarding the datasets published in this diploma, I have not included shot numbers for any of the lines published on the horizontal scale; only the scale bar is included for the horizontal axis. This applies for all seismic lines presented in the following sections.

3. Detailed interpretation of selected seismic 2D lines from Sassenfjorden, Reindalen and Eastern Svalbard

Chapter 3 presents the main work and results achieved for this master diploma thesis. At the end of each sub-section the figures referred to in the text can be found.

Triassic tectonics of Eastern Svalbard

The focus for the study of some selected lines from Eastern Svalbard is motivated by the fact that there is a regional, roughly E-W oriented extensional fault system in this region, as outlined in a recent paper by Braathen et al. (2011; Force meeting, Stavanger). This fault system is poorly known. As outlined in the Chapter 1.5 (Introduction), these faults can be observed in sea-cliffs of Hopen and Edgeøya, where they characteristically bound up to 100 m deep basins, as shown by Edwards (1976) and Høy and Lundschien (2011). The fault systems and associated basins are of upper Triassic to lowermost Jurassic age, and interact with the regional NW-directed infill of the shallow, middle-Late Triassic shelf, as described in Riis et al. (2008).

Braathen et al. (2011) document complex geometries and interactions between shallow-rooted ad deep-rooted faults, as shown in Figure 4.3 and Figure 1.7. Many of these faults have a significant listric/curved geometry downwards into prodelta shales. These onshore observations have been used for a guide for the offshore study. Of significance for the seismic study are the facts:

1) The geometries are extremely complex, in cases with multi-level detachments.
2) There are some deeper rooted faults that are predicted to cut the near-top Permian reflector.
3) The growth fault basins are up to 100 m and in extreme cases 200 m deep, which suggest seismic configurations within 100-150 ms TWT (with an inferred velocity of 3 km/s for poorly lithified sandstone-shale successions). The basin infill show cyclic successions of massive sandstone, thin-bedded sands-shale units, and prodelta shales, with thickness up to 30-40 m.

The onshore observations, with complex fault geometries and shallow basins with heterolithic basin fill, make the interpretation work challenging. As the fault system is predicted to be approximately E-W oriented, selected lines are oriented with a high angle to the faults, i.e., they strike N-S. In the seismic interpretation, careful outlining of reflector systems combined with the use of conceptual models of the onshore fault systems in sum unravel tectonic activity in mainly Triassic strata. This thesis represents the first attempt to analyze these systems in the seismics.

The quality of the seismics from this region many places are rather poor and have misleading artifacts. Much of this noise is related to late Cretaceous intrusions, of which

some sills have been unroofed and sit as high-velocity bodies on the sea floor, masking underlying reflectors. Further, side sweeps effects from both dikes and edges of sills seem common.

3.1 Line NH8802-32

A) Brief description of the line:

Line NH8802-32 is located onshore in the valley of Reindalen, as shown in Figure 3.1. A well was drilled by Hydro in 1993 on this seismic section; see Figure 5.1 in the Appendix for the position of this well. Previous work on this seismic line include an interpretation in Bælum and Braathen (2012; Their Fig. 8). In this study, I have concentrated on post-, syn-and pre-rift formations, identification and description of seismic facies and sequences found in the basin. As this study goes deeper into detail than Bælum and Braathen (2012), some new information -and characterization of the basin infill has been unraveled, as shown in Figure 3.3.

B) Introduction to faults, folds, basin and cap rocks:

The near top Permian and intra-Triassic reflector(s) show both folding (syncline-anticline pair) and signs of fold decapitation, as described and discussed in Bælum and Braathen (2012). As the focus here is on the Carboniferous to lower Permian basin, these structures are not further discussed.

There are major faults and fold structures visible in this line at depth. In Figure 3.3 the approximate position of the east-dipping Drønbreen and Balliolbreen faults are indicated, along with additional smaller faults, boundary surfaces and seismic facies. The major Drønbreen and Balliolbreen faults are not easily located, as their position is basically indicated by a general break in reflector belts, variations in dip domains, and otherwise poor, inconsistent reflectors in steep, fairly broad zones. Hence, the detailed outline of the faults offers significant uncertainty.

The reflectors in the basin infill are very strong for parts of the line. In addition to these strong amplitude sequences there are sequences in between which show weaker amplitude response and less continuous reflection patterns. The rift basin reflectors show both wedge and -lenticular shaped geometries, including thickening towards the footwall, and deposits curving and thinning above the Balliolbreen fault, respectively. Another key observation is that reflectors of the syn-rift sediments are partly dragged upwards near the Balliolbreen fault and some reflectors can even be traced onto the footwall block; this is seen in Figure 5.6 towards the Balliolbreen fault.

C) Seismic facies and their appearance:

There are many seismic facies with good and laterally continuous reflectors to be identified in this line. The syn rift sediments show vertically stacked, - wedge – and lenticular shaped geometries of reflector belts. However, there is a general thickening towards the west, setting up an overall half-graben geometry (towards the Balliolbreen Fault). In between the seismic facies with very strong amplitudes and relatively constant thickness, there are reflectors with more chaotic patterns and weaker amplitude response. These facies thicken towards the west. They deviate

from the otherwise seemingly continuous deposition of the strong and continuous amplitude facies. There seems also to be some kind of tectonic disturbance within the early syn-rift sediments, as is marked with red fault lines (number 1 and 2 in Figure 3.3).

The area between the Balliolbreen and Drønbreen faults, which is a high standing fault block or terrace, has the geometry of a rotated half graben block, and appears to be analogue to the geometry of the Viking graben of the northern North Sea. The reflectors within the block towards the Drønbreen fault appear dragged up along the fault plane, but with a significantly lower angle than the reflectors dragged up along the Balliolbreen fault.

The positions of the identified seismic facies are showed in Figure 3.3. The yellow facies named A1, A2 and A3 consist of very strong, continuous reflectors that are located mainly inside the basin. The brown facies B1 and B2 are found in between the yellow facies. At places there are onlap terminations onto the yellow facies where the brown facies are thinning towards the East. The B1 and B2 facies are not as continuous as in the facies A1-3, and seem to fill in the accommodation space between each of the yellow facies (A1-3). Facies C is relatively thick (about 100 ms at the most), and is only found as the last clear synrift section of the half-graben basin. The base of this facies shows onlap towards the east, whereas the top makes up a through-going boundary surface. Towards the footwall and the Balliolbreen fault the reflectors in facies C are dragged upwards. Above facies C, I have identified a facies which consists of strong and continuous reflectors, facies D. As this unit and overlying reflectors do not show signs of thickness changes, I have interpreted this section to have a post-rift status. However, there is a boundary surface between facies C and D, with downlap termination of reflectors in facie D onto facies C, and toplap terminations in the drag zone of facie C. Also the facies A and B show drag up along the footwall, though the pattern of the reflectors are more chaotic for these syn-rift facies.

D) Link between seismic facies, stratigraphic units and possible lithologies:

When following the interpretation given in Bælum and Braathen's (2012) Figure 8, the facies identified can be linked to formations and groups identified in the mentioned article (see Figure 3.3 for the identified sequences referred to in the following text): Starting with the Gipsdalen Group, the Top Gipsdalen Group horizon is about 600 ms deep at the easternmost part of my line in Figure 3.2, and corresponds to the top facies D. Top Wordiekammen sits about 100 ms below the Top Gipsdalen Group, and there seems to be almost constant thickness between these two tops. The Wordiekammen Formation is roughly equivalent to facies C. Accordingly, the top Wordiekammen Formation is therefore basically the boundary surface between facies D and C. The Minkinfjellet Formation is underneath the Wordiekammen Formation and corresponds roughly to the shallowest yellow facies

A1, and Top Minkinfjellet is close to the boundary between this shallowest yellow facies and facies C. The reflectors in the Minkinfjellet Formation are very strong and continuous with high amplitudes. The Ebbadalen Formation is believed to start somewhere in facies A2, -possibly at the top-, and continue to the bottom of facies A3; here the Top Billefjorden Group starts (about 1100 ms at the easternmost part of the line). The Billefjorden Group has a pre-rift status. Accordingly, the main pre-rift succession is found between the Wordiekammen Formation at the top and the Billefjorden Group at the base.

Although some general stratigraphic considerations are possible through the Reindalen well and Bælum and Braathen's (2012) link of this well to the seismics, much is left uncertain around the sedimentary rocks of the basin fill. As highlighted in Braathen et al. (2011), there are significant lateral facies changes in the basin, and detailed mapping would require a 3D overview. In this isolated 2D line, my interpretation indicates that all reflector belts of striking similarity, which have similar seismic amplitude response (very strong amplitudes) and geometry, also have similarity in lithology, although I acknowledge that the similar amplitude response could be caused by other effects. The depocenter geometry of this line suggests that a fault-tip monocline formed at three stages, consistent with seismic facies B1 and B2 and C, which all show related lenticular basin shapes. –For seismic facies' A1, A2 and A3 there are only mild thinning to the east. Accordingly, they reflect more regional infill, which may also have been present in the terrace in the hanging wall of the Drønbreen fault, and later removed by erosion of a high-standing block. Overall, the A1-3 reflector facies is suggested to be caused by thick, well-bedded units giving significant velocity contrasts, such as thick marine carbonates, or thick sandstone sections such as alluvial fans and fan deltas. The B1-2 reflector facies could be significantly more heterolithic, with changing evaporites, thin carbonates and siliciclastics. For facies C, the thicker unit with syn-rift affinity is likely micritic carbonate of the lower Wordiekammen Formation, as proposed by Maher and Braathen (2011) and Braathen et al. (2011).

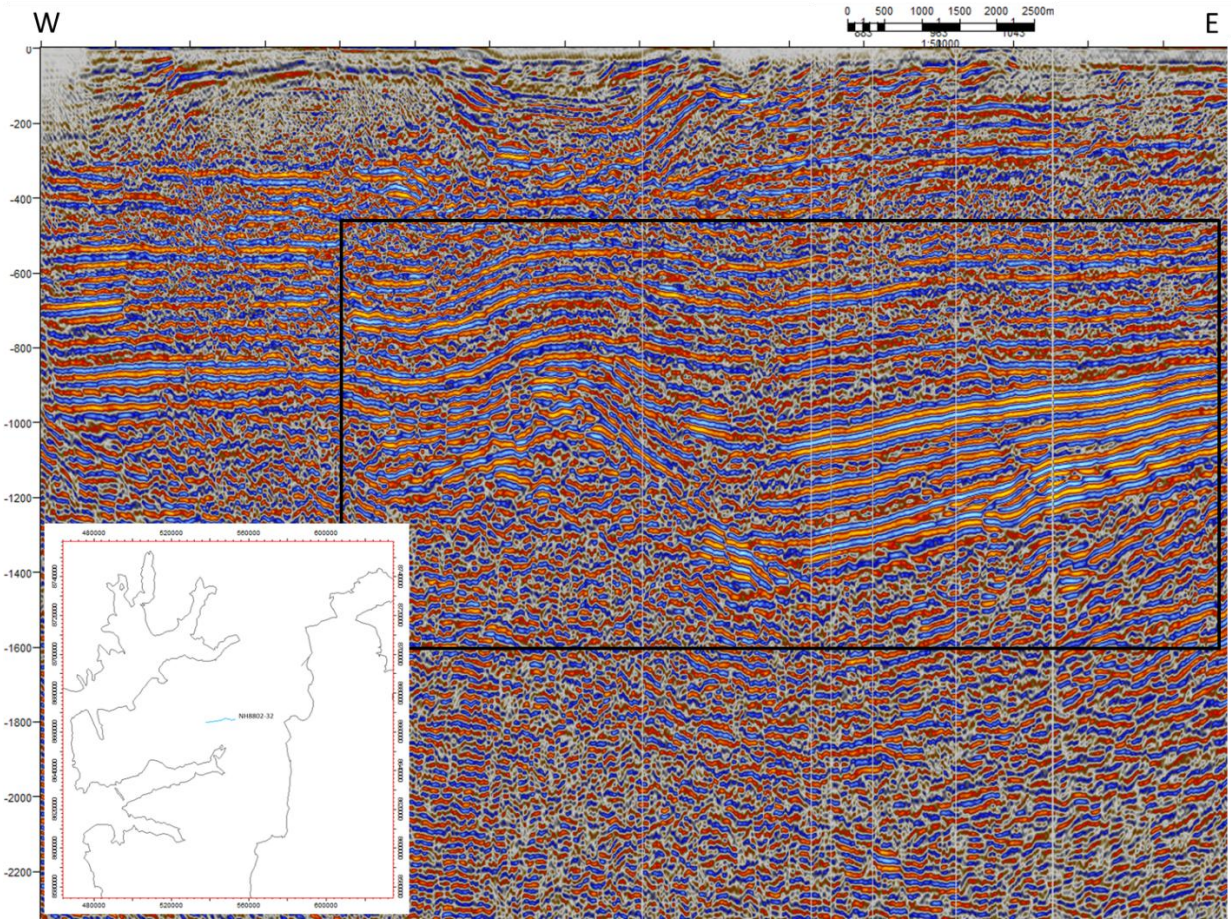

Figure 3.1 Seismic 2D line NH8802-32 with overview map.

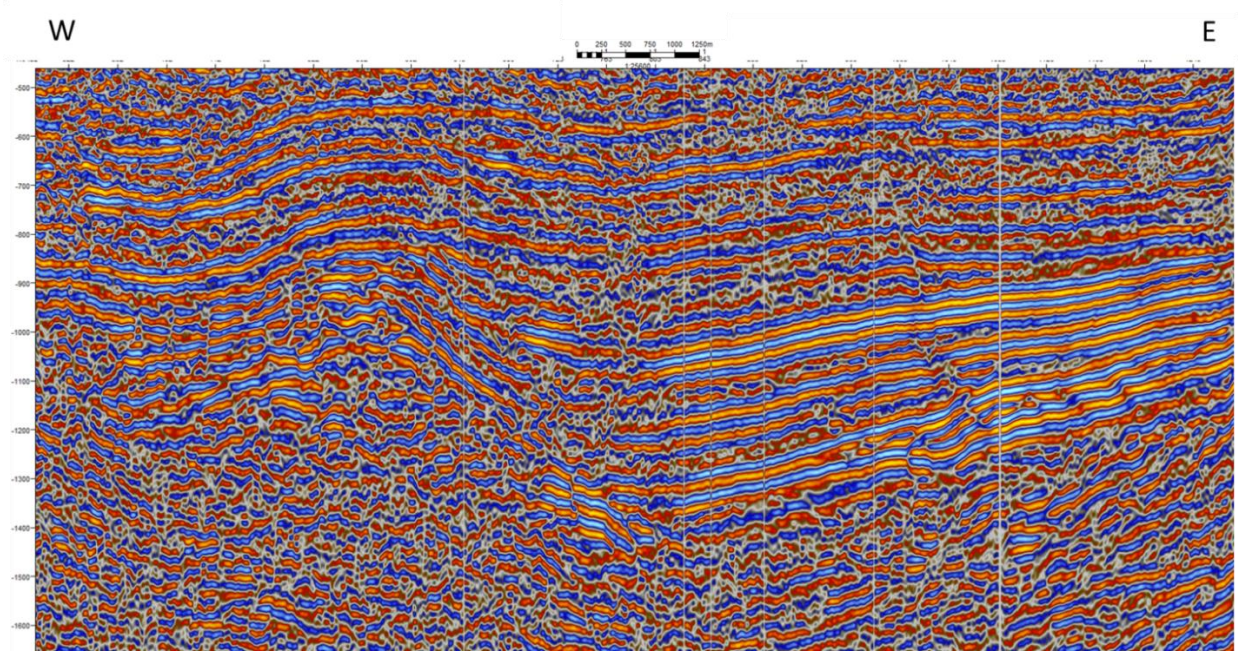

Figure 3.2 Detailed interpretation area of seismic 2D line NH8802-32.

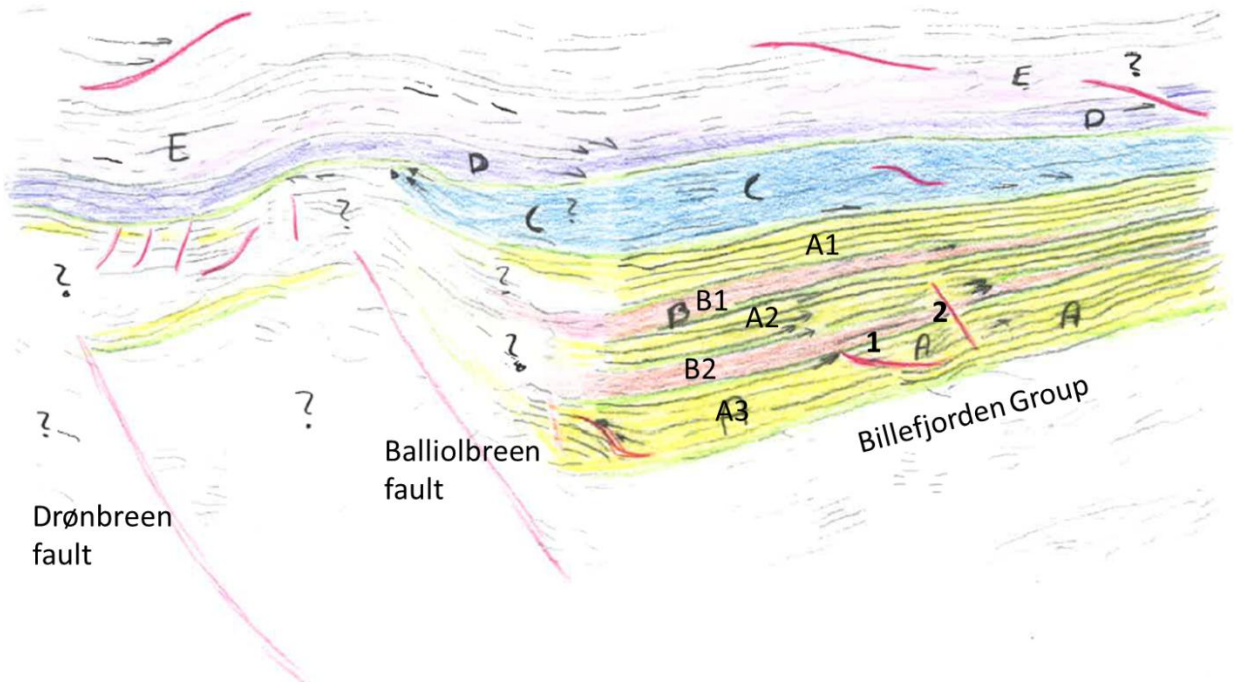

Figure 3.3 Main results of interpretation of line NH8802-32.

3.2 Lines NH8706-404 and NH8706-210

A) Brief description of the lines:

The 2D lines NH8706-210 and NH8706-404 are located offshore in Sassenfjorden and Tempelfjorden, respectively; as shown in Figure 3.4 that offers a map view of the two lines. Line NH8706-210 is roughly W-E trending, whereas line NH8706-404 is more SW-NE trending. I have made a composite line of these two lines at the point where they intersect with each other. For the most part the reflective pattern on both sides of the intersection is consistent between the lines. The interpretation is done separately and presented individually, and in Figure 3.11 the composite interpretation of the lines is presented. I have included the seismic composite line in the Appendix; see Figure 5.3 and Figure 5.4. The line NH8706-210 is close to the position of line ST-8515-121, which is interpreted by Bælum and Braathen (2012); see Figure 7. Note that I have concentrated on the area from the Drønbreen Fault (roughly the start of the Nordfjorden Block) and eastwards to the area where the line intersects with line NH8706-404.Hhere the interpretation continuous on line NH8706-404 (the cropped part of the lines is showed in Figure 3.6 and Figure 3.9).

B) Introduction to faults, folds, basin and cap rocks:

Line NH8706-210 from Sassenfjorden shows the Nordfjorden Block as a clearly visible high, and the formations are thinning towards it on both sides. I have indicated the position of the Drønbreen Fault and the Balliolbreen Fault in Figure 3.7. There are some anticlinal structures at the top of the Nordfjorden Block, of which two are rather clearly observed on the seismic, but there is a possibility of more anticlines to be identified had the resolution of the seismic line been better. These anticlines are discussed in Bælum and Braathen (2012), and are outside the scoop of this contribution.

The two master fault planes are interpreted to be where the reflectors terminate, and the seismic becomes noisy between the two master faults in the high standing Nordfjorden block. The reflectors towards the Drønbreen faults western side are dragged up along the fault plane, with an intermediate (-low) angle, and then the angle for the dragged reflectors gradually increases upwards. The reflectors terminating towards the Balliolbreen fault plane show no clear signs of significant drag up along the fault plane, other than the reflectors in the shallow facies termed K (further described in the following sections). Here the reflectors show steep angles close to the fault zone, and some are almost parallel to the fault plane in facies K.

There are important observations regarding major faults and basin fill on the 2D lines. In the basin east of the Nordfjorden Block there are also many boundary surfaces, some that could be regional and some less extensive. The reflective pattern in between the Drønbreen Fault and the Balliolbreen Fault (the Nordfjorden Block) is complicated, and accordingly challenging to interpret.

C) Identification and description of seismic facies

See Figure 3.7, Figure 3.10 and Figure 3.11 for the position of the seismic facies.

In the following description, the focus is predominantly on the area within the main rift basin east of the Nordfjorden Block. The intersection of the lines NH8706-210 and NH8706-404 is marked in the following figures, and the same colors for the facies are used where the lines cross and where the facies continues. The facies are labeled A – to K, starting from the top. A general observation is that the sequences A to J are thinning towards the NE.

Facies A is colored light grey and consists of a weak reflective package with variable thickness. This facies fills in between the Balliolbreen fault and a high standing block close to the seafloor. Past this high standing block, towards the NE, a new facies is identified (colored yellow). The reflectors in facies A close to the Balliolbreen Fault are not dragged, but deposited as a drape following the topography at the time of deposition.

Facies B has some long, persistent reflectors in an otherwise rather chaotic pattern. The strongest reflectors are closest to the underlying facies, facies C, and between these two facies I have marked a boundary surface. This surface is the bottom of facies K, and where facies K thins towards NE the reflectors in K terminate (possibly downlaps) onto this surface. Another reason for making this a boundary surface is the sudden change in reflector strength, from weak in facies K, to stronger where the boundary surface is marked. Facies B stops towards the same high standing block as facies A.

Facies C has reflectors that show possible fault truncation onto the fault in the west, and also thins towards the west. This reflector belt seems to have a monoclinal shape towards the fault. I have interpreted C and D as being separable as facies since the reflectors in C continues over the extensional fault to the west with a curved shape, whereas the reflectors in D terminates towards the same fault. There are some blurry areas in the seismic in facies C and D, especially close to and within the high standing block where several faults are marked. Both for facies C and D it applies that they could continue through this high standing block and further to the NE, thus underlying the yellow sequence here (NE of the block).

Between the facies D and E a boundary surface is identified where some reflectors in D downlap on this horizon, and there is an increase in reflectivity for this boundary surface.

Both facies E and F are identified in an area where the geology seems complex close to the Balliolbreen fault, but further to the NE the reflectors are easier to follow for both facies. They both seem to have trough-going geometry, thinning towards the E-NE. Between facies E and F there exist some kind of subtle boundary surface (only marked by a change of color from one facies to the next in the figures). This is seen as an increase in reflector strength for the surface in between E and F, no clear terminations of the reflectors are observed along this boundary. The reflector

strength in both facies E and F is generally weak, with some strong amplitude events occurring.

A very strong, thin reflector belt separates facies F from the underlying facies G. This reflector belt is marked as a boundary surface. Facies G has many strong reflectors, especially close to where the reflectors start to bend upwards, and some faults are marked in the interpretation. This increase in reflection strength could also be a tuning effect, where reflectors start to thin below tuning thickness and merge together.

Facies H fills in the lower part of the trough-structure below facies G. Beneath the facies H the seismic becomes rather chaotic. Facies G is deposited over a fault zone to the NE and the reflectors in facies H terminate towards the same bounding fault zone.

Facies K is present in the shallow part line NH8706-210 and is in contact with more than one boundary surface. This facies continues in the high standing Nordfjorden Block. The reflectors are characterized by weak amplitude response, except for where boundary surfaces are marked in contact with this facies, here the reflectors increase in strength. Also, close to the fault planes (Drønbreen and Balliolbreen fault planes). The reflectors are dragged up along the fault planes on both sides of the Nordfjorden Block, with highest angle on the north-eastern side of the high standing block (towards the Balliolbreen fault plane).

Facies I is found in line NH8706-210, between facies G and H. The reflectors in this facies show termination towards a bounding fault on the western side of the facies. The reflectors beyond this fault, further west, dip in the opposite direction, and also terminate towards this fault plane.

Facies J is present in line NH8706-404, beneath facies G. This facies thins from NE towards the fault zone it overlies, and is interpreted to disappear (-thin below tuning thickness?) approximately where facies H (early basin fill) is ending towards the fault plane marked. The reflector belt in facies J contain some strong amplitudes, but the majority of the reflectors are weak laterally.

D) Seismic facies versus stratigraphic units and lithologies for the NH8706 lines

(This part is included in the next section together with line NH8706-405)

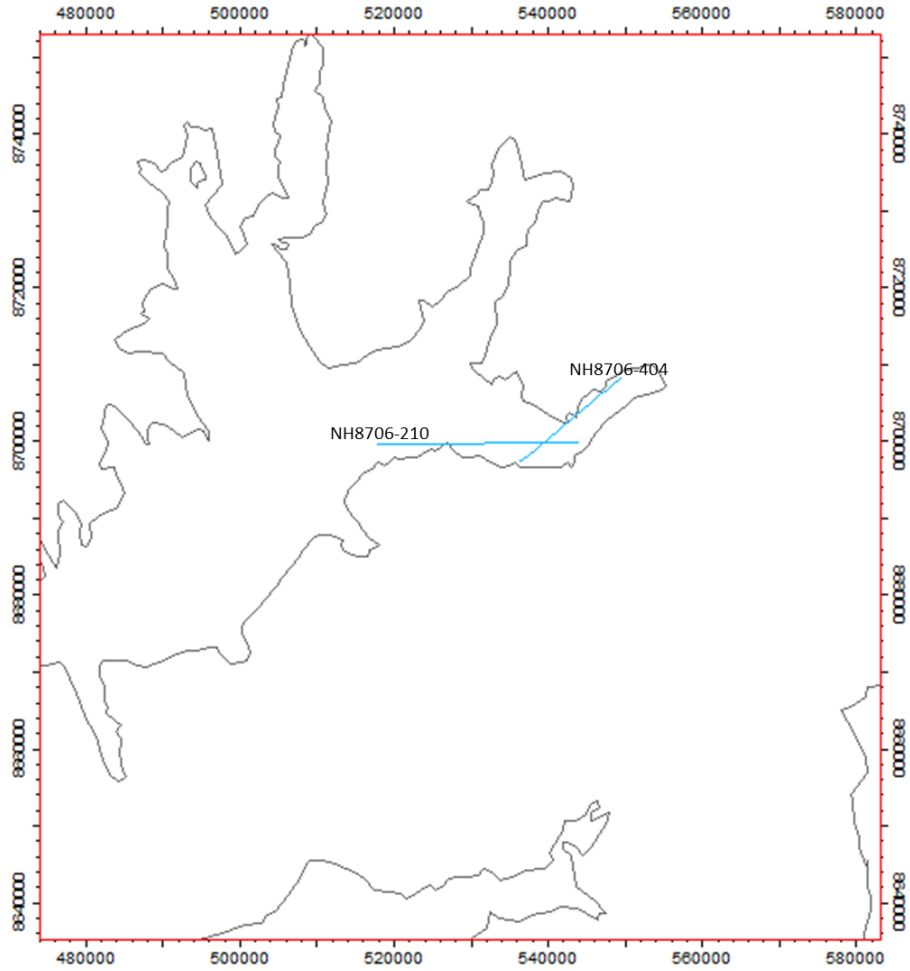

Figure 3.4 Position of lines NH8706-210 and NH8706-404 (note point of intersection) from offshore Tempelfjorden and Sassenfjorden.

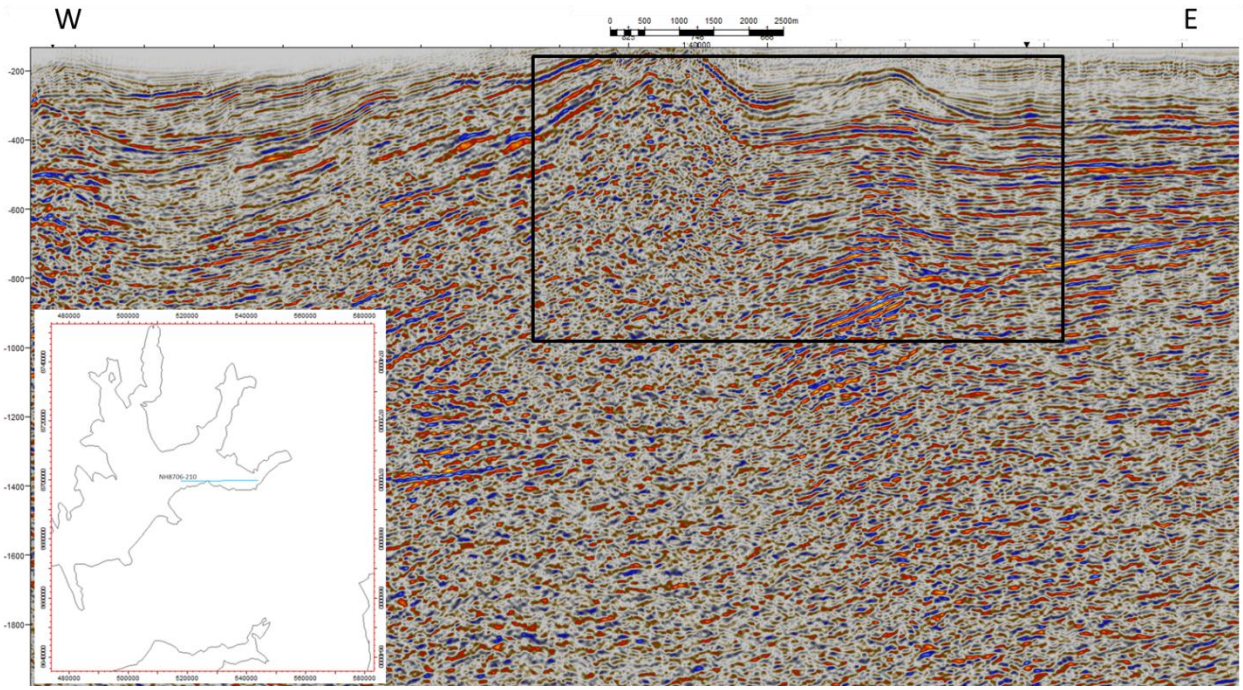

Figure 3.5 Seismic 2D line NH8706-210 with overview map.

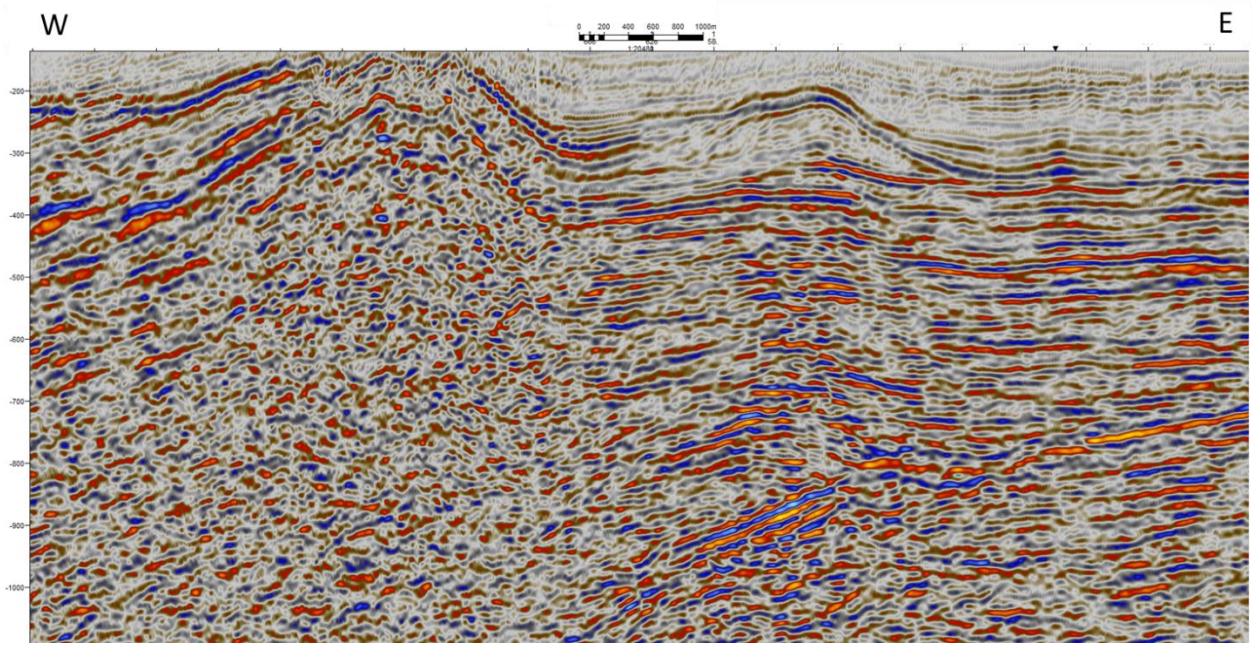

Figure 3.6 Interpreted area of seismic 2D line NH8706-210.

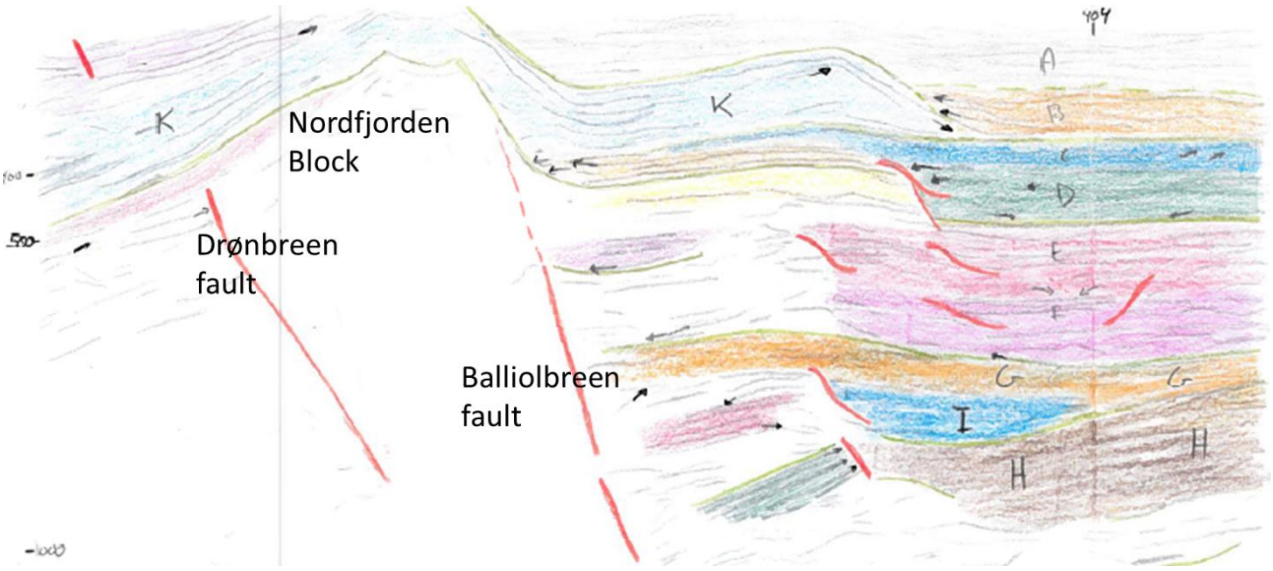

Figure 3.7 Main results of interpretation of line NH8706-210.

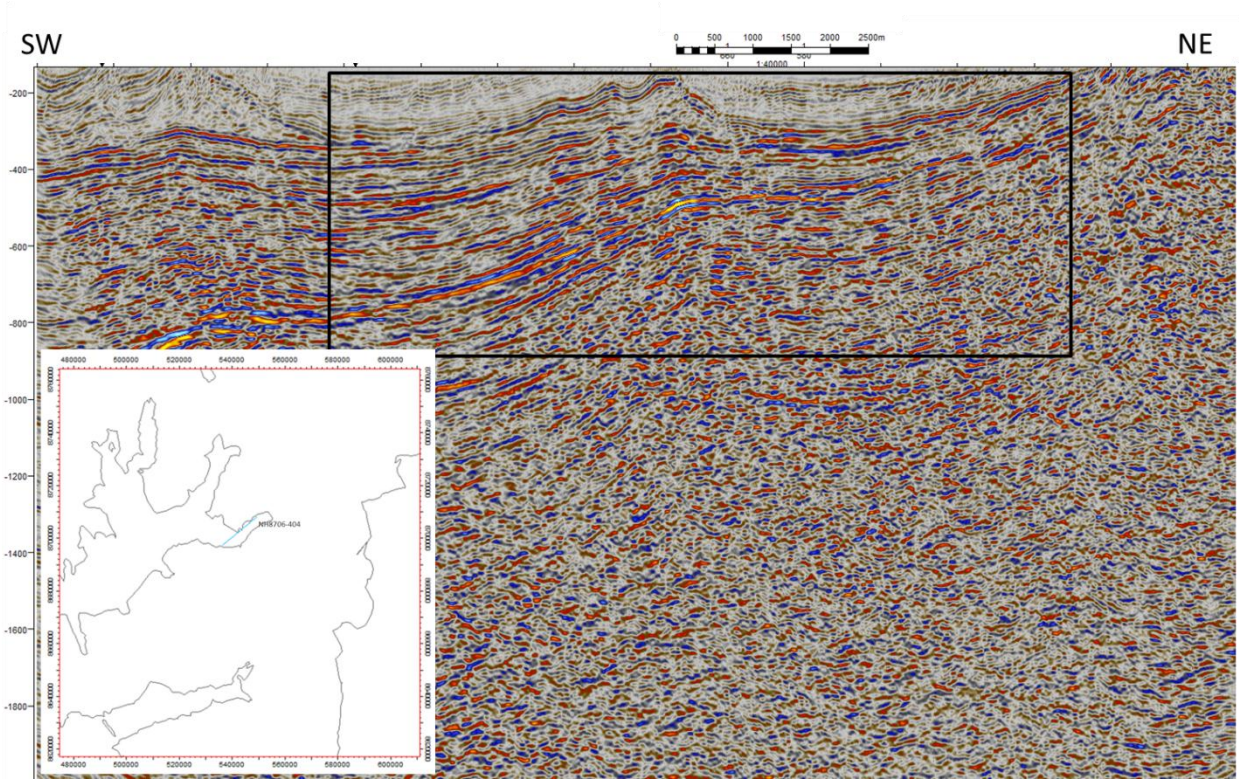

Figure 3.8 Seismic 2D line NH8706-404 with overview map.

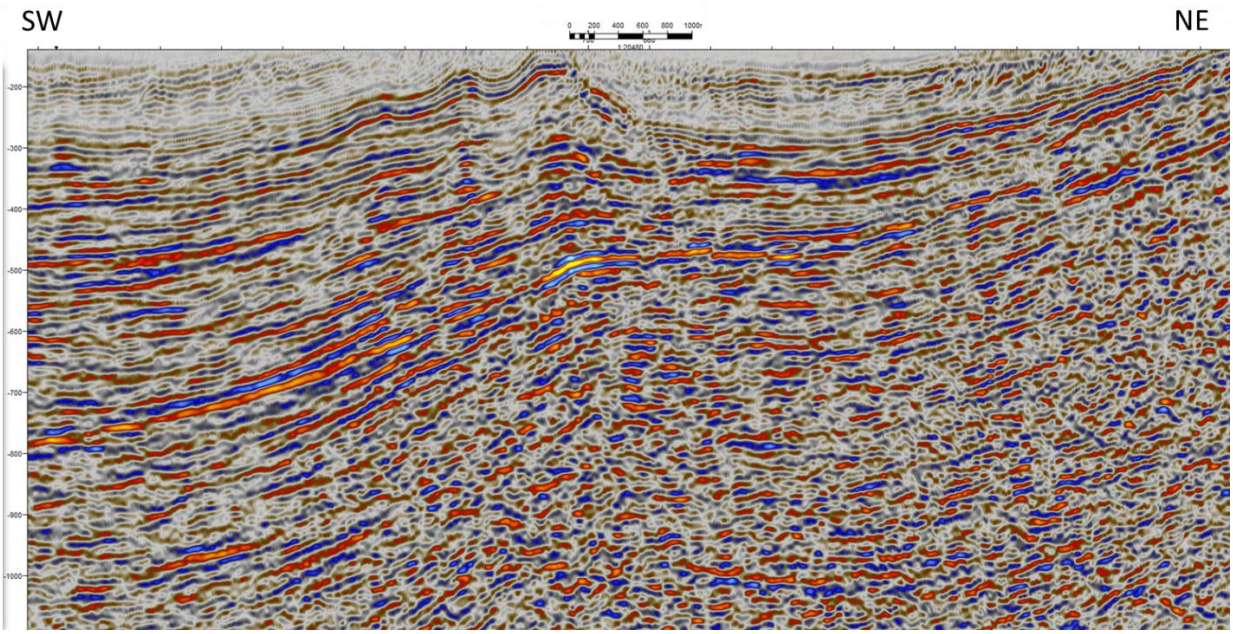

Figure 3.9 Interpreted area of seismic 2D line NH8706-404.

Figure 3.10 Main results of interpretation of line NH8706-404.

Figure 3.11 Main results of interpretation of lines NH8706-404 and NH8706-210 as a composite line.

3.3 Line NH8706-405

A) Brief description of the line

Line NH8706-405 is located offshore in Sassenfjorden and Tempelfjorden; see Figure 3.12 for map view. This is not a straight seismic line, but curving and following the fjord close to shore. From approximately the middle of the line (see Figure 3.13) this line is similar to the line NH8706-404 described above. There are several similarities between the lines NH8706-210 and NH8706-404. I have chosen to split this line in two when undertaking the detailed interpretation, to establish a higher content of details. Note that **Feil! Fant ikke referansekilden.** in the Appendix shows a composite of Figure 3.15 and Figure 3.18.

B) Introduction to faults, folds, basin and cap rocks

The Balliolbreen Fault is clearly visible, as is the wedge shaped rift basin east of the Balliolbreen Fault. This is similar to the area of the nearby seismic line NH8706-404 interpreted in the previous section. The reflector packages in the rift basin are also similar to the lines NH8706-210 and NH8706-404, for instance the facies with strong amplitudes inside the rift basin at roughly at the same depth. It is worth noting that reflectors close to the Balliolbreen fault are dragged up along the fault plane, and the angle increases upwards. The Drønbreen fault is not as clear as in line HN8706-210, and the reflectors in between Drønbreen and Balliolbreen faults are fairly straight and undisturbed with an upwards dip eastwards.

This is a curved 2D seismic line, and therefore the distance between the Drønbreen Fault and the Balliolbreen Fault is exaggerated.

C) Seismic facies description

I have tied together the two figures by identifying and color the same seismic facies and boundary surfaces at the place of intersection between lines, continuing them from part 1 to part 2. The seismic facies are termed A to –F, and some additional observations 1-3 for part 1 of the interpreted line.

The top of seismic facies A is not a clearly visible boundary surface, and this shallow part of the seismic is likely to be affected by noise and a variable seafloor topography together with noise generated from the fjord sides. This facies consists of a weak reflector package, and also show some chaotic patterns with dipping reflectors. The facies stops towards the Balliolbreen fault plane, and thins out towards the east where reflectors terminate, and a new facies is observed (in purple). Between the facies' A and B I have interpreted a boundary surface marked with green, due to abrupt change in the reflector pattern from facies A to facies B, and some downlapping reflectors in facies A onto this surface.

Seismic facies B shows increased reflector strength compared to facies A, and the reflectors are easy to follow laterally eastwards away from the Balliolbreen fault

plane. The thickness of the facies is fairly constant, and the reflectors show a slight curved shape with low angle updip to the east.

Reflectors in seismic facies C have many of the same characteristics as facies B has. An overall thinning eastwards is observed for the facies, but the reflector pattern in the eastern part gets more complex.

Seismic facies D show downlap reflectors onto the contact with facies E. The surface between facies' D and E has very strong amplitudes, and could be a lateral intrusion-which would explain the high amplitudes not found above or below this thin reflector belt/surface separating facies E and D. Also, volcanic intrusions are known to occur in this area (Alvar Braathen; Personal communication, 2012).

Seismic facies E has both strong reflectors and some more transparent areas in the seismic. The facies thins towards the eastern part of the line.

Seismic facies F has a stretched sigmoidal-oblique shape in between facies C and D and eastwards its thickness is more or less constant, except for possible thinning of the facies in an area all the way to the east of the interpreted part where the reflector belt becomes challenging to follow. The indications of a boundary between facies F and the facies C and D, is the direction of the reflectors in D which downlap onto the surface between facies D and E, and reflectors in F follow the shape of facies D, but deviate from the direction of the downlapping reflectors

In part 1 of this line (see Figure 3.15) the area marked with numbers from 1-3 will be further described. Site number 1 is in a shallow area where the reflectors dip in several directions, and there are reflection terminations for the boundary surface above and below (marked in green), arrows mark the terminations. There could be erosional surfaces associated with the terminations of the reflectors.

Site number 2 is a facies with both strong and weak reflectors associated with the high standing block west of the Drønbreen fault, and the facies wedges towards the Balliolbreen fault. The reflectors close to the Drønbreen fault is dragged up along the plane.

Site number 3 is a facies where the reflectors show some drag pattern up along the Drønbreen fault plane, and the reflectors in this facies are slightly increasing in strength towards the east and the Balliolbreen fault-this could be a tuning effect where the reflectors merge together when the facies is thinning.

D) Seismic facies versus stratigraphic units and lithologies for the NH8706 lines

When following the interpretation in Bælum & Braathen's (2012) Figure 7, the following formation tops and groups can be proposed for the seismic lines of the Sassenfjorden -Tempelfjorden area: The Gipsdalen Formation could be equivalent to at least the upper part of the K facies in line NH8706-210 and facies A in line NH8706-405. The Wordiekammen Formation has late-syn rift or post-rift status in this area (e.g., Bælum & Braathen, 2012), and the top of the Wordiekammen Formation is likely found within facies K, at about 300 ms TWT close to the Balliolbreen Fault for

line NH8706-210. For line NH8706-405 this is equivalent to the bottom of facies A- Top Wordiekammen roughly corresponds to the transition between facies A and B. The top Minkinfjellet Formation is interpreted to be at approximately 400 ms depth close to the Balliolbreen Fault, which corresponds to an identified boundary surface above facies C in line NH8706-210/404 and the boundary between facies A and B in line NH8706-405. The top Ebbadalen Formation is predicted at about 550 ms depth close to the Balliolbreen Fault, and could correspond to approximately the top of facies E (where there is a prominent boundary surface) and top of facies C in line NH8706-405. Accordingly, the Ebbadalen Formation could basically match facies E and maybe also include facies F in line NH8706-210/404. In line NH8706-405 this corresponds to the facies' C, D and F. The facies G in line NH8706-210 /404 and facies I (small basin filling facies) in line NH8706-210 could be part of the Hultberget Formation, where the top of facies G is the approximate horizon for the top of the Hultberget Formation. In line NH8706-405 this roughly corresponds to facies E, where top Hultberget Formation then would be expected as the boundary surface separating facies' D and E. The top of the Billefjorden Group is believed to be consistent with facies H in line NH8706-210, potentially continuous all the way towards the Balliolbreen fault, and the top of H would in that case end up at about 1000 ms depth at the point of contact with the Balliolbreen Fault. In line NH8706-405 the Billefjorden Group does not seem to have a clear top surface, and for the seismic below facies E the reflectors are challenging to follow laterally.

As seen regionally, the Billefjorden Group continuous down to the metamorphic basement (e.g., Braathen et al. 2011).

There are some complex monoclinal lenticular shapes and fault structures just east of the position of the Balliolbreen Fault which makes the sequences challenging to follow from the Balliolbreen Fault and eastwards. The amount of throw of present faults here cannot be accurately determined with the limited information the 2D lines offer.

When comparing with the lithology proposed for the identified link between formations and facies for line NH8802-32, a link between the identified seismic facies and lithology is also suggested here: As for line NH8802-32, the interpretation of the NH8706 lines indicates that all reflector belts of striking similarity, with similar seismic amplitude response and geometry, also have similarity in lithology, even though I acknowledge this could be the cause of other effects. There are significant lateral changes in many of the facies in general, and so the lithological composition proposed could be varying from east to west on the interpreted section of the seismic. The NH8706 lines interpreted show similar reflector packages for the facies proposed to be the Wordiekammen Formation (similar characteristics as facies C in line NH8802-32). Hence, the lithology is likely carbonate, and micritic towards the base, as suggested for the Wordiekammen Formation in line NH8802-32 (Braathen et al., 2011; Maher & Braathen, 2011).

The thick, well-bedded sequences found as basin fill eastwards from the Balliolbreen Fault (facies B-F in line NH8706-405 and facies B-G in line NH8706-210/404) is likely to comprise thick marine carbonates, or thick sandstones (such as fan deltas and alluvial fans which can be expected for this area), and more heterolithic units of evaporites, carbonates and siliciclastics likely to be occurring in these facies. With lateral changes in the sequences, a change of lithology can be an explanation.

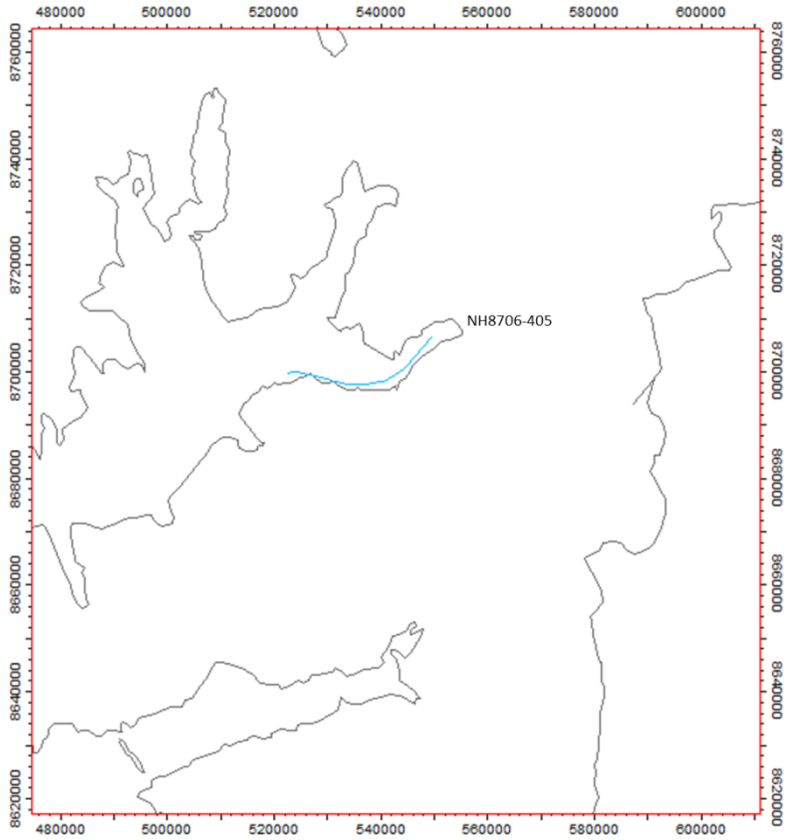

Figure 3.12 Position of line NH8706-405 from offshore Sassenfjorden.

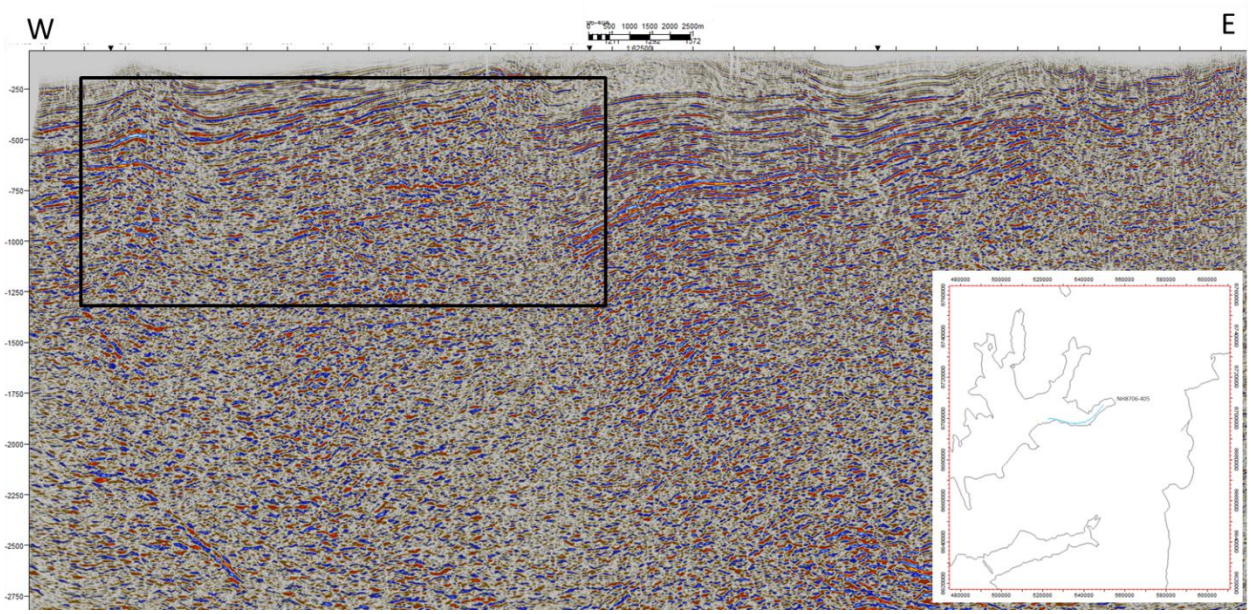

Figure 3.13 Seismic 2D lines NH8706-405 with overview of first part area interpreted.

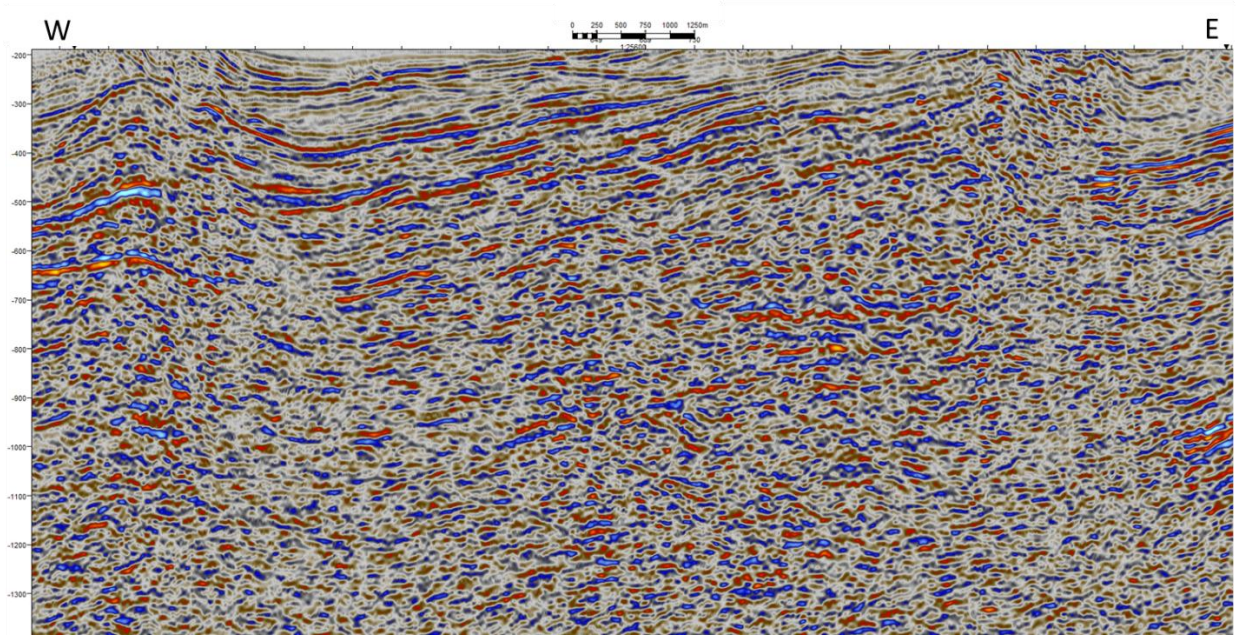

Figure 3.14 Interpreted area of seismic 2D line NH8706-405, first part.

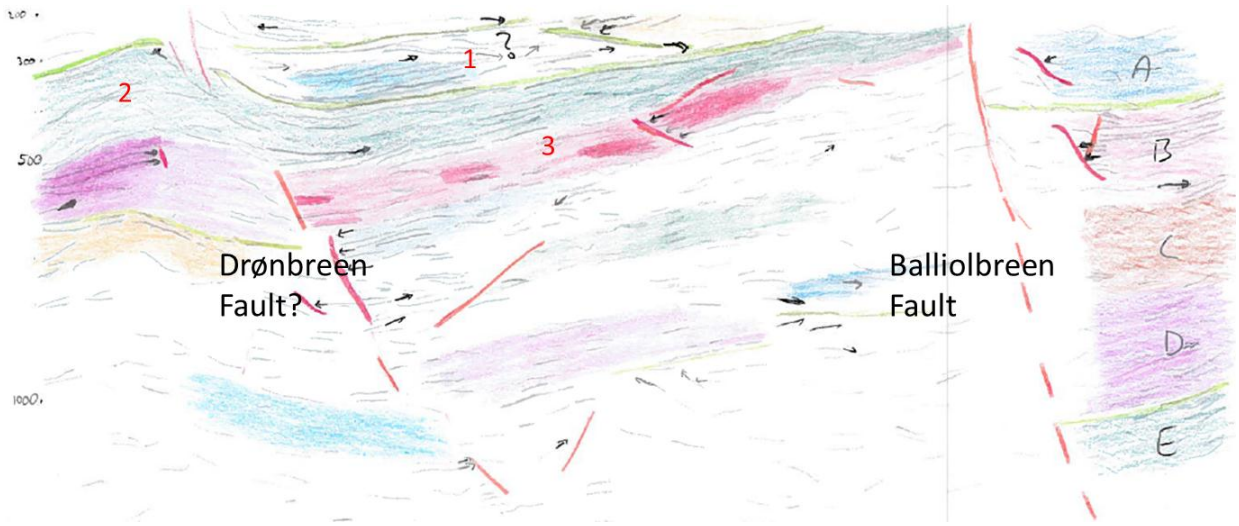

Figure 3.15 Main results of interpretation of line NH8706-405, first part.

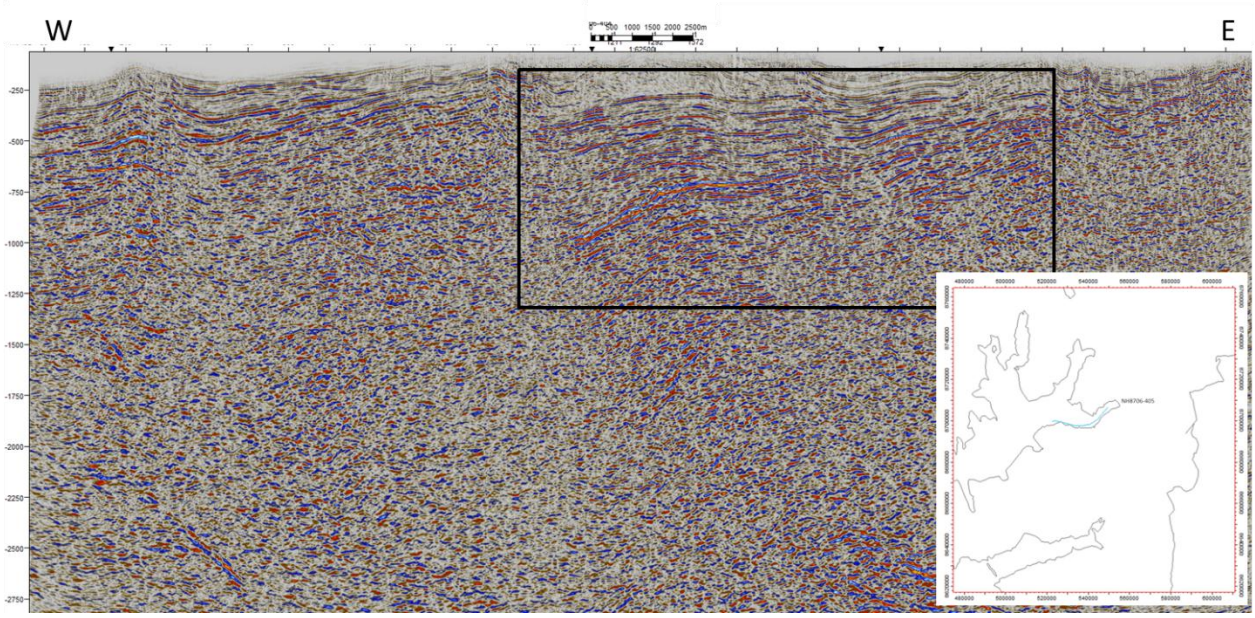

Figure 3.16 Seismic 2D lines NH8706-405 with overview of second part area interpreted.

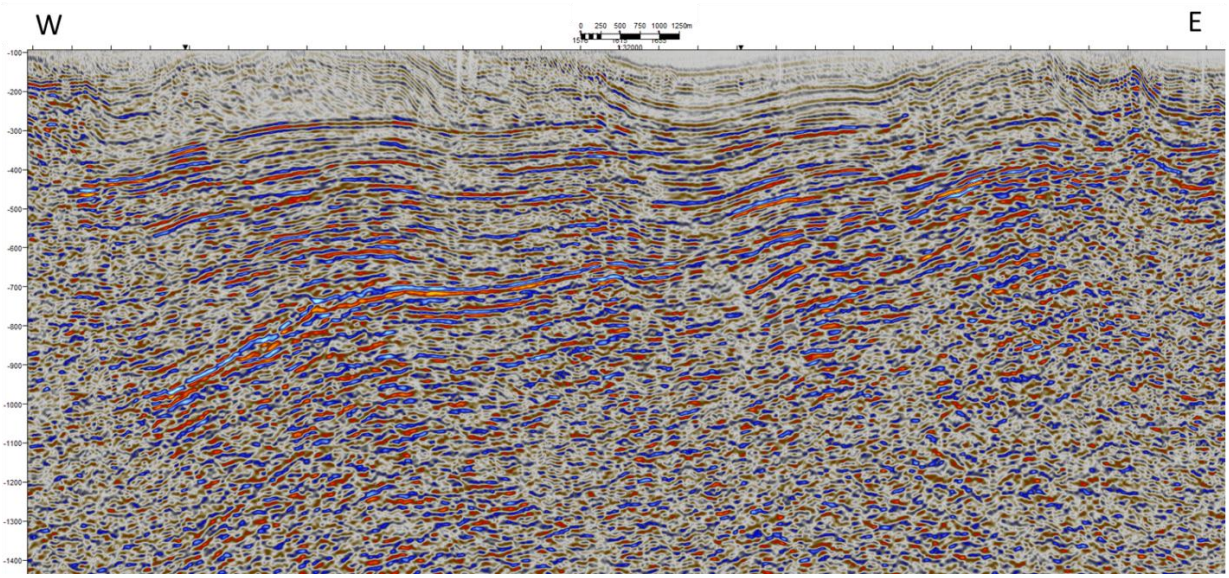

Figure 3.17 Interpreted area of seismic 2D line NH8706-405, second part.

Figure 3.18 Main results of interpretation of line NH8706-405, second part.

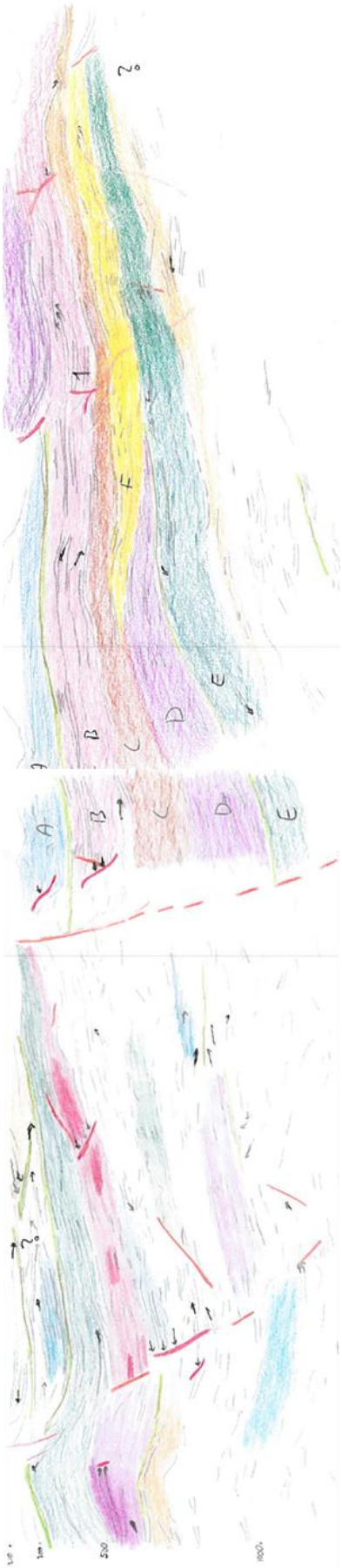

Figure 3.19 Main results of interpretation of line NH8706-405.

3.4 Line 2045-92 A

A) Brief description of the line

Line 2045 92 A is from a 2D seismic dataset from Eastern Svalbard, in Figure 3.21 the line is located in map view and the studied segment positioned.

The quality of the seismic at times can be very poor and have misleading artifacts (side sweeps etc. from frequently occurring intrusions).

B) Introduction to faults, folds, basins, and cap rocks

Faults with listric geometry and hanging wall growth basins are suggested for the Triassic succession of this dataset, in the studied window. The detailed analysis outlines several fairly convincing examples of tectonic activity. In the same area, nearby to the north, a well-expressed clinoform system, with a northerly vergence, can be mapped out. The clinoforms unravel a steep and upward curving shelf edge trajectory, as indicated with a black curve in Figure 5.21.

Listric faults and growth faults are common for the Triassic basin area this dataset covers, and there are a number of good examples of this faulting activity for this line.

The main feature for the faults is believed to be growth faults and listric faults.

C) Description of seismic facies and boundaries

The interpreted near top Permian reflector is just below the study area of this line, as shown in Figure 3.22. The overall dip direction of overlying reflectors is northwards, except for the lower part (just above the near-top Permian reflector) where reflectors dip southwards beneath a boundary surface. Several seismic facies have been identified, labeled A to F in Figure 3.24. There are evident boundary surfaces that restrict the spatial extent of the seismic facies. Further, there are some belts of strong, dipping reflectors separated by reflectors with less clear signature, allowing a subdivision of facies belts.

Seismic facies A is a belt of strong reflectors which mainly are slightly dipping towards the north (note 2D). Abrupt lateral terminations suggest the facies belt is interrupted by faults, cutting through the belt in some places.

The reflectors in seismic facies B are less pronounced than in seismic facies A. The reflectors in B show a more wavy characteristic than in A, and they are also partly weak and scattered. Laterally, the amplitude strength varies, but no trend is observed, mostly weak amplitudes are seen for the reflectors in facies B. At places facies' A and B seem to interfere/interfinger, as shown by the arrow in Figure 3.24. Overall, B is thicker in TWT than A.

Seismic facies C (dark brown) is a very thin facies, characterized by weak horizontal reflectors. C is restricted to what is interpreted as a small basin bound by two low angular faults and facies A can be found to each horizontal side of this basin.

Seismic facies D (purple) is found above seismic facies C, and is characterized by changing amplitude strength of the reflectors, although the majority of the reflectors

are weaker than for instance facies A. The lower part of D could be an upper fill of the same basin as seismic facies C.

Seismic facies E is found in between two boundary surfaces and is interpreted to be thickening towards the north. E is characterized by strong reflectors, and the reflectors at the base of E show onlap onto the boundary surface here. The top of facies E is marked by another boundary surface, where the above-lying facies show onlap/downlap in the transition. There seems to be a fault zone coming up into E, and the upper part of facies E is continued further north. Hence, the biggest part of the reflectors in facies E terminates towards this fault, whereas the upper part bypasses the fault, continuing into the footwall.

Seismic facies F has reflectors which dip northwards, and most have strong amplitudes. F is thinning northwards, and is limited by boundary surfaces above and below. The surface above is recognized by a change of dip in the reflectors, there are also examples of termination of reflectors onto the top of F. The surface below F is recognized where some of the reflectors show downlap. There are also some listric faults marked coming up into F.

Seismic facies G is characterized by some very strong reflections where it is adjacent to facies B.

Seismic facies H has straight, horizontal reflectors, and some strong amplitudes towards the top of the facies. A listeric fault with clear reflector terminations and offset reflectors is the limiting factor for this facies.

Seismic facies I is interpreted to be a local facies in between two listeric faults. The reflectors have strong amplitudes and are tilted up northwards. The reflectors in this facies show termination towards the faults on both sides.

There are several evident boundary surfaces (in green) that restrict the spatial extent of the facies as well as listric and growth faults which can have an effect on the temporal and spatial development of the facies; see Figure 3.24. The boundary surfaces identified for this line is mainly determined by downlap/onlap and a change of dip in reflectors. Starting at the bottom, the boundary surface at the bottom of facies F could be an erosional surface, some of the underlying reflectors terminate with a steep angle towards this surface. The next surface is between facies' G and F where reflectors in G onlap onto this surface, though the reflectors are in general weak and hard to follow laterally for both facies' F and G. Above facies A and facies C another boundary surface is marked. This is based on the change of reflector characteristics, as well as onlapping reflectors onto this surface from the above-lying facies' B (?) and D above facies C. The last two surfaces are above and below facies E. Facies E shows onlap onto the surface below, and above E there is termination of reflectors in more than one direction onto the boundary surface here, some chaotic reflector patterns can be seen above facies E.

D) Link between seismic facies, formations and lithology

Facies A, with its strong reflectors slightly dipping towards the North, could be siliciclastic material interrupted by faults that cut through some places. Heterogeneous channels offer an explanation for the seismic signature towards the top where the reflectors increase in strength. Facies A is interpreted to be a prograding delta sequence.

I have marked especially one extensive low angular fault in facies B, which may indicate weak lithology, and together with low reflectivity this could be a shaly facies - lower energy environment than in facies A. So fault geometry (low angular faults) combined with seismic facies signature indicates facies B is a delta-front sequence.

Seismic facies C sits as late infill in a basin, and could be thin-bedded lithologies or even prodelta mud.

Seismic facies D is separated from C due to that D is deposited after C has filled in the small basin (boundary surface in between C and D where reflector pattern change slightly). The weak, horizontal layered reflectors indicate low energy depositional environment and lithology with high shale content, similar seismic response as facies B, and is possibly also a delta front sequence.

The lower reflectors in seismic facies E onlap onto a boundary surface southwards, opposite of the prograding delta sequences. The strong reflectors point in the direction of competent lithologies like siliciclastic sandstone. E could be a heterogeneous channelled sequence.

Seismic facies F is a chaotic (dip of reflectors change) and spatial limited facies (boundary surfaces at top and bottom of F), and could be a local facies (point bar?).

Seismic facies G could be a heterogeneous, channeled facies, the reflector strength increase significantly upwards.

The weak, horizontal layered reflectors in seismic facies H indicates low energy depositional environment. The low angle of the listric fault cutting the reflectors is also consistent with weak, layered lithology.

Seismic facies I could be clastic basin infill (local small basin in between listric faults).

On this line there are good examples of prograding clinoform sets, with direction of progradation in northwards direction. The stacking of the clinoform sets is nearly vertical in the lower part before curving and becoming significantly more lateral in the upper part. This suggests an earlier phase of nearly true aggradation, followed by a series of clinoforms that filled accommodation space that was already in place (Høy & Lundschien, 2011). This early aggradation event could have several reasons, but with the observed faulting nearby, a possible explanation is that faulting temporally arrested the shelf-edge progradation. This could cause deepening of a nearby basin off the shelf, that later was filled as the fault system was bypassed.

On this line there are good examples of prograding clinoform sets, with direction of progradation (note 2D) towards the North. The stacking of the clinoform sets is significantly more lateral than vertical. This suggests that the accommodation space

was already in place before the sediment infill was deposited (Høy & Lundschien, 2011).

The reflectors near the bottom of the interpreted area (beneath facies F) show some discontinuity and listric/growth faults may have relocated the facies here. Since the Botneheia shale succession is expected to be found near the Top Permian horizon (which is just below the interpreted area, see Figure 3.22), facies F could be part of the Tschermakfjellet Formation, prodelta shales which comprise the lower foreset to bottomset for clinoforms of Anisian-Ladinian age. This also applies for facies H, and possibly facies G as well.

The prograding reflector belts (for instance facies A and B) are consistent with that the accommodation space was already in place before deposition (Høy & Lundschien, 2011), and is interpreted to be part of the De Geerdalen Formation, which can be categorized as shallow marine to continental deposits, basically of coastal affinity, and dominated by sandstone, of Carnian age. Also facies' D and E could be part of the De Geerdalen Formation.

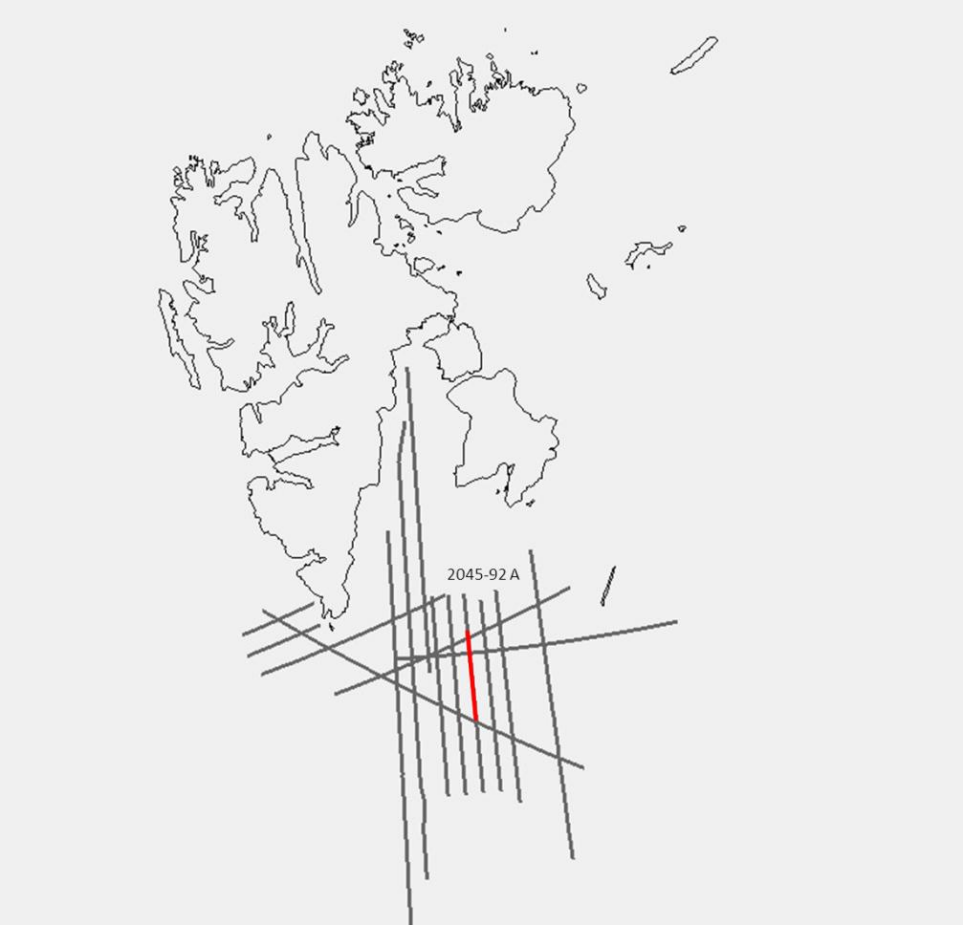

Figure 3.20 Position of line 2045-92 A from offshore Eastern Svalbard. The red line represents 2D seismic area showed in the following figure.

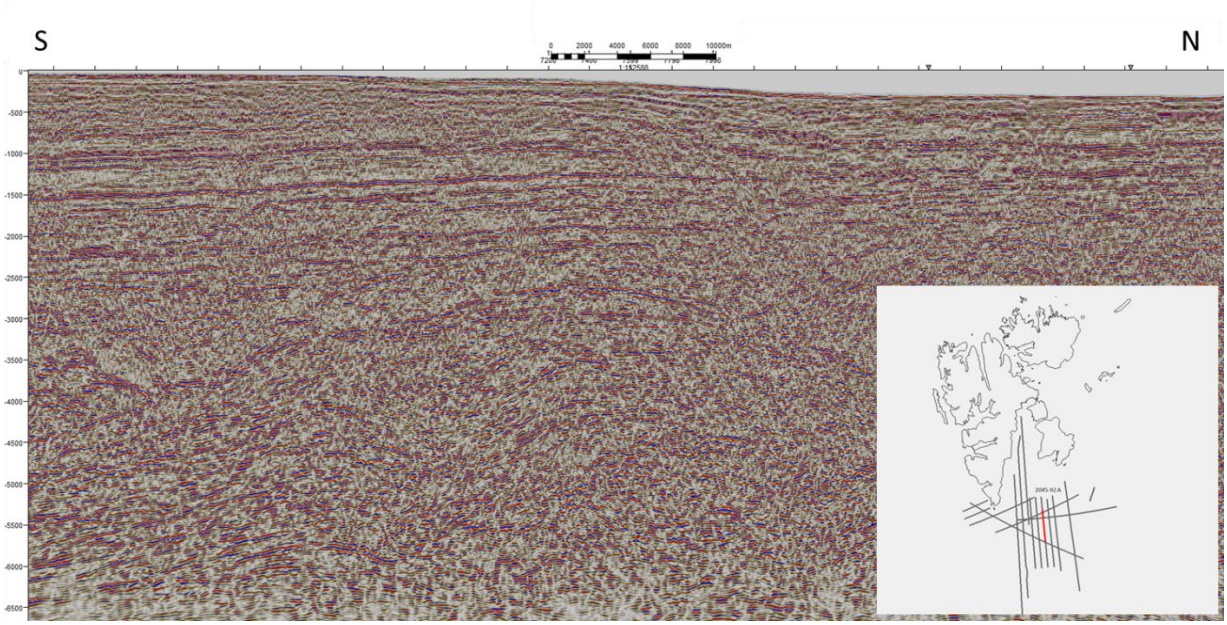

Figure 3.21 Seismic 2D line 2045-92 A with overview map.

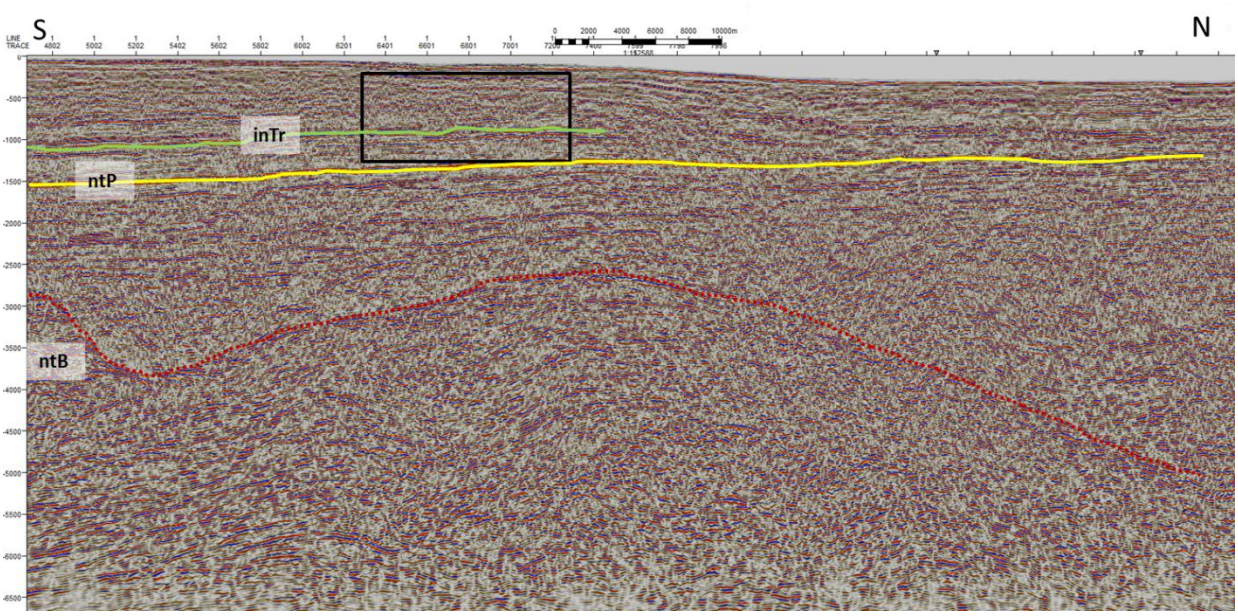

Figure 3.22 Seismic 2D line with overview of area interpreted. Near top basement, near top Permian and intra-Triassic horizons are indicated.

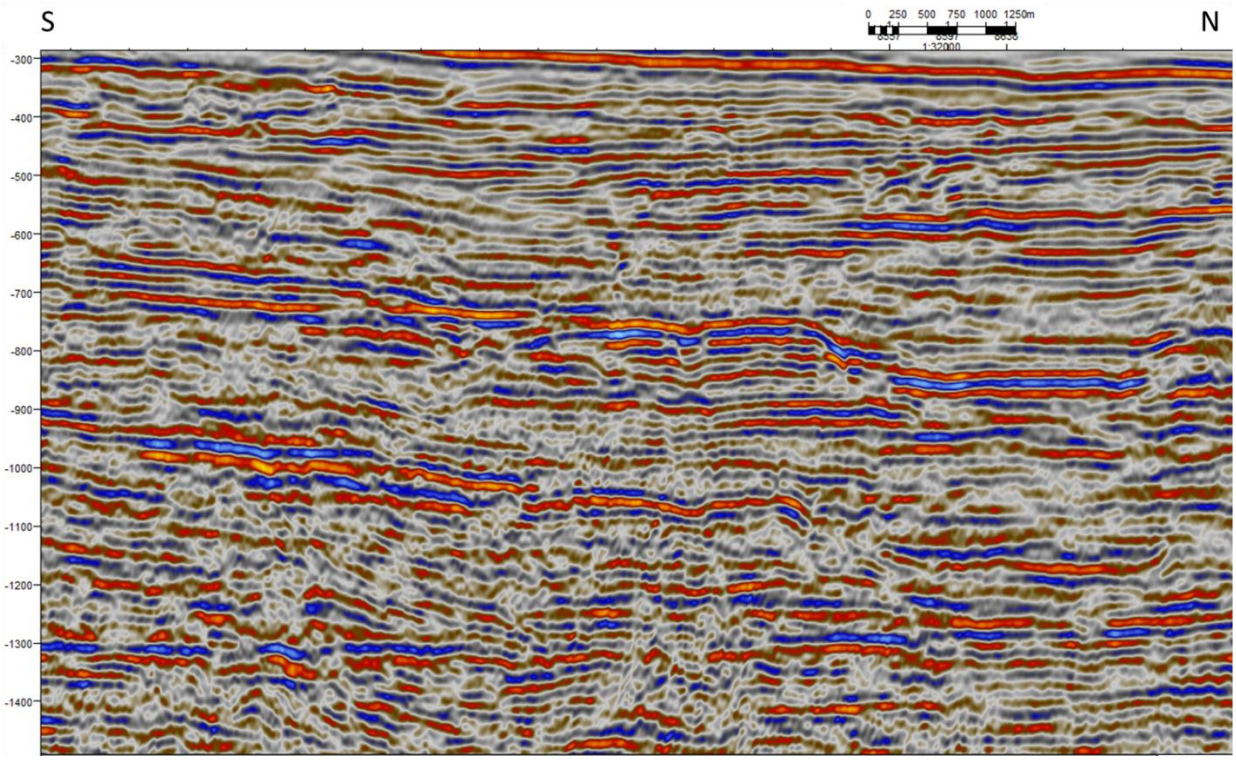

Figure 3.23 Detailed interpretation area of seismic 2D line 2045-92 A.

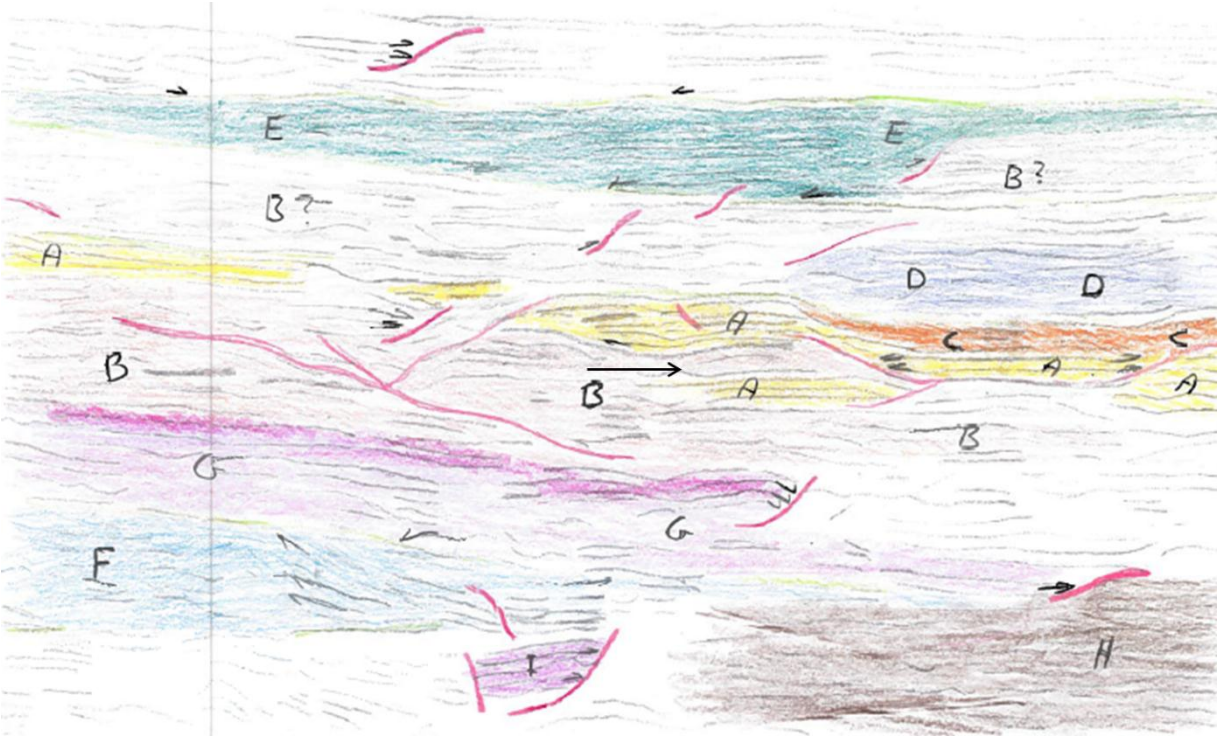

Figure 3.24 Main results of interpretation of line 2045-92 A.

3.5 Line 2300-81

A) Brief description of the line

See Figure 3.25 for position of this seismic 2D line from Eastern Svalbard. The seismic has relatively low resolution in general, and there seems to be some fault areas also affected by noise artifacts (vertical blurry zones, see Figure 5.5 in the Appendix). Still, the Triassic fault activity is highly visible in this line, and the area chosen for interpretation shows some interesting examples; see Figure 3.27.

B) Introduction to faults, folds, basins, and cap rocks

There is a lot of fault activity in the Triassic part of the basin on this line, this is particularly evident laterally for the seismic facies' A and B, and also on a small scale in general there are many faults in the interpreted section. In Figure 3.27 I have indicated an intra-Triassic reflector (inTr) and a near top Permian horizon (ntP). The facies show a slight dip towards the North, more pronounced dip of the facies close to the approximate top basement reflector at the southern end of the line.

C) Identification of seismic facies:

Three facies are identified, which will be described in the following section named A-C, in addition some interesting site observations are commented which are numbered 1-4; see Figure 3.28. There are more facies colored in addition to facies A, B and C, especially in between A/B and C, as can be seen in Figure 3.28. In the cropped interpreted area there are two main belts of strong reflectors, one of which is beneath the interpreted near top Permian horizon and facies A.

Numbered observations (site 1-4) and the facies' A-C can be seen in Figure 3.28.

Seismic facies A is a band of strong reflectors, expanding or splitting up southwards in my interpreted area (varies on the line in general). Where the seismic facies expands, the amplitudes between is less reflective than the thinner seismic facies more towards the north, and this is interpreted to be seismic facies B, which is possibly a part of an expanded seismic facies A.

Seismic facies C is interpreted to be between two boundary surfaces, and is disturbed by faults (about in the middle of the seismic section interpreted). This seismic facies seems to be thinning on both sides towards a high made by faulting roughly in the middle of the seismic facies. Also the top boundary surface is interpreted to be a near top Permian (ntP) reflector. The seismic signature for this seismic facies is weak, but directly below there are some strong reflectors. Site number 1 is seismic facies A in between two bounding faults. These faults (or fault zones-blurry seismic) have a curved shape.

Site number 2 is within seismic the facies' A and B where the strong reflector belt (seismic facies A) splits into at least 3 thinner strong belts, and in between the seismic signature is less reflective (seismic facies B).

Site number 3 is in seismic facies C just beneath the near top Permian horizon. There are clearly visible downlapping reflectors onto the marked boundary surface defining the bottom of seismic facies C.

Site number 4 is in an area of discontinuous reflector patterns (faulting activity), some continuous horizontal reflectors can be observed in between the faults, and seismic facies C is interpreted to extend just above this fault area as a thinner seismic facies, as a drape.

D) Link between seismic facies, formations and lithology

Facies A with strong and prograding reflectors is likely to have little shale content, for instance heterogeneous channeled facies, and prograding delta environment. Facies B in between reflectors of facies A have a more smeared appearance, and could represent more shaly lithology than A, and hence less energy in the depositional environment. The facies' A and B are interpreted to be shallow marine to continental sandstone of the Carnian De Geerdalen Formation.

The area of the seismic in the middle of the section between facies' A/B and C is likely to contain more shale than the facies A due to less clear reflectors and chaotic appearance, and thus reflect a depositional environment with lower energy than prograding delta, possibly prodelta shales. Between the ntP surface marked on top of facies C and facies A the facies' here are interpreted to be the Tschermakfjellet Formation, and hence of Anisian-Ladinian age (about 1300 ms-2000 ms for the interpreted section).

The seismic signature of facies C is characterized by strong bright reflectors for the bounding reflectors at the top (ntP) and bottom, but more smeared expression in between. Since facies C is close to the ntP, it is also likely to associate C with the deep marine black shales of the Botneheia Formation of Anisian (-Ladinian) age.

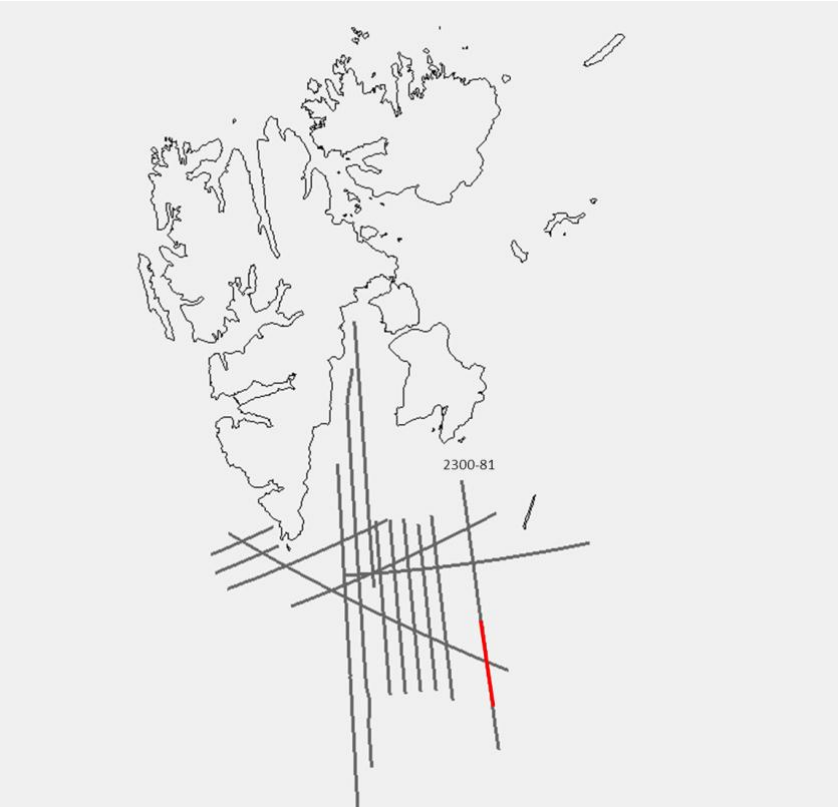

Figure 3.25 Position of line 2300-81 from offshore Eastern Svalbard. The red line represents 2D seismic area showed in the following figure.

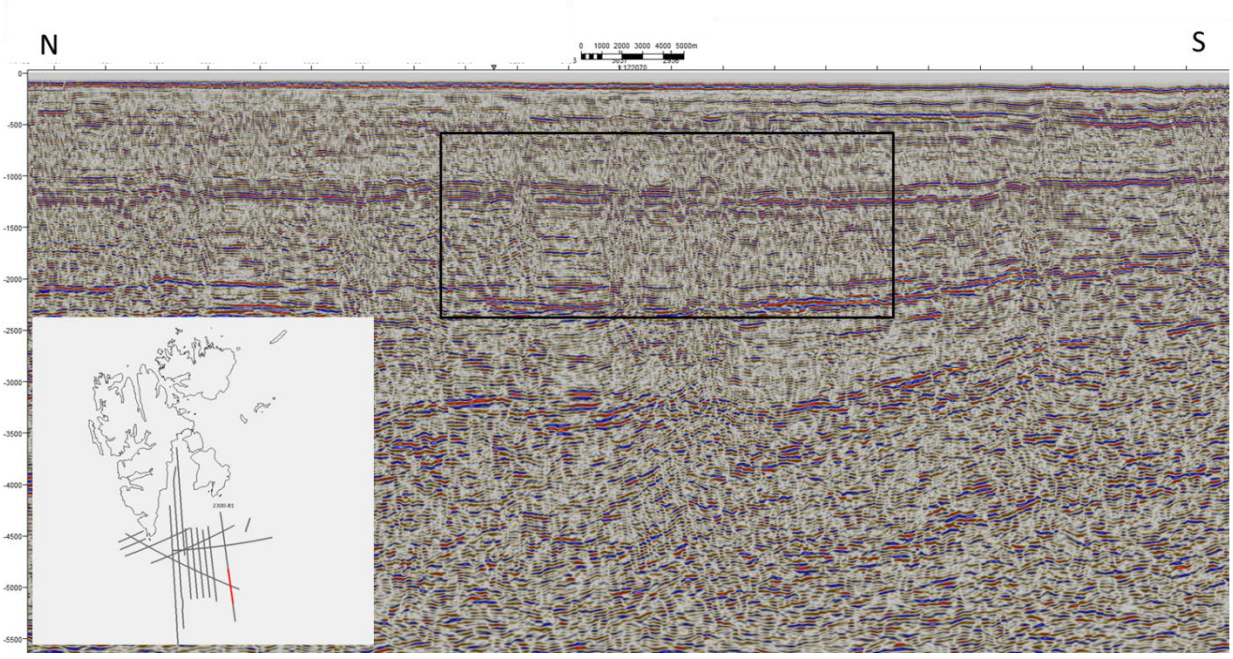

Figure 3.26 Seismic 2D line 2300-81 with overview map.

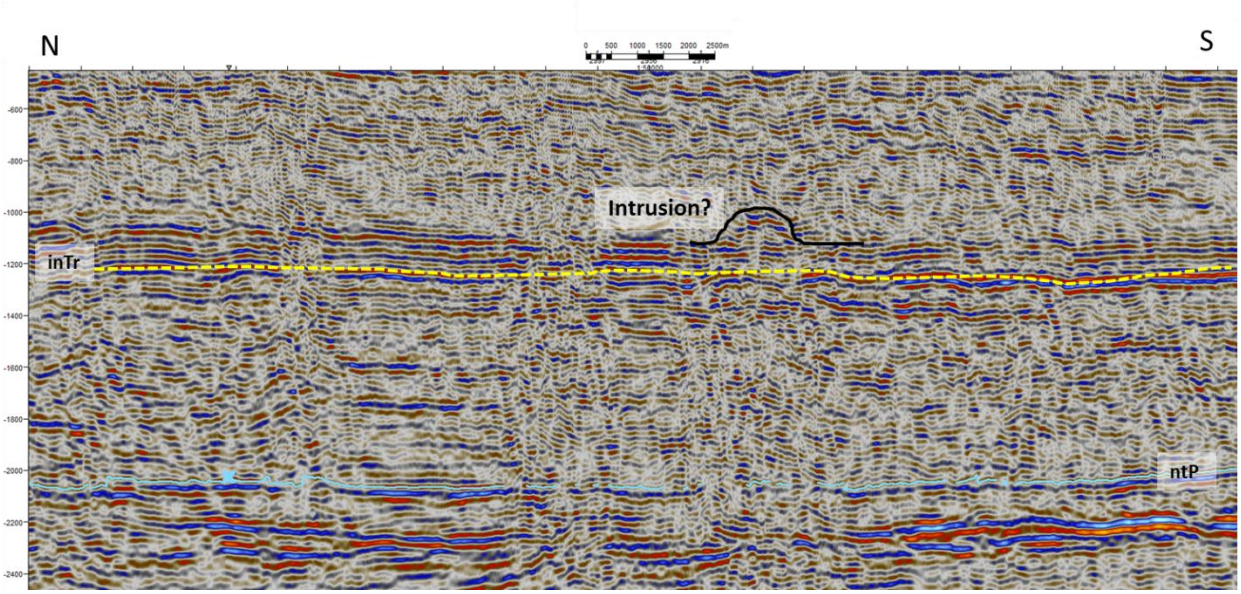

Figure 3.27 Some additional observations on seismic 2D line 2300-81, same area as in the previous figure.

Figure 3.28 Main results of interpretation of line 2300-81.

3.6 Line 2145-92

A) Brief description of the line

This line is nearly N-S oriented and has approximately the same orientation as the two previous lines; see Figure 3.29 for position in map view. The red part of the line outlines the part of the seismic section showed in Figure 3.30. This is a complex seismic section, with potentially intrusions that affect the quality of the seismic (strong reflectors which are laterally continuous). These intrusions can cause complex reflections, noise and multiples.

B) Introduction to faults, folds, basin, and cap rocks

Listric faults and growth faults are common for the Triassic basin area this dataset covers, and there are several good examples of this type of faulting activity for this line.

The start and end point of the faults interpreted were at times challenging to decide, due to complexity of the lines. The seismic facies identified are labeled A-G, as shown in Figure 3.32. The interpretation of this line with regards to seismic facies A, B and C offers many details. In order to explore some of these details, some site numbers are added in Figure 3.32. At these locations, more detailed descriptions are given, offering several sub-seismic facies.

C) Identification of seismic facies

The seismic signatures for the interpreted section show well-defined, continuous and very gentle north-verging monoclinal shape for the topmost seismic facies' A and B.

Seismic facies A is characterized by wavy reflectors with strong and clear amplitudes.

Seismic facies B is characterized by wavy reflectors, slightly less amplitude strengths than in facies A, but they both have similar shape of the reflector packages. There are several blurry zones in facies B, with listric faults marked, and local small basins may have developed accordingly (facies G).

Seismic facies E is characterized by changing reflector strength (a few very strong reflectors close to the boundary surface directly beneath E). There are some listric faults limiting the spatial distribution of E.

Seismic facies F is characterized by wavy reflector belts, as in the facies' A and B. The strength of the reflectors in F is seen as alternating bands of strong and weak reflectors stacked on top of each other.

Seismic facies G is in between two bounding faults, where the reflectors show drag up along the fault planes (on both sides). The strength of the reflectors is generally weak, but a few reflectors have strong amplitudes, approximately in the middle of G.

For the lower seismic facies' C and D the signature is characterized by less continuous reflectors and a distinct change in the dip domain compared to A and B. The monoclinal structures in the seismic facies' A and B vs. the more horizontal reflectors

in facies' C and D can best be observed in Figure 3.31 (together with Figure 3.32 for comparison with the seismic facies).

There are 3 major boundary surfaces identified which are persistent throughout the interpreted area of the line, marked in green; see Figure 3.32.

Starting at the bottom, the boundary surface here marks the bottom of seismic facies D. There is a very strong amplitude where the green surface is marked, especially to the south. I have not marked any onlap or downlap reflectors associated with this boundary, the reflectors directly above and beneath are chaotic, and much weaker than the strong reflection of the boundary.

The next surface is marked where there is a change of dip direction for the reflectors, also the reflectors beneath the surface are fairly straight, and above the surface the reflectors have wavy shape. The last surface marks the top of facies A, and is marked on a very strong amplitude reflection. The reflectors immediately above the surface are laterally straighter than the wavy facies A.

D) Link between seismic facies, formations and lithology

The interpretation of this line with regards to some of the thicker facies, where there is a lot of details, is probably too general. Some site numbers are put on in Figure 3.32, where more details in the facies are addressed, the facies could be consisting of several sub-facies.

From approximately the boundary between facies' A and B and upwards there is continuous onlap onto strong reflectors, in the reflector belts between. This is flooding surfaces with progradational small clinoform systems.

Signs of Triassic faulting activity are suggested by truncations and offset of the reflector bands of seismic facies' A and B, with associated rather complex reflections from what likely are small/shallow growth basins. At the base of seismic facies B, there is a distinct down-N downlap onto the boundary surface towards facies C.

The seismic facies' C and D are dipping very gently towards the south. This difference in dip direction at the top of facies C a possible erosional (hiatus?), along the boundary surface is marked in green. They could maybe be split into several thinner sub-seismic facies.

On a more detailed level, several observations suggest faulting and basin formation. In the following, four numbered sites will be further explored. Site number 1 is found in an area where reflector truncations suggest there could be two steep, oppositely dipping faults that sole out in seismic facies B. In between the faults, a shallow extension basin in the shape of a fairly symmetrical graben can be mapped out. Most reflectors around this area are strong and continuous, but some smeared and blurry zones can be seen especially toward the faults.

Site number 2 is above a possible growth fault close to the lower part of seismic facies C, again indicated by the sharp truncation of reflectors and a potential basin in

the hanging wall. This basin resembles a shallow lenticular shape, where the reflectors of the basin infill has a chaotic appearance.

Site number 3 is either directly below, or within seismic facies B. Identified faults continue downward towards the underlying boundary surface, but do not offset this marker.

Site number 4 is close to a low-angle, reflector cutting fault that soles out in seismic facies C. This fault could continue further down into seismic facies D where there seems to be another similar fault. These faults dip in the same direction, but the lower fault is steeper. If connected, the composite fault consists of two strands. When exploring this area in even greater detail, there are many small truncations of reflectors, offering signs a complex fault zone. In valid, there are many smaller faults in addition to the larger faults marked in the Figure 3.32.

Starting at the bottom, the deepest marked boundary surface in Figure 3.32 (bottom of facies D) is interpreted as the near top Permian horizon which should then be close to the deep marine black shale of the Botneheia Formation., Hence facies D is likely of Anisian-Ladinian age, and could comprise the transition between Botneheia and Tschermakfjellet formations. D is interpreted as being prodelta shales, consistent with the Tschermakfjellet Formation and the seismic signature of facies D.

Facies C is also interpreted to be part of the Tschermakfjellet Formation-prodelta shales.

As of facies E the Carnian De Geerdalen Formation is believed to start, and continue up to the top of facies A. The seismic signatures for these facies' are consistent with the lithology of De Geerdalen-shallow marine to continental sandstone dominated lithologies.

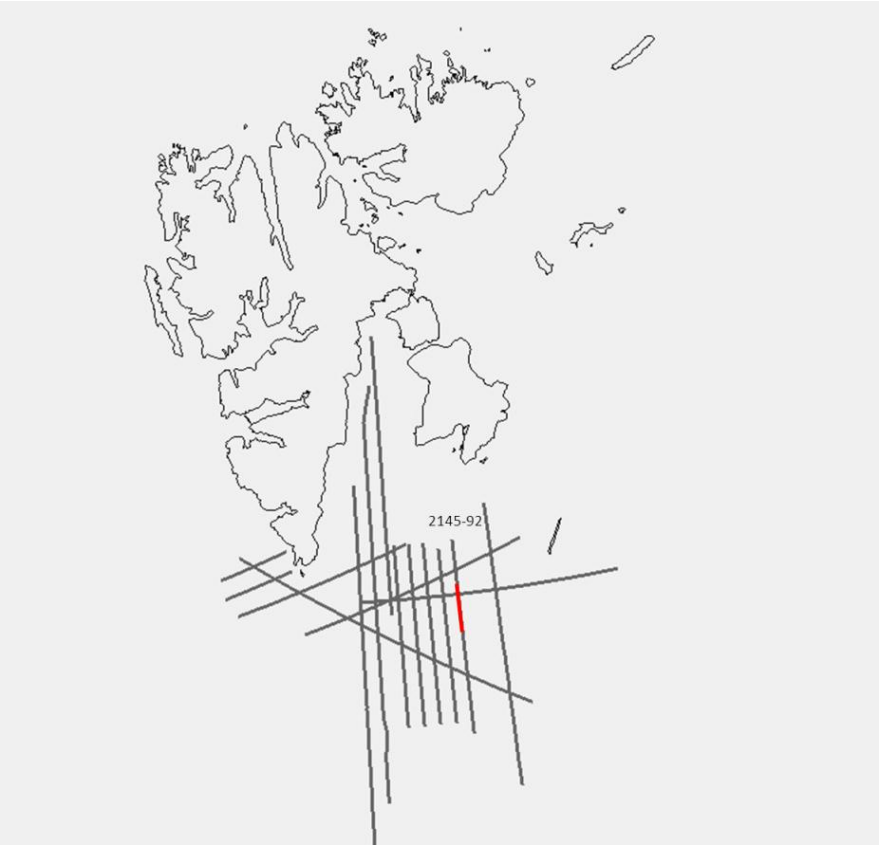

Figure 3.29 Position of line 2145-92 from offshore Eastern Svalbard. The red line represents 2D seismic area showed in the following figure.

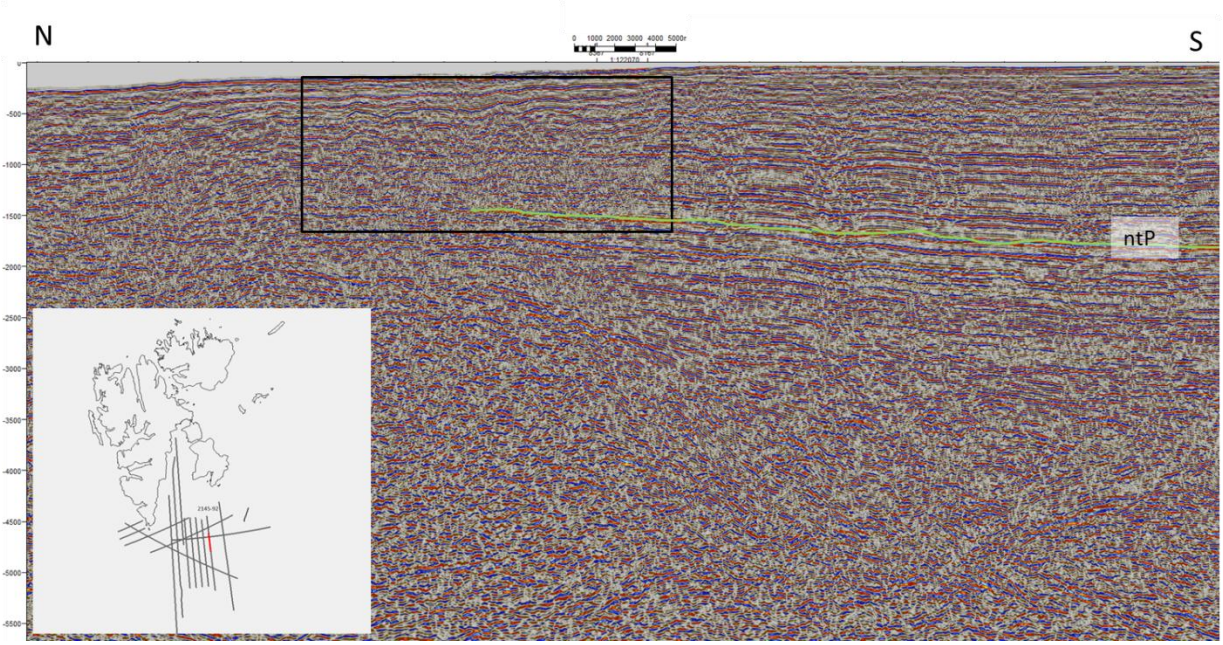

Figure 3.30 Seismic 2D line 2145-92 with overview map.

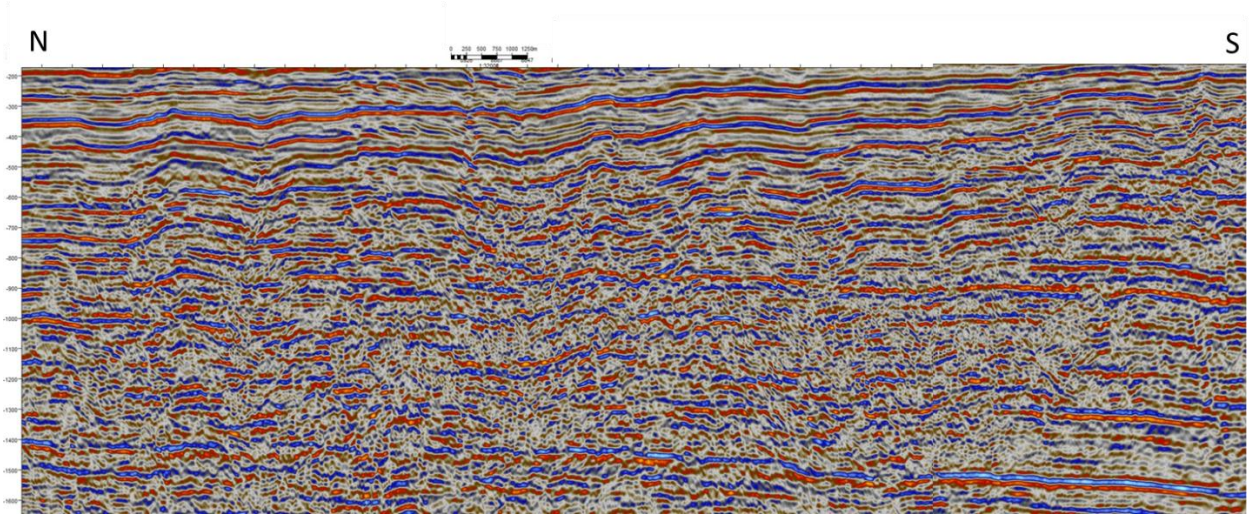

Figure 3.31 Interpreted area of seismic 2D line 2145-92.

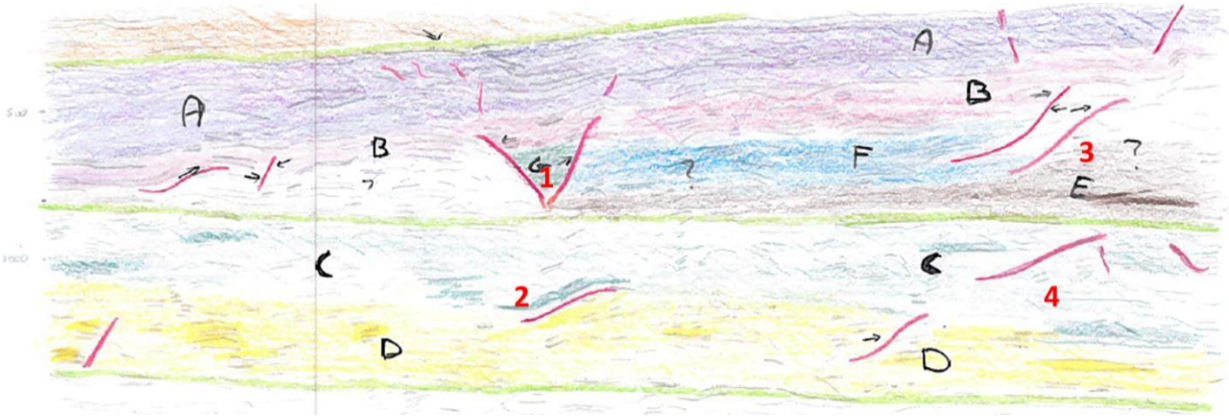

Figure 3.32 Main results of interpretation of line 2145-92.

4. Discussion and conclusions

4.1 Carboniferous rift basin(s) of Central Spitsbergen

As outlined in Chapter 2, the seismic dataset is from the Sassenfjorden - Tempelfjorden area and another line is from Reindalen. All lines are approximately E-W oriented, all crossing the N-S trending Billefjorden Fault Zone, with the middle-upper Carboniferous Billefjorden Trough in the eastern hanging wall basin. This basin is asymmetric, deepening towards the master fault segments in the west, showing half-graben geometry. The depth of the basin is at places as much as 2500 m in the west, thinning and finally wedging out over 20-30 km eastward (Bælum and Braathen 2012). The basin fill reflects interaction between fault movement and basin fill (e.g., Johannessen and Steel 1992; Maher and Braathen 2011; Braathen et al. 2011), with geometries and fill characteristics common for growth fault basins (Braathen et al., 2011; R. Gawthorpe & Hardy, 2002; R. L. Gawthorpe & Leeder, 2000; Jackson et al., 2006; Sharp et al., 2000).

The Billefjorden Trough is the result of a complex basin evolution history, as proposed with the reconstructions of Braathen et al. (2011). Outcrop studies in the northern Billefjorden area shows a basin that changes basin depocenter geometry, from a lenticular shape to a wedge shape and then back to a lenticular shaped basin. As debated in Braathen et al. (2011), these changes may have several causes, but seem partly controlled by varying weak (evaporites) and stiff lithologies (sandstones, carbonates) and their spatial thickness. However, the fundamental geometry comes from either; 1) fault movement, or 2) fault-tip monocline growth. The former would enhance a wedge-shaped basin deepening towards the fault with distinct truncation of bedding, whereas the monocline would offset the basin away from the fault, with a growth basin potentially onlapping the monocline, as seen from classic cases of for instance the eastern Suez Rift (Sharp et al. 2000; Jackson et al. 2006).

The syn-rift succession of the Hultberget, Ebbadalen and Minkinfjellet formations (Gipsdalen Group) are restricted to the Billefjorden Trough, and can also partly be found east of the Billefjorden Fault Zone's western margin, within the blocks of the Billefjorden Fault Zone (Bælum & Braathen, 2012). The Hultberget Formation is mid Carboniferous in age and is believed to mark the initiation of the rifting, whereas the post-rift (immediate post-rift) Wordiekammen Formation is Late Carboniferous to Early Permian in age. However, new evidence advocates the lower Wordiekammen to be involved in the basin-forming event, suggesting a status of this succession as late syn-rift (Maher and Braathen, 2011; Braathen et al. 2011).

<u>Reindalen line:</u>

The fundamental pattern of wedge – and lenticular-shaped basins is a basic observation that would be expected to be discernible in the Billefjorden Trough seismics. For instance, the reflector geometric patterns are very intricate in the Reindalen line, and the discussion around results of correlation with the well drilled here (position of well in Figure 5.1) and reflectors, as presented in Bælum & Braathen (2012), suggests that the faulting initiated on the Balliolbreen fault, whereas the western Drønbreen fault became

activated at a later stage. The Balliolbreen fault truncated the pre-rift Billefjorden Group and accommodated the first rift fill, the lower Ebbadalen Formation. This unit was successively folded up along the fault plane, suggesting development of an early fault-tip monocline. Then, close to the fault, the above-lying angular contact at the base of the overlying succession of the middle Ebbadalen Formation could either be reflecting a lenticular depocenter and/or a shear zone in evaporites, as documented from the basin father north (Maher and Braathen 2011). At the same time, a deeper wedge-shaped depocenter developed in the hanging wall of the Drønbreen Fault to the west, which now had become active (Bælum & Braathen, 2012). This growth section experienced drag-folding into a gentle syncline, which gradually developed in the rift fill next to the fault. Subsequently, both faults seem to have been active, with basin development and deposition of the lower Hultberget Formation. However, this interpretation is questioned by an erosive surface that developed across the uplifted fault block shoulder in the footwall of the Balliolbreen Fault (Bælum & Braathen, 2012), challenging a link for this level across the high-standing block. After this event, faulting was focused on the Drønbreen Fault.

To summarize the points above, a dominant depocenter with a lenticular shape is present in the basin east of the Balliolbreen Fault throughout the entire basin development. The basin sitting in the hanging wall to the east of the Drønbreen Fault contains two wedge shape successions, correlated with the upper Ebbadalen and upper Minkinfjellet formations times, as outlined in Bælum and Braathen (2012). Between the wedging events the lower parts of Minkinfjellet and Wordiekammen formations show depocenters with lenticular shape. As discussed for the Pyramiden area (Braathen et al. 2011), when major fault segments joined and thereby focused deformation, such as the link between the Odellfjellet fault and the Balliolbreen fault across the Pyramiden relay zone, basin floor subsidence was likely enhanced in parallel with the development of a wedge-shaped basin (e.g., Bælum & Braathen, 2012). Using this wedge-shape as a guide for enhance fault-driven subsidence, two such fault-focusing events can be indicated for the Reindalen line; during the upper Ebbadalen and Minkinfjellet formation times.

Following the description of the Pyramiden area by Maher and Braathen (2011), the geometry of the depocenter shape is believed to be partly controlled by the rift fill. Weak lithologies, for instance evaporites, can trigger the formation of fault-tip monoclines. This is because evaporites are known to give a low fault-throw to propagation ratio (e.g., Sharp et al., 2000). Also, the variable compaction for clastic sediments, carbonate and evaporites cannot be depreciated regarding a possible effect on the geometry. Gypsum may, during transition to Anhydrite, compact significantly more than what is common (or even possible) for other lithologies. For the Reindalen line, similar geometry as described for the Løvehovden depocenter is observed on for the depocenter in the seismic line NH8802-32. The basin fill in the depocenter west of the Balliolbreen Fault plane also has dominant lenticular geometry, and together with very strong reflectors, is believed to have a very high content of evaporites. The depocenter in the hanging wall of the Drønbreen Fault has a more complex shape with combined wedge-lenticular geometry; this suggests lithologies like

sandstones and carbonates. Also, the basin between the Drønbreen and Balliolbreen faults is closer to the basin margin, and therefore closer to the clastic source area. Accordingly, alluvial fans would be expected to impact the basin in the hanging wall of the Drønbreen fault, and less so for the Balliolbreen Fault, which is more distal to the source area. The block between the Drønbreen and Balliolbreen faults is tilted, and partly eroded on the crest. This crest would have contributed to restrictions in the basin drainage and sediment flux, and potentially causing less siliciclastic sediment input into the basin in the hanging wall of the Balliolbreen fault. The majority of sediments into this basin are believed to have come down the hanging wall dip-slope, from the east towards the Balliolbreen Fault (Bælum & Braathen, 2012). The distinct reflector facies A1 is corresponding to the Minkinfjellet Formation, A2,3 and B1,2 corresponds to the Ebbadalen Formation and facies' C and D corresponds to the Wordiekammen and Gipsdalen formations, respectively (see Figure 3.3). Lithologies has also been proposed for the facies', see Chapter 3.1. This facies classification is consistent with the interpretation of the same formation tops in Bælum and Braathen (2012).

The depocenter geometry of this line suggests that a fault-tip monocline formed at three stages, consistent with seismic facies B1 and B2 and C, which all show related lenticular basin shapes. –For seismic facies' A1, A2 and A3 there are only mild thinning to the east. Accordingly, they reflect more regional infill, which may also have been present in the terrace in the hanging wall of the Drønbreen fault, and later removed by erosion of a high-standing block. Overall, the A1-3 reflector facies is suggested to be caused by thick, well-bedded units giving significant velocity contrasts, such as thick marine carbonates, or thick sandstone sections such as alluvial fans and fan deltas. The B1-2 reflector facies could be significantly more heterolithic, with changing evaporites, thin carbonates and siliciclastics. For facies C, the thicker unit with syn-rift affinity is likely micritic carbonate of the lower Wordiekammen Formation, as proposed by Maher and Braathen (2011) and Braathen et al. (2011).

Sassenfjorden-Tempelfjorden lines

The associations between identified seismic facies and formations present for the lines interpreted in the Sassenfjorden-Tempelfjorden are shown in Figure 3.7, Figure 3.10, Figure 3.15 and Figure 3.18, and described in Sections 3.2 and 3.3. The facies and boundaries between them identified in the Reindalen line coincide fairly well with the depth of the formations expected to be present as basin fill, when comparing with the interpretation of Bælum and Braathen (2012). For the Sassenfjorden-Tempelfjorden lines, the outlined formations and groups are the pre-rift Billefjorden Group, followed by the syn-rift Gipsdalen Group (Hultberget, Minkinfjellet and Ebbadalen formations), and the overlying late- to post-rift Wordiekammen Formation. The exact location of the tops of the formations and groups are challenging to interpret correctly without any well information, and is now based on the tops/bottoms of facies identified and boundary surfaces and the interpretation of line ST-8515-121 in Bælum and Braathen (2012).

The syn-rift facies of the Sassenfjorden-Tempelfjorden lines show folding structures towards the master fault of Balliolbreen, highlighted in Figure 4.1 . The shape of the accommodation space created in the Billefjorden Trough during rifting strongly indicates that there is a direct connection between fault growth and the fault propagation. Weak, evaporittic facies is a plausible explanation for the formation of monoclinal structures in the Reindalen line, as well as in the Sassenfjorden-Tempelfjorden lines.

A challenge of the interpretation work is the fact that reflectors often change laterally and/or split into several reflectors. They can therefore be hard to follow. Considering this is 2D seismic data, the possibility of checking the interpreted reflectors on the place of intersection with other lines can be highly uncertain. As shown by Prosser (2003), the seismic signature of growth-strata in rift basins offers significant complexity, due to the spatial interaction between subsidence and uplift, and gradual block rotation, with implications for temporal accommodation creation and drainage development. In addition, eustatic sea-level changes and even climatic impact could play a role (e.g., Densmore, Allen, & Simpson, 2007). Accordingly, the many boundaries within growth-successions of rift basins (downlap, onlap, toplap) are best addressed in 3D studies.

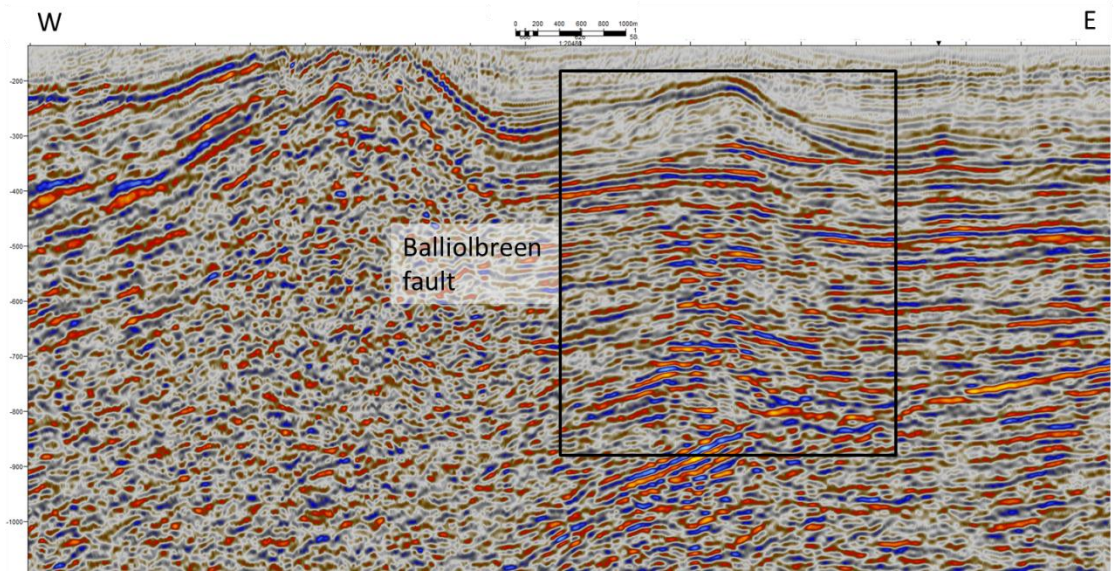

Figure 4.1 Folding structures in the reflectors proximal to the Balliolbreen fault plane on line Nh8706-210.

Conceptual discussion of the Carboniferous rift-basin characteristics

The geometry of the Carboniferous rift basin in the Reindalen line and the Sassenfjorden-Tempelfjorden lines differ in several ways from the illustration of rift basins as presented in Figure 1.3, of Prosser (1993). Nevertheless, one prominent similarity is the drag of reflectors up along the master fault plane, which can be the Prosser's (1993) S3 reflectors coinciding with the time of maximum rifting. The influence of fault-propagation folding in the studied rift basins are, however, very important for the geometry of the basin east of the Balliolbreen Fault in the lines interpreted, and the geometry can be linked to that of rift

basins studied in the Gulf of Suez (e.g., Jackson et al., 2006; Sharp et al., 2000). In Figure 4.2, from Sharp et al. (2000), highlighting the link between fault-propagation folding, fault growth and basin development, and comparing these structural styles with observations from the Billefjorden Trough, several striking similarities can be observed. Noticeably, the offset of the maximum thickness of depocenter away from the maximum displacement of the fault is also described for the Suez rift basin (e.g., Jackson et al., 2006; Sharp et al., 2000). Also, across the Løvehovden intra-basin fault of the Billefjorden Trough, asymmetric lenticular sub-basin geometry is observed (e.g., Braathen et al., 2011). As faults grow over time, the majority of associated folds will respond by gradually increasing amplitude and intensity (Schlische, 1995). Accordingly, fill into the related accommodation space would discern an upward onlapping configuration that becomes enhanced over time. In the Reindalen line, onlap towards the monocline is indicated for the Minkinfjellet Formation (facies A1), down to the lower Ebbadalen Formation (facies B2/A3). Also for the Wordiekammen Formation (facies C) it can be argued that onlap towards the monocline can be observed. This onlap configuration has geometry consistent with higher angles between the fold-limb and temporal deposits as the fold grows, along lines discussed by Schlische (1995).

Another aspect of importance is the temporal relationship between faults and sedimentary fairways into the basin, as shown by Gawthorpe and Leeder (2000). In Maher & Braathen (2011) addressing the Billefjorden Trough in the north, for instance, the footwall block of the Løvehovden fault experience uplift and erosion, with development of a erosional lag breccia and even a paleovally. This likely had significant impact on the sedimentary fairways, focusing sediment flux into distinct channels that were reaching the basin at a few given apexes. For instance, the character of alluvial fans is linked to fault margin evolution, and is highly relevant for siliciclastic fairways into the basin realm, especially in light of high-standing fault blocks and fault scarp surface expressions. For the Reindalen line, a similar erosional high is indicated for the footwall block of the Balliolbreen fault. Similarly, in the Sassendalen-Tempelfjorden lines, the Nordfjorden Block is an erosional high standing block. This hints at intricate basin development and focused sediment flux over time. With the analyzed open-grid 2D dataset, however, the resolution required for identifying the link between source areas and siliciclastic sinks is not available.

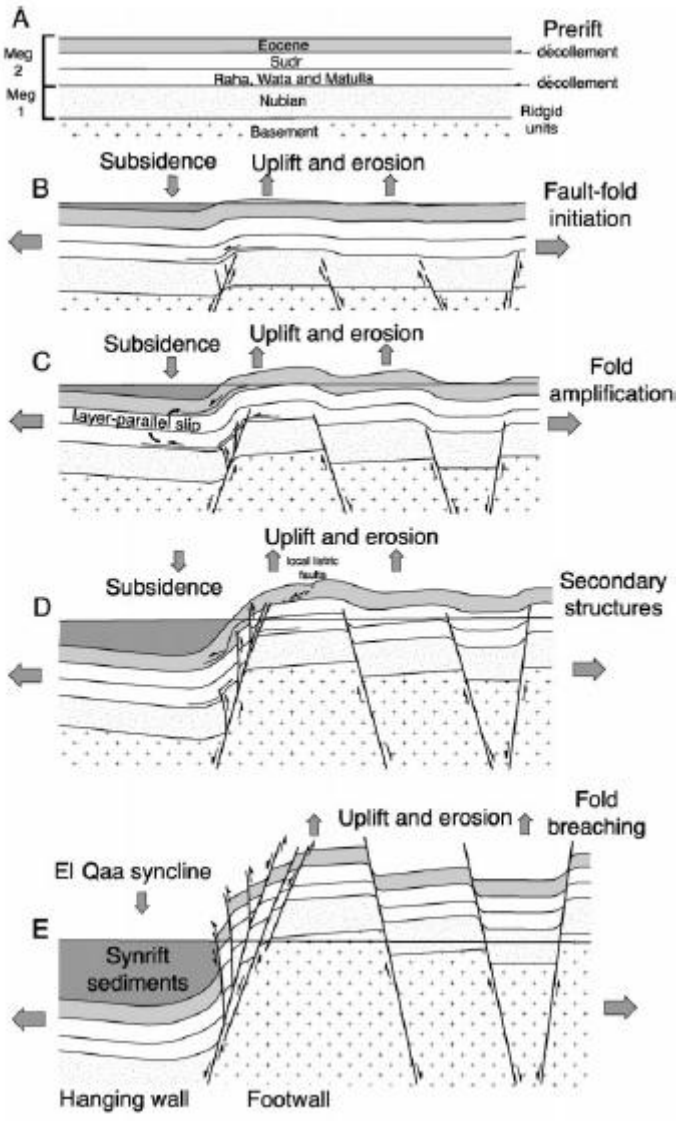

Figure 4.2 Fold propagation fold model from the publication by Sharp et al. (2000).

4.2 Triassic fault-bound basins of Southeast Svalbard

In the lines interpreted from the Eastern Svalbard, the focus has been on the Triassic part of the succession. The motivation for these analyses is the faulting observed in coastal cliffs of Edgeøya and Hopen, showing complex interaction between shallow-rooted and deep-rooted faults, as outlined in Braathen et al. (2011b). Figure 1.6, Figure 1.7 and Figure 4.3 and Section 1.5 further show the outcropping expression of this fault and basin system, and outline the background for this discussion. As this approximately E-W trending fault system has a regional distribution, they are expected to appear in seismic sections of the same stratigraphic interval. Accordingly, in this study a screening of lines resulted in the selection of a few cases for further analysis. As pointed out, these lines are challenging to interpret, as the intricacy of faulting and their associated shallow basins (< 200 m; up to 150 ms deep) offer both complex geometries and limited seismic resolution. Anyhow, the presented examples can be seen as first assessments of the seismic imaging of such basins.

The regionally well-expressed near-top Permian reflector represents a regional marker that can be used to discern deeper-rooted faulting from shallow-rooted faulting. This reflector correlates with the transition from the Permian to the Triassic, which is a globally recognized boundary of mass extinction of life. In the northern Barents Sea, this period was characterized by a gradually subsiding Barents Shelf in parallel with a noticeable change of climate (Grogan et al., 1999). Instead of open-shelf cold-water carbonate deposition of the upper Permian, this climatic change led to more clastic deposition characterizing the Mesozoic. At the same time, the Uralides developed as a major mountain chain in the east. With increased crustal thickness from thrust-nappe stacking, the foredeep basin deepened, as seen in the easternmost Barents Shelf. Here, Triassic deposition reached more than 7 km in thickness. This major succession gradually thin to around 1 km as approaching the Svalbard region in the west.

Clinoform characteristics and development

As the Triassic foredeep basin was filled in, the broad shallow marine shelf experienced sequences in a laterally stacked pattern, as documented by distinct, large-scale clinoform systems of the northern Barents Sea area (e.g., Høy and Lundschien 2011). Sediment transport is believed to be mainly from the SE towards the NW, and Høy and Lundschien (2011) also propose that the provenance area is found in the Caledonides, the Kola Peninsula and in the Uralides of the easternmost Barents Shelf and their continuation along Siberia.

The toe of the clinoforms (Anisian and Ladinian age) in the Eastern Svalbard area make up the Triassic source rock of the Botneheia Formation (Høy & Lundschien, 2011). The progradation of the delta responsible for filing in the Eastern Svalbard Triassic basin include the Botneheia Formation as a pro-delta bottom set (Høy & Lundschien, 2011). They are found to be gradually younger from SE towards NW. Riis et al. (2008) identify four principal seismic facies and associated depositional environments for a study area that is located further east than Eastern Svalbard. However, with progradation of the deltaic system, similar

facies should be present in Eastern Svalbard. The Palaeogeography of the Anisian, Ladinian and Carnian of the northern Barents Sea is described in Riis et al. (2008), where the Anisian and Ladinian comprise the Middle Triassic, and the Carnian marks the start of the Upper Triassic. The Botneheia Formation (Anisian age) is deposited in a foredeep setting. In the Ladinian, the Eastern Svalbard area changes to a shallow shelf environment, which subsequently (Carnian) is influenced by a prodelta to delta top setting (Riis et al., 2008). The Botneheia (Anisian-Ladinian deep marine black shale), the Tschermakfjellet (Ladinian age-prodelta shales) and the de Geerdalen formations (Carnian age-prograding delta) are the Triassic sequences with facies associations for the Eastern Svalbard lines interpreted, outlined in Chapters 3.4-3.6.

All the studied lines of Eastern Svalbard show the clinoform systems. The general pattern is that of northward progradation for large-scale clinoforms.. Bringing the sedimentary system of clinoforms into the discussion, further knowledge can be added to lithologies. For instance, the interpreted area of line 2045-92 A as seen in Figure 3.24 offers reflectors with strong amplitude response of facies A, which is likely dominated by sandstones due to the prograding nature of the facies. A delta-top succession is likely the depositional environment for this seismic facies (A).

Underneath this, the Botneheia Formation supposedly makes up a c. 100-150 m thick layer of black shales before the top-Permian contact is reached, mimicked by the near-top Permian reflector. This succession is seen as a seismic facies of transparent to weak and discontinuous reflectors, as mimicked by the seismic facies C in line 2300-81 of Figure 3.28.

Braathen et al. (2011b) also argue that the clinoforms show nearly vertical stacking, or aggradation, when arrested by faults. This could well be the case for the clinoform system of Line 2045-92 A (Figure 4.5), where the clinoform shelf-edge break has a nearly vertical trajectory for the lower part. As the sedimentary system bypass the faults, the trajectory changes to a lower-angle progradation trend.

Growth faults and basin fill

The interpreted faults in the Triassic succession can be divided into two main types. Several places, there are faults offsetting the near-top Permian reflector, cutting as high as the Triassic level. These faults are generally steeper, and have semi-planer geometry compared to the overall listric, shallow-rooted faults limited to the Triassic level. Their downward continuation suggests they are rooted in the Carboniferous or even in the basement. With deeper Carboniferous fault-bound basins at depth, reactivation of such deep faults is a viable model for the faults penetrating up to the Triassic level. Braathen et al. (2011b) argue that the instability caused by such deep faulting is the cause for the intra-Triassic faulting rooted in shale horizons.

The shallow-rooted growth fault systems are widespread, as for example seen by the general disturbance of layering in lines 2045-92 A and 2145-92 (Figure 3.23 and Figure 3.31). A pattern of overall wavy reflectors and complex reflector patterns is the first order

appearance of these systems. Further, the instability terminates before reaching the near-top Permian reflector, which seems undisturbed by the deformational system.

Interpreted faults vary significantly in geometry, from low-angle and listric to steeper and more planar. In the latter case, the faults likely have a sharp bend into layering of weak shale horizons. Fault throw is overall small, with growth basins reaching 100-150 s thickness. This is well displayed in line 2045-92 A (Figure 4.4). In the same line, there are indications for both rollover-folding and drag-folding towards faults. The growth basins would accordingly show either wedge or lenticular shape, as discussed for the Carboniferous basins (see above).

The listric faults of the Triassic of Eastern Svalbard seem to have significant curvature, with very low angles (see for instance the faults in facies' A and B for line 2045-92 A in Figure 3.24) before flattening out in shale layers, making the faults hard to detect. At places the faults have a steeper angle in the sandstones, which could signify higher shear strength, or that the fault approaches the surface. From the onland studies, it seems clear that faults sole out in various levels of pro-delta shale, with a fundamental lower boundary in the Botneheia Formation black shales. This pattern is indicated by the seismics, where faulting seems rooted at several levels (e.g. Figure 3.28).

Braathen et al. (2011b) arguments also address the regional extent of the faulting, by that suggesting that the delta-front collapse model of Edwards (1976) is less viable. However, for the shallow-rooted fault system, the geometries are strikingly similar to those ascribed to delta collapse (e.g., Bhattacharya and Davies 2001, and references therein). Hence, some sort of vertical load as a driving force, for example by outbuilding delta lobes, could have assisted the dynamics of the fault system.

Linking the basin fill of the shallow Triassic basins with conceptual models for growth-strata geometries, as outlined in Gawthorpe and Hardy (2002) and Prosser (1993), is not trivial. The main concern is the shallow depth of the basins, which allow little information from the growth-strata. Hence, a clear subdivision into early-, syn- and late-rift growth sections is not really discernible, in contrast to the conceptual models, building either on onland detailed observations or deeper rift basins. Further, the lateral facies changes as documented from cliffs of Edgeøya and Hopen (Figure 4.3 and Figure 1.7) are not directly reflected in the seismics, although the basins at places show internal reflectors that could mimic the geometry of the fill. Such links would require even more detailed analysis then undertaken here.

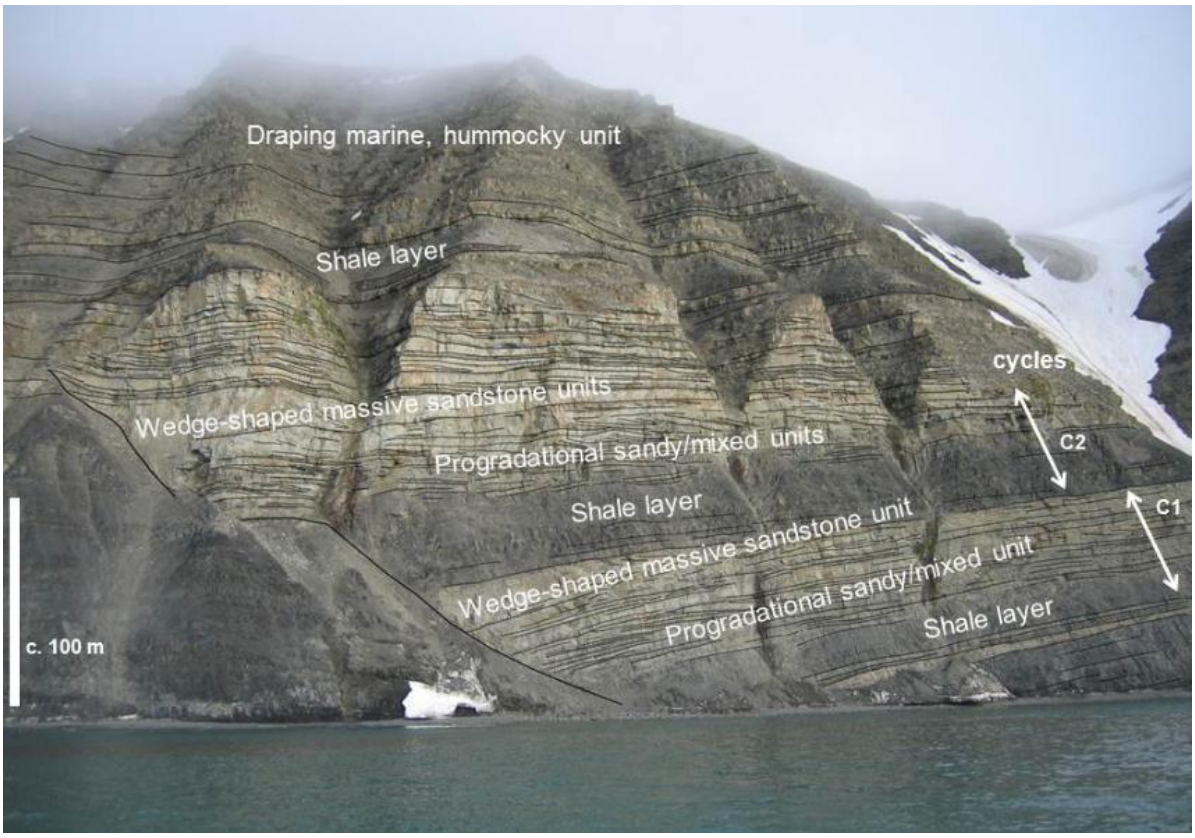

Figure 4.3 Photograph's with interpretations of extensional listric faults with Triassic growth basins in the hanging wall from Kvalpynten, SSW Edgeøya. The view is to the east. Photographs by A. Braathen.

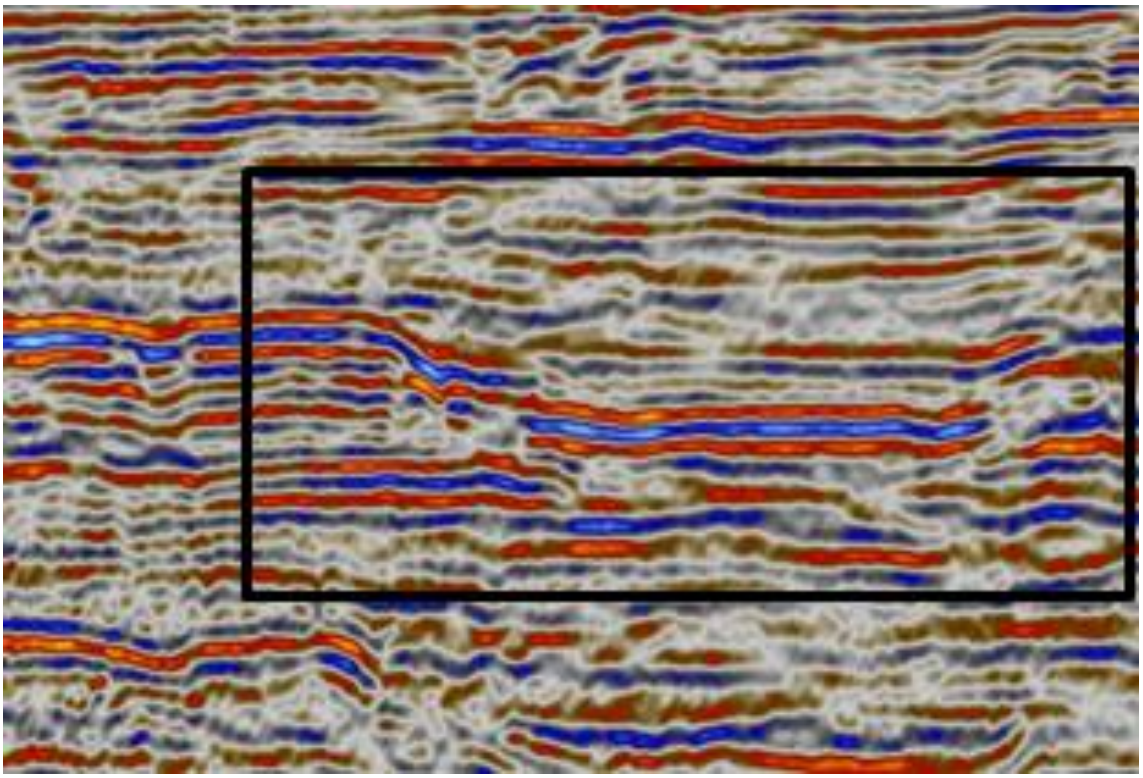

Figure 4.4 Cropped area of line 2045-92 A with example of drag of reflectors associated with growth fault.

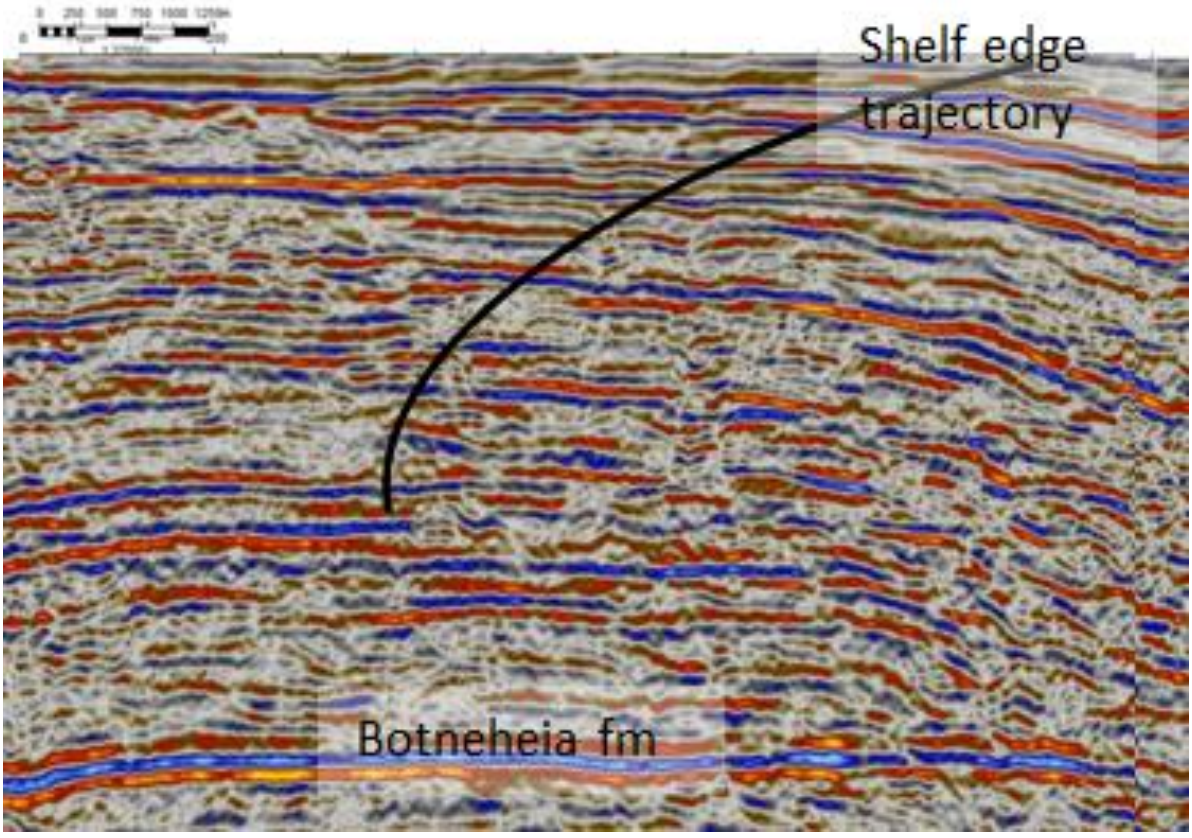

Figure 4.5 Line 2045-92 A with examples of clinoform systems and indications of the shelf edge trajectory.

4.3 Comparison between Carboniferous rifting and Triassic extension

The scale of the half-graben Carboniferous basin of Central Spitsbergen is significantly larger than the Triassic extensional growth-basins in the Eastern Svalbard lines. One major difference is the size of drag-folds, or monoclines. In the Reindalen line there is a major up-folding of reflectors towards for instance the Balliolbreen fault, basically creating a lenticular and offset (-from-the-fault) growth basin in the hanging wall (Figure 4.1).Similar drag-folds are potentially visible for the Eastern Svalbard seismics, suggesting that lenticular growth-basin shapes are present there as well (Figure 4.4). However, in the latter case the small scale of the basin limits further analysis.

The growth-strata lithology is different as well. In the Billefjorden Trough, the growth succession is dominated by sandstone and carbonates along the basin margins, which are interfingering with mostly evaporites making up the main lithology of the basin center. For Triassic extensional basins, the accounts by Edwards (1976), Høy and Lundschien (2010) and Braathen et al. (2011b) points to mainly three sedimentary facies; (i) shale succession of pro-delta origin, (ii) heterolithic, thin bedded and prograding sandstone-shale successions, and (iii) massive sandstone bodies. The three units all show thickness variations related to localized accommodation creation expansion in the subsiding fault blocks. Compared to the Billefjorden Trough, the mechano-stratigraphy in the Triassic basins is different, but this may not significantly have impacted the structural style. What seems clearer is the influence of evaporites in the Billefjorden Trough, which have been argued to enhance or even trigger fault-tip monocline formation (e.g., Braathen et al. 2011a). The pro-delta shales of the Triassic growth-basins could play a similar role; however, their importance as floors to faulting seems more important, as shown in Figure 1.7 and Figure 4.3. Similar floor-faults are not observed in the dataset from the Billefjorden Trough, although Maher and Braathen (2011) document down-dip, layer-parallel shear zones in evaporites where these layers have significant dip in the forelimbs of monoclines.

Conclusions

1) The Billefjorden Trough is the result of a complex basin evolution history, as proposed with the reconstructions of Braathen et al. (2011). Outcrop studies in the northern Billefjorden area shows a basin that changes basin depocenter geometry, from a lenticular shape to a wedge shape and then back to a lenticular shaped basin.
2) In the Reindalen line there is a major up-folding of reflectors towards for instance the Balliolbreen fault, basically creating a lenticular and offset (-from-the-fault) growth basin in the hanging wall.
3) Drag-folds, similar to the ones observed for the Reindalen and Sassenfjorden-Tempelfjorden lines, are potentially visible for the Eastern Svalbard seismics, suggesting that lenticular growth-basin shapes are present there as well. The small scale of the basin limits further analysis.
4) The listric faults of the Triassic of Eastern Svalbard seem to have significant curvature, with very low angles before flattening out in shale layers, making the faults hard to detect. At places the faults have a steeper angle in the sandstones, which could signify higher shear strength, or that the fault approaches the surface. From the onland studies, it seems clear that faults sole out in various levels of pro-delta shale, with a fundamental lower boundary in the Botneheia Formation black shales. This pattern is indicated by the seismics, where faulting seems rooted at several levels.
5) A challenge of the interpretation work is the fact that reflectors often change laterally and/or split into several reflectors. They can therefore be hard to follow for the seismic sections.

References

Bergh, S. G., Maher, H. D. J., & Braathen, A. (2011). The Adriabukta deformation event: Evidence for Early-Mid Carboniferous transpressional uplift of the Sørkapp-Hornsund High, Southern Spitsbergen. . *Journal of the Geological Society, London*, 168, 441-456.

Braathen, A., Bælum, K., Maher Jr, H. D., & Buckley, S. J. (2011). Fault influence on a mixed siliciclastic-evaporite-carbonate riftbasin system; the Carboniferous Billefjorden Trough, Svalbard.

Braathen, A., Osmundsen, P. T., & Olaussen, S. (2011b). Tectonic events of the NW Barents Shelf; on-offshore correlations with implications for development of the eastern shelf area. *Invited lecture, FORCE petroleum seminar, Stavanger, October 11-12.*

Bælum, K., & Braathen, A. (2012). Along-strike changes in fault array and rift basin geometry: The Billefjorden Trough of Svalbard, Norway.

Cocks, L. R. M., & Torsvik, T. H. (2007). Siberia, the wandering northern terrane, and its changing geography through the Palaeozoic. *Earth-Science Reviews, 82*(1-2), 29-74.

Densmore, A. L., Allen, P. A., & Simpson, G. (2007). Development and response of a coupled datchemnt-fan system under changing tectonic and climateic forcing. . *Journal of Geophysical Research 112, F01002, doi:10.1029/2006JF000474.*

Edwards, M. B. (1976). Growth faults in Upper Triassic deltaic sediments, Svalbard. *American Association Petroleum Geologists Bulletin, 60*, 341-355.

Gawthorpe, R., & Hardy, S. (2002). Extensional fault-propagation folding and base-level change as controls on growth-strata geometries. *Sedimentary Geology, 146*(1-2), 47-56.

Gawthorpe, R. L., & Leeder, M. R. (2000). Tectono-sedimentary evolution of active extensional basins. *Basin Research, 12*(3-4), 195-218.

Grogan, P., Østvedt-Ghazi, A. M., Larssen, G. B., Fotland, B., Nyberg, K., Dahlgren, S., & Eidvin, T. (1999). *Structural elements and petroleum geology of the Norwegian sector of the northern Barents Sea*.

Høy, T., & Lundschien, B. A. (2011). Triassic deltaic sequences in the northern Barents Sea. *Geological Society, London, Memoirs, 35*(1), 249-260.

Jackson, C. A. L., Gawthorpe, R. L., & Sharp, I. R. (2006). Style and sequence of deformation during extensional fault-propagation folding: examples from the Hammam Faraun and El-Qaa fault blocks, Suez Rift, Egypt. *Journal of Structural Geology, 28*(3), 519-535.

Johannessen, E., & Steel, R. (1992). Mid-Carboniferous extension and rift-infill sequences in the Billefjorden Trough, Svalbard. *Norsk Geologisk Tidsskrift, 72*(1), 35-48.

Leever, K. A., Gabrielsen, R. H., Faleide, J. I., & Braathen, A. (2011). A transpressional origin for the West Spitsbergen fold-and-thrust belt: Insight from analog modeling. *Tectonics, 30*(2), TC2014.

Maher, J., H.D, & Braathen, A. (2011). Løvehovden fault and Billefjorden rift basin segmentation and development, Spitsbergen, Norway. *Geological Magazine, 148*(1), 154-170.

Maher Jr, H. D., & Braathen, A. (2010). Lovehovden fault and Billefjorden rift basin segmentation and development, Spitsbergen, Norway. *Geological Magazine, 148*(1), 154.

McCann, A. J., & Dallmann, W. K. (1996). Reactivation history of the long-lived Billefjorden Fault Zone in north central Spitsbergen, Svalbard. *Geological Magazine, 133*(01), 63-84.

Nøttvedt, A., Livbjerg, F., Midbøe, P., & Rasmussen, E. (1993). Hydrocarbon potential of the central Spitsbergen basin. *Arctic Geology and Petroleum Potential, 2*, 333-361.

Prosser, S. (1993). Rift-related linked depositional systems and their seismic expression. *Geological Society, London, Special Publications, 71*(1), 35-66.

Riis, F., Lundschien, B. A., Høy, T., Mørk, A., & Mørk, M. B. E. (2008). Evolution of the Triassic shelf in the northern Barents Sea region. *Polar Research, 27*(3), 318-338.

Schlische, R. W. (1995). Geometry and origin of fault-related folds in extensional settings. *AAPG Bulletin-American Association of Petroleum Geologists, 79*(11), 1661-1678.

Sharp, I. R., Gawthorpe, R. L., Underhill, J. R., & Gupta, S. (2000). Fault-propagation folding in extensional settings: examples of structural style and synrift sedimentary response from the Suez rift, Sinai, Egypt. *Geological Society of America Bulletin, 112*(12), 1877.

Steel, R., & Worsley, D. (1984). Svalbard's post-Caledonian strata—an atlas of sedimentational patterns and palaeogeographic evolution. *Petroleum geology of the North European margin*, 109-135.

5. Appendix

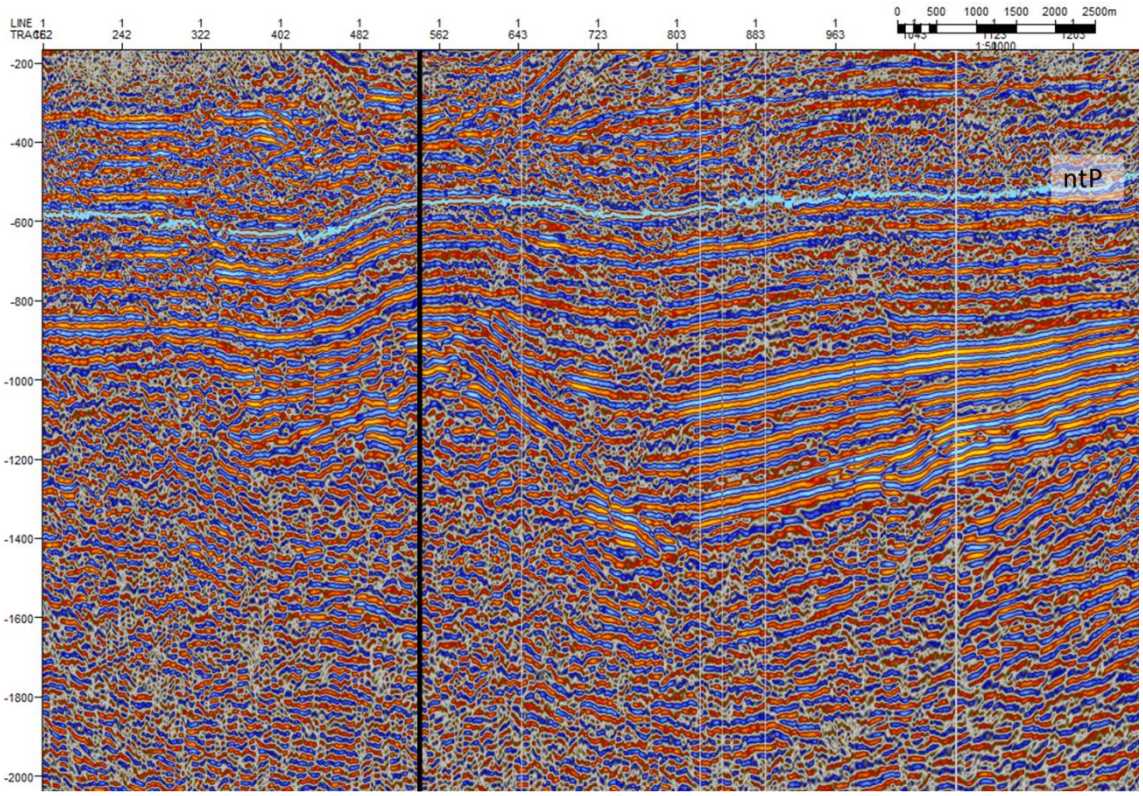

Figure 5.1 Line NH8802-32 with position of the well drilled by Hydro indicated with the black vertical line and the near top Permian interpretation in blue.

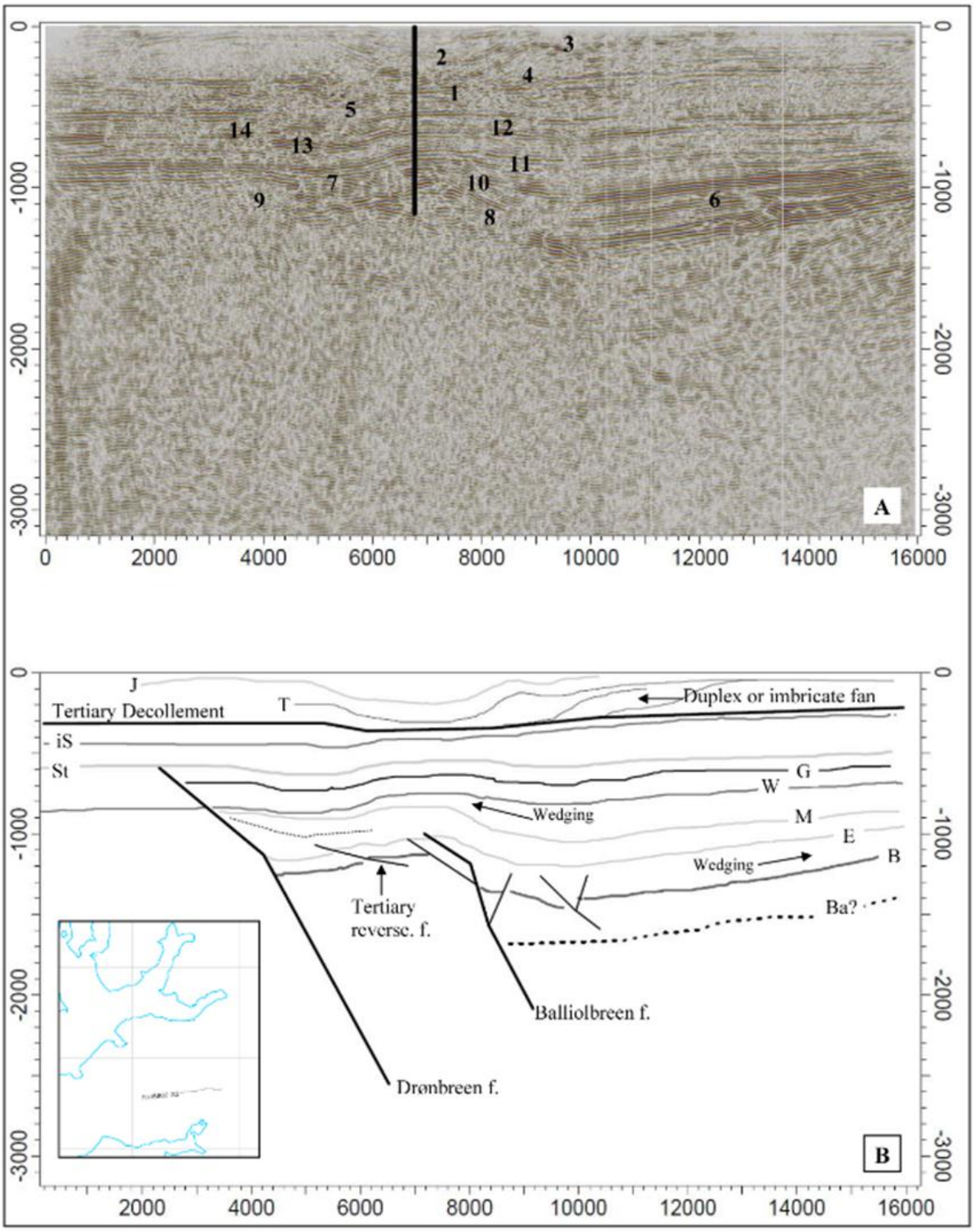

Figure 5.2 The interpretation of line NH8802-32 by Karoline Bælum from the article Bælum and Braathen (2012).

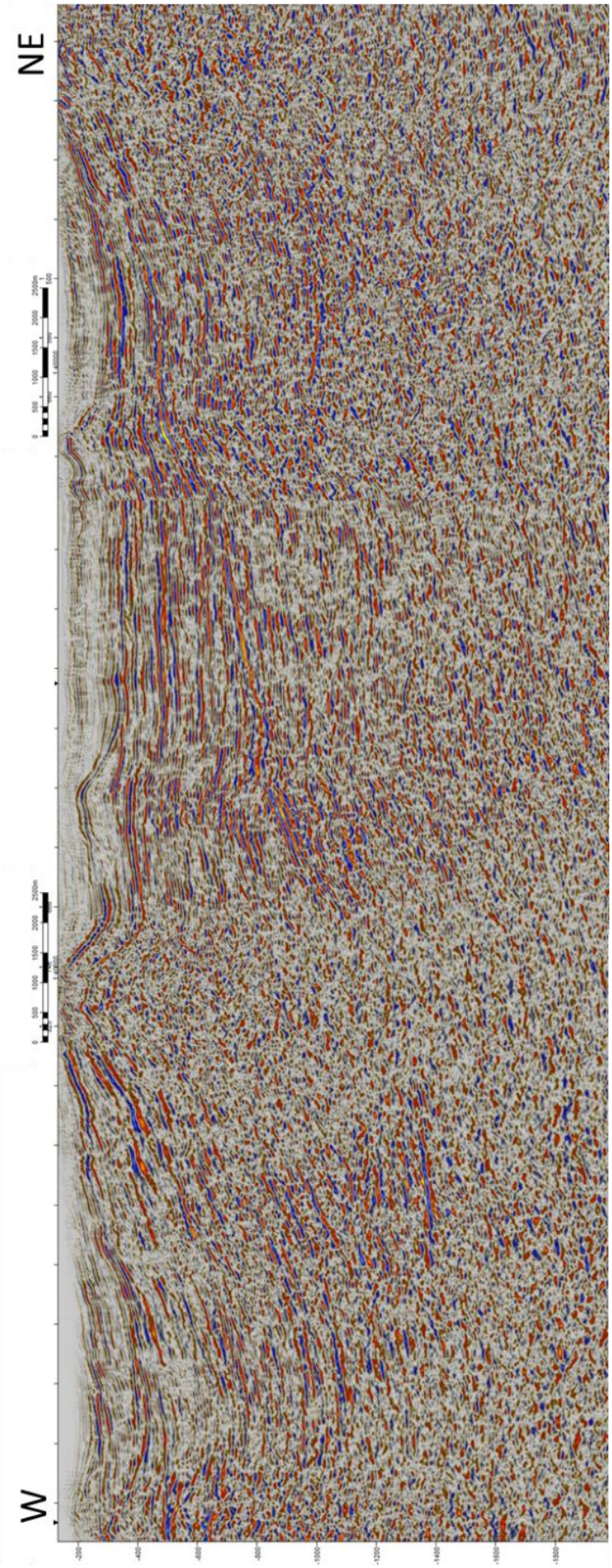

Figure 5.3 Composite line of NH8706-210 and NH8706-404

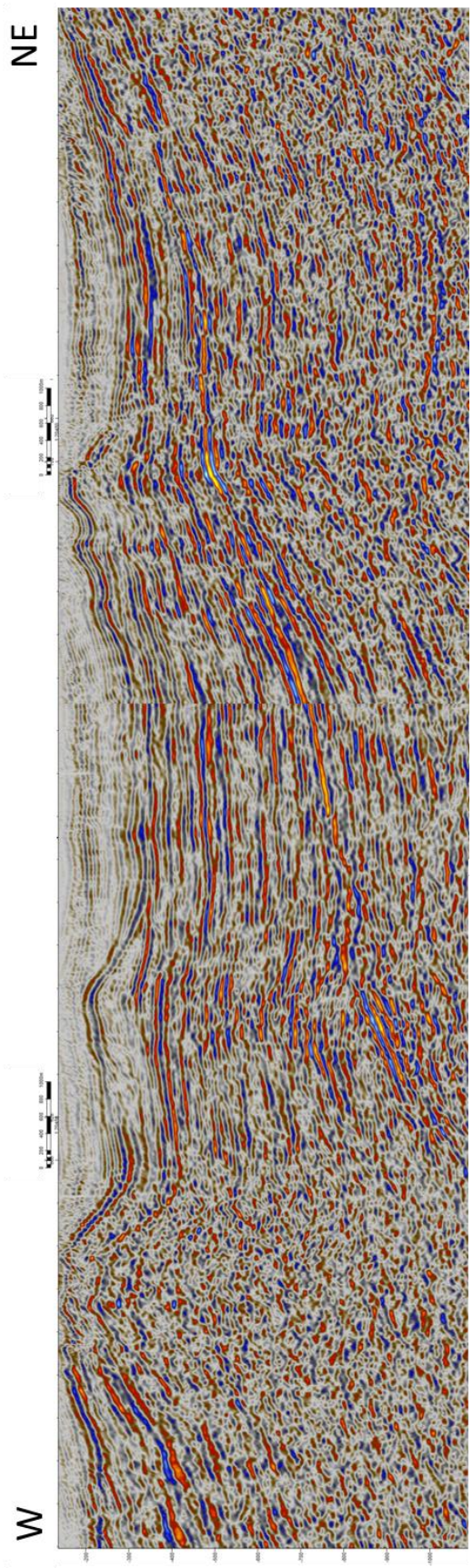

Figure 5.4 Composite line of NH8706-210 and NH8706-404

Some highlighted areas from the interpreted area of line 2300-81. Fault zones, also possibly affected by noise downwards. There also appears to be a number of small interesting rift basins associated with the extensional fault zones for the strong reflector belts above ntP (blue horizon). These basins may also be beneath the seismic resolution, so that much of the interesting details in these small-scale Triassic basins in the fault zones are missing.

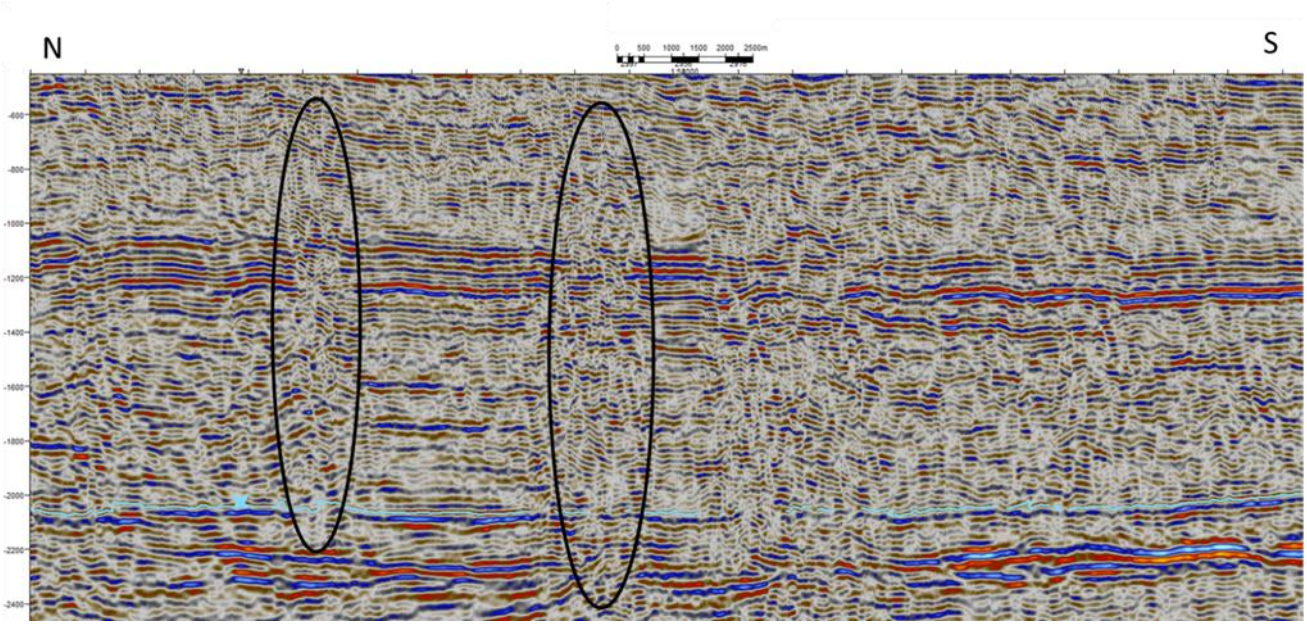

Figure 5.5 Line 2300-81 with indicated fault zones possibly mixed with noise artifacts.

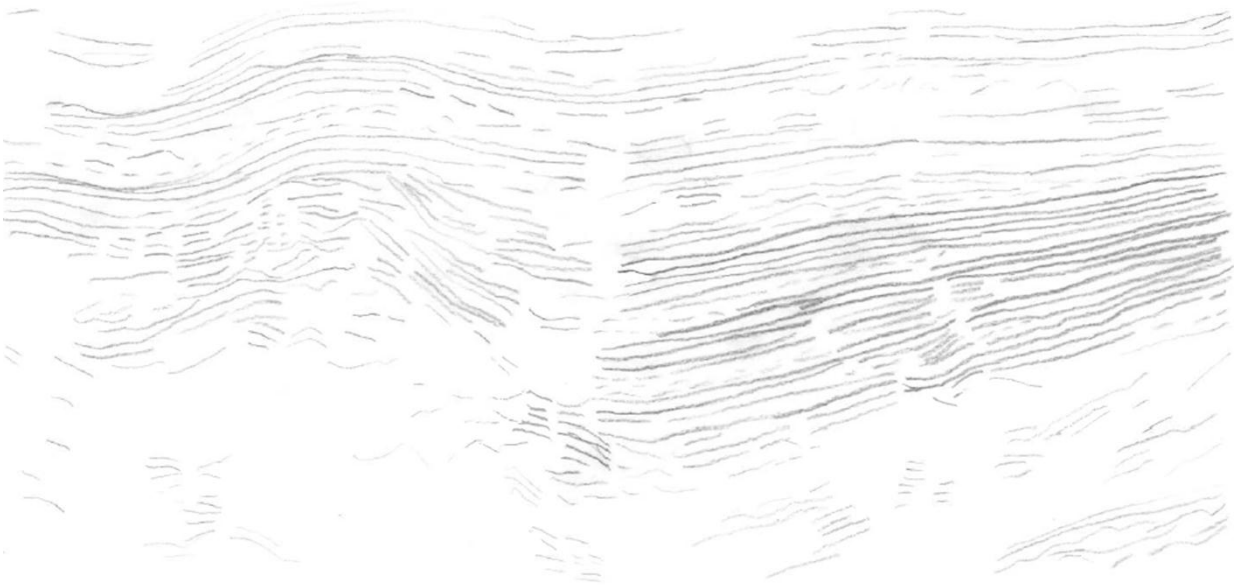

Figure 5.6 Line NH8802-32 drawn with pencil on transparent paper.

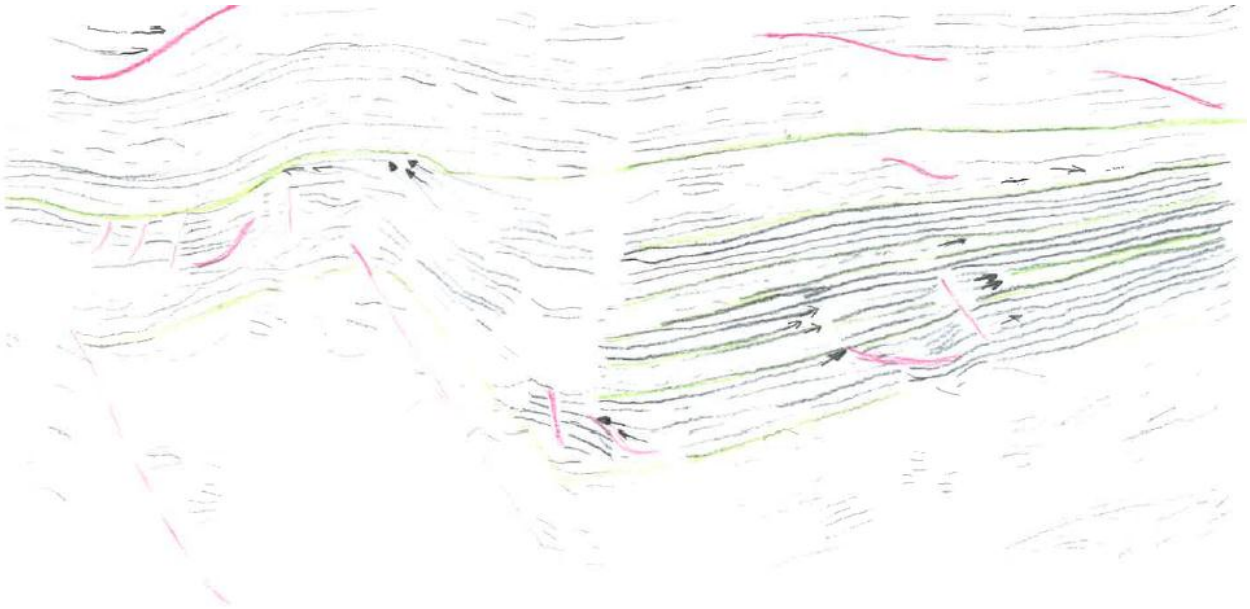

Figure 5.7 Line NH8802-32 with main boundary surfaces in green and faults in red. Arrows indicate terminations of reflectors.

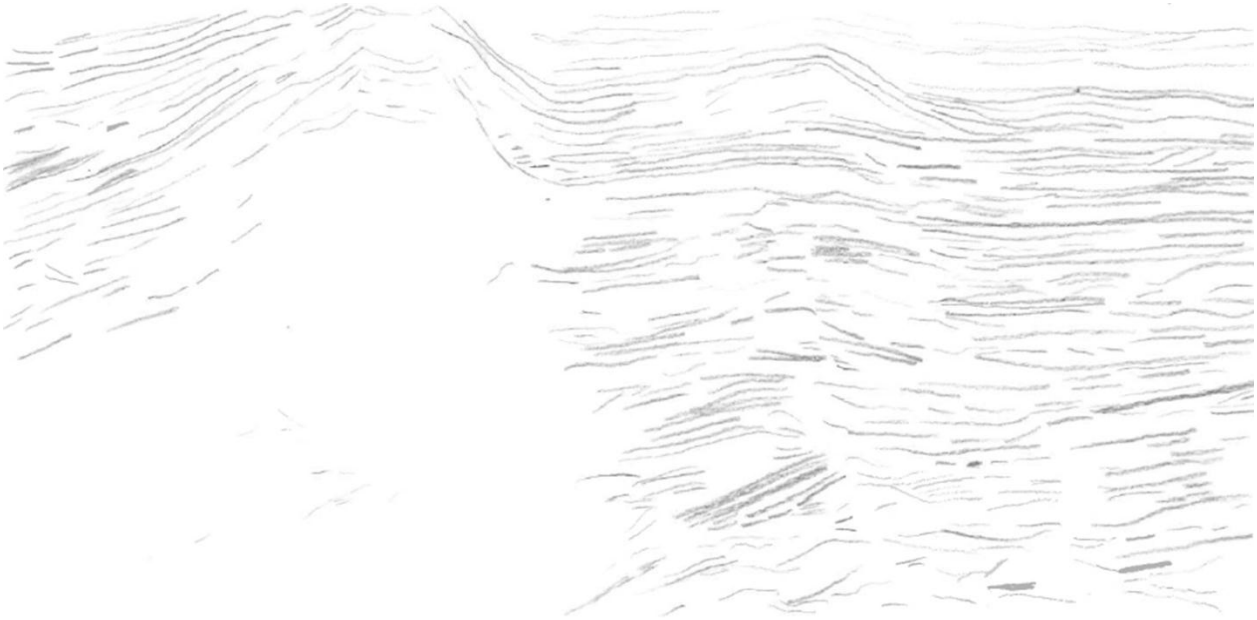

Figure 5.8 Line NH8706-210 drawn with pencil on transparent paper.

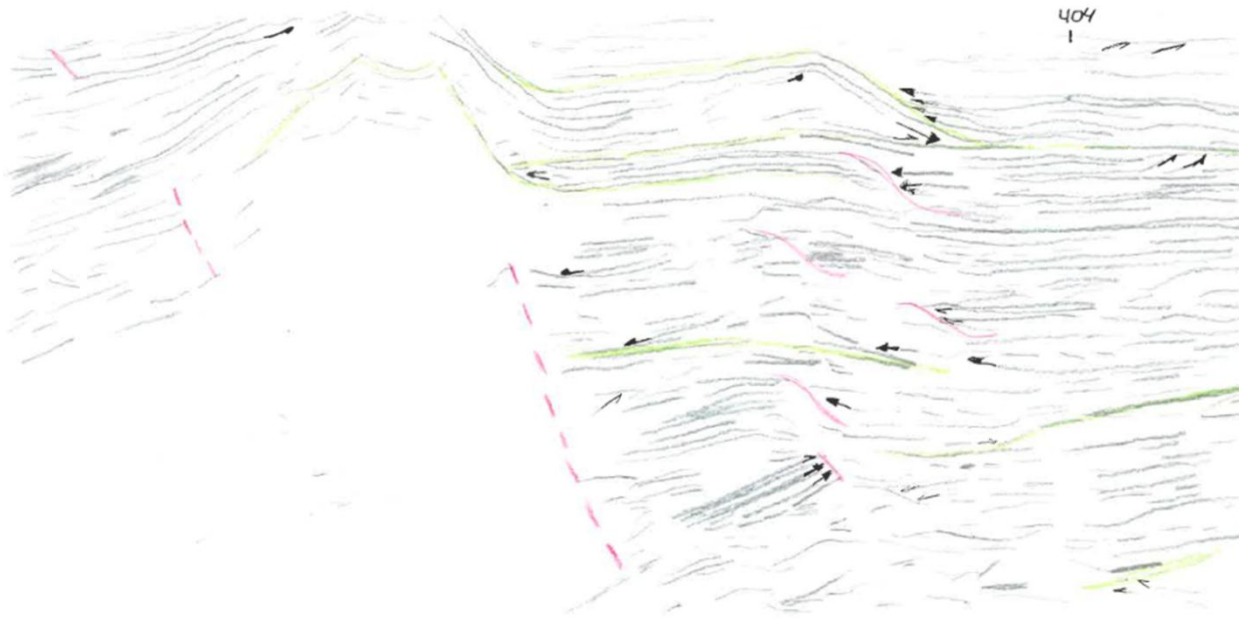

Figure 5.9 Line NH8706-210 with main boundary surfaces in green and faults in red. Arrows indicate terminations of reflectors.

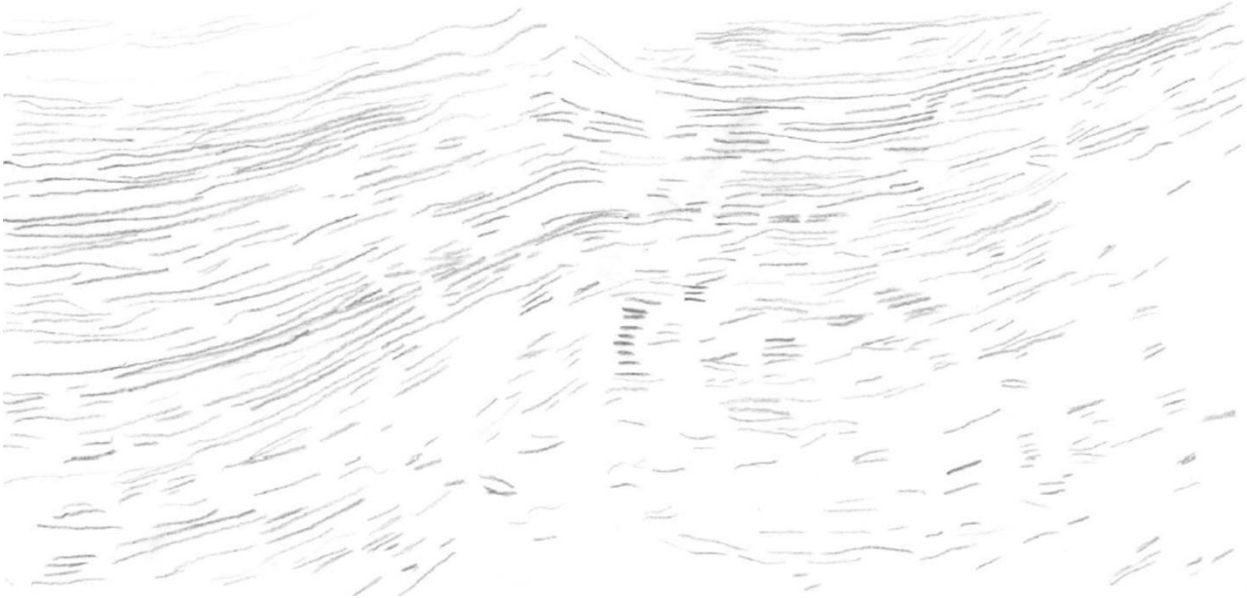

Figure 5.10 Line NH8706-404 drawn with pencil on transparent paper.

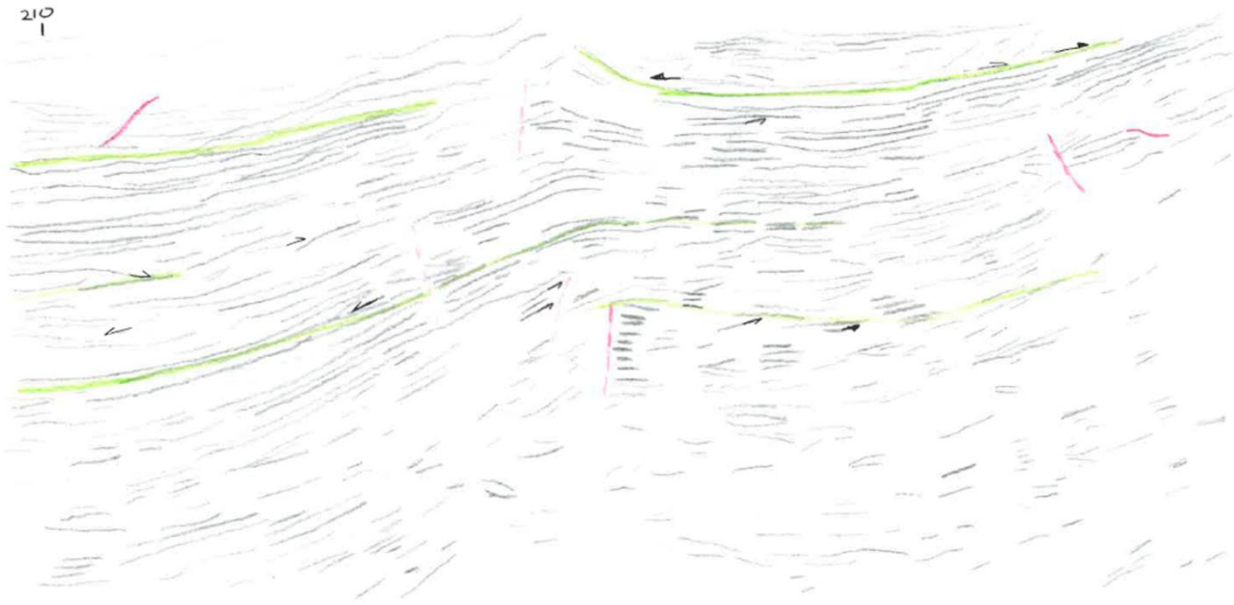

Figure 5.11 Line NH8706-404 with main boundary surfaces in green and faults in red. Arrows indicate terminations of reflectors.

Figure 5.12 First part of line NH8706-405 drawn with pencil on transparent paper.

Figure 5.13 First part of line NH8706-405 with main boundary surfaces in green and faults in red. Arrows indicate terminations of reflectors.

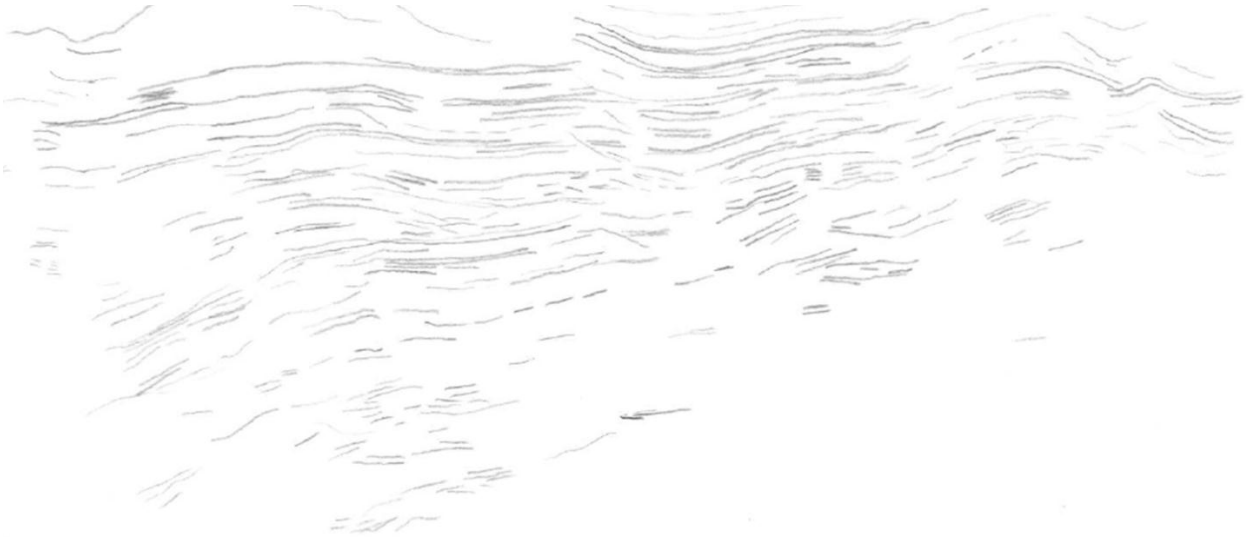

Figure 5.14 Second part of line NH8706-405 drawn with pencil on transparent paper.

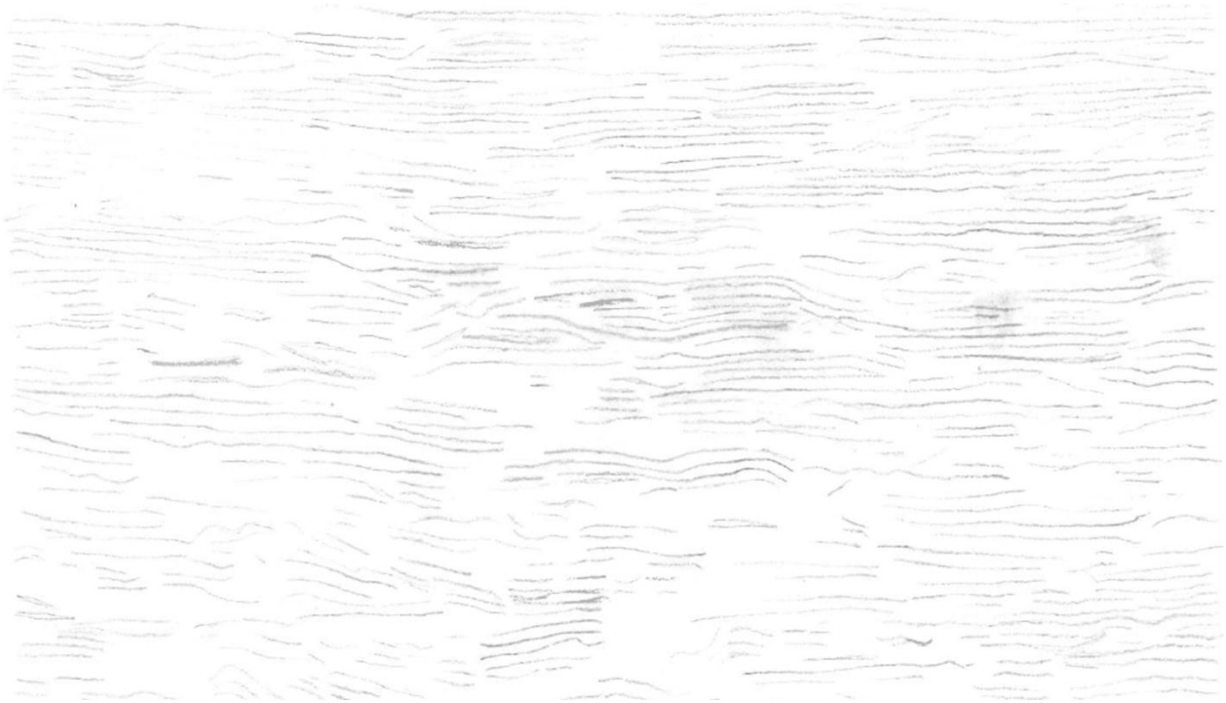

Figure 5.15 Line 2045-92 A drawn with pencil on transparent paper.

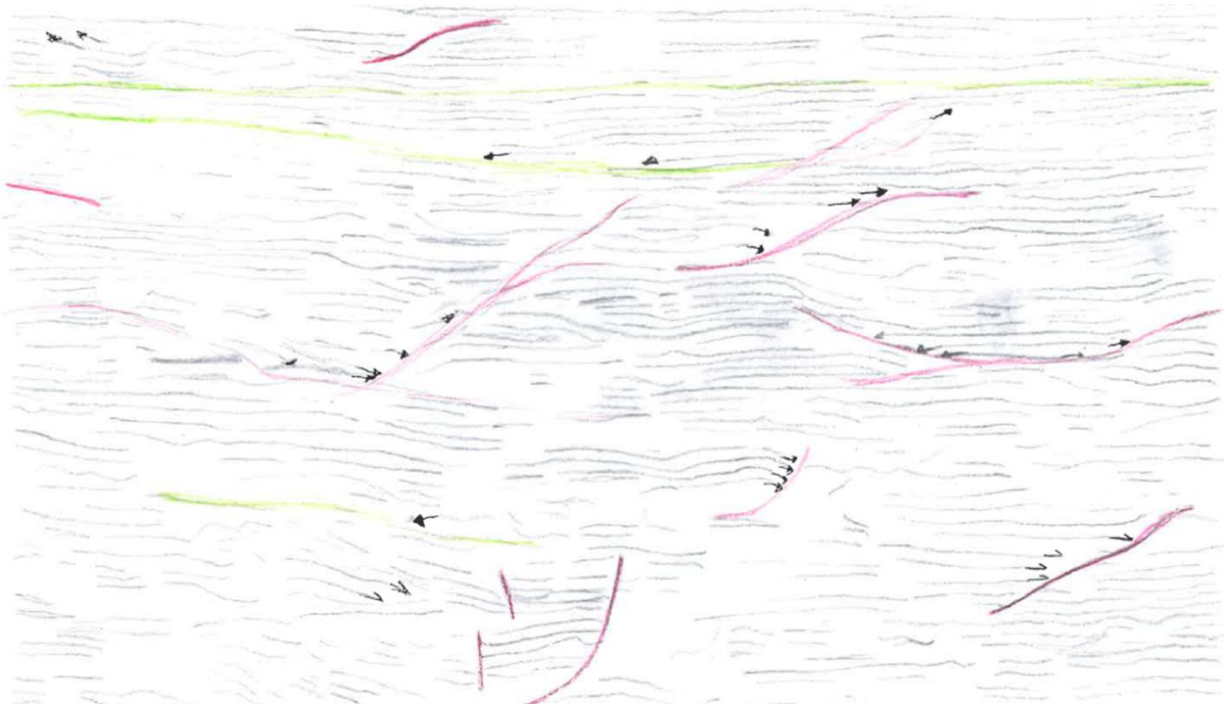

Figure 5.16 Line 2045-92 A with main boundary surfaces in green and faults in red. Arrows indicate terminations of reflectors.

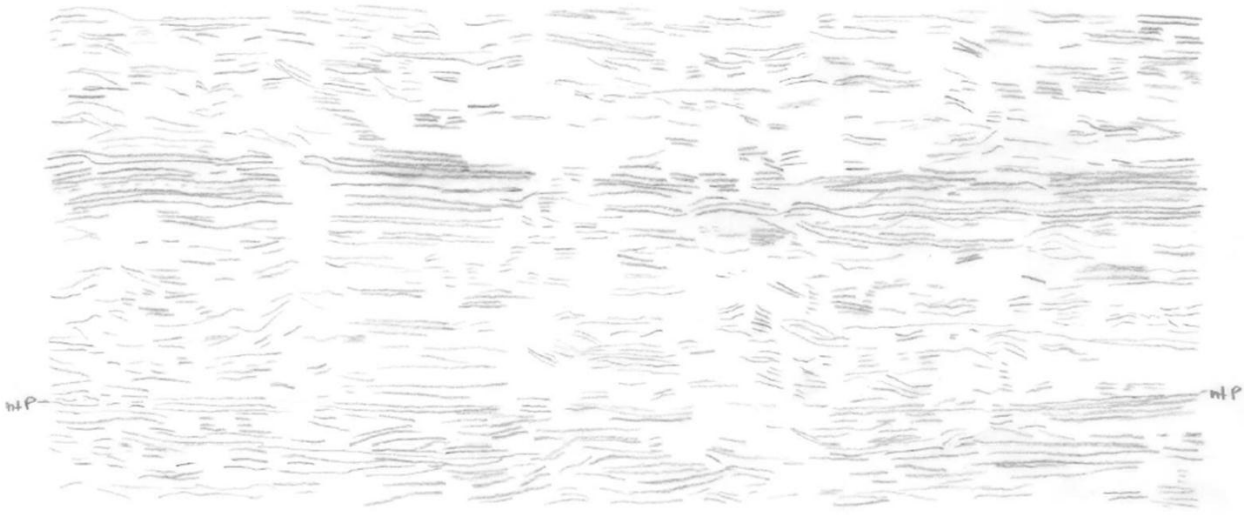

Figure 5.17 Line 2300-81 drawn with pencil on transparent paper.

Figure 5.18 Line 2300-81 with main boundary surfaces in green and faults in red. Arrows indicate terminations of reflectors.

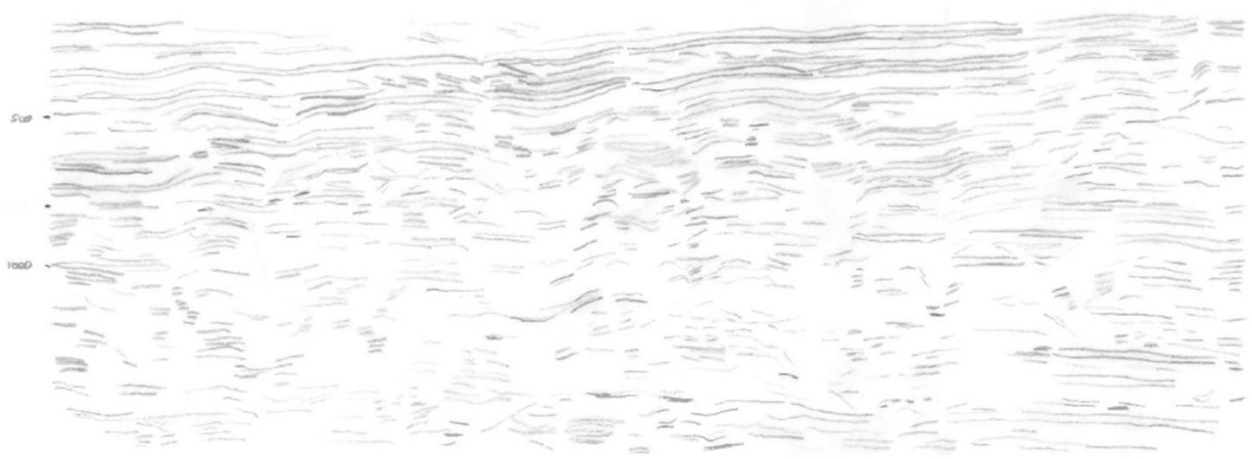

Figure 5.19 Line 2145-92 drawn with pencil on transparent paper.

Figure 5.20 Line 2145-92 with main boundary surfaces in green and faults in red. Arrows indicate terminations of reflectors.

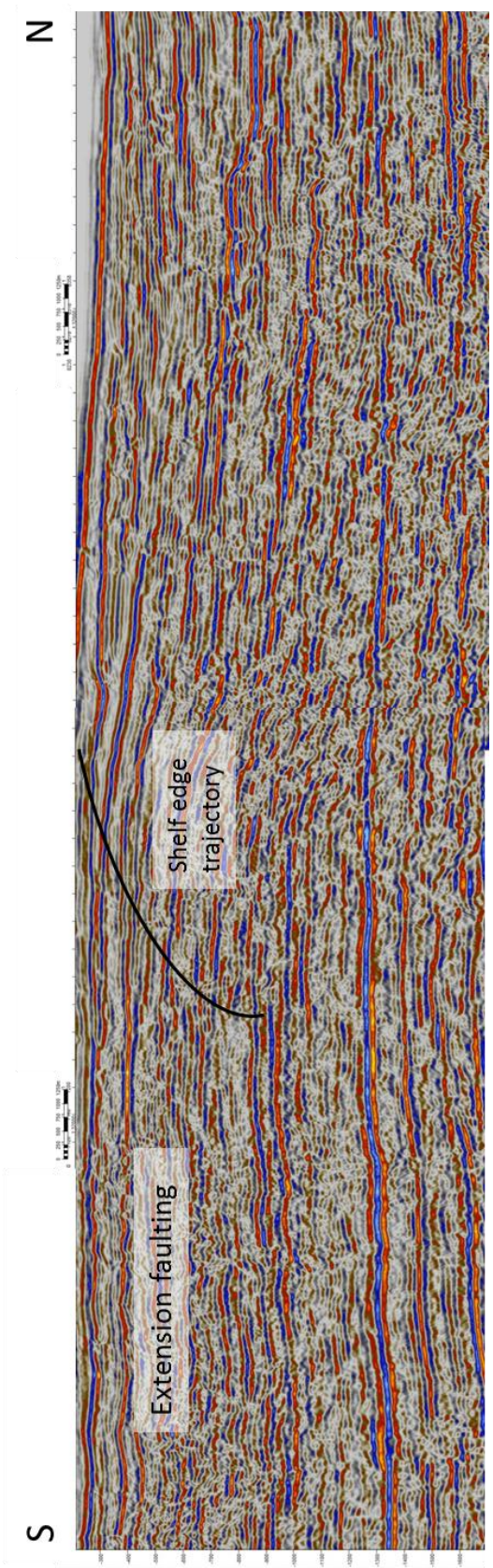

Figure 5.21 Line 2045-92 A with some additional observations.